

## Hydrophobic Substituents on Isatin Derivatives Enhance Their Inhibition against Bacterial Peptidoglycan Glycosyltransferase Activity

Yong Wang<sup>‡</sup>, Wing-Lam Cheong<sup>‡</sup>, Zhi-Guang Liang, Lok-Yan So, Kin-Fai Chan, Pui-Kin So, Yu-Wai Chen, Wing-Leung Wong and Kwok-Yin Wong<sup>\*</sup>

State Key Laboratory of Chemical Biology and Drug Discovery, Department of Applied Biology and Chemical Technology, The Hong Kong Polytechnic University, Hunghom, Kowloon, Hong Kong, P. R. China.

<sup>‡</sup> The authors contributed equally to this work.

<sup>\*</sup> Corresponding author

E-mail: kwok-yin.wong@polyu.edu.hk

### Abstract

Moenomycin A, the well-known natural product inhibitor of peptidoglycan glycosyltransferase (PGT), is a large amphiphilic molecule of molecular mass of 1583 g/mol and its bioavailability as a drug is relatively poor. In searching for small-molecule ligands with high inhibition ability targeting the enzyme, we found that the addition of hydrophobic groups to an isatin-based inhibitor of bacterial PGT significantly improves its inhibition against the enzyme, as well as its antibacterial activity. The improvement in enzymatic inhibition can be attributed to a better binding of the small molecule inhibitor to the hydrophobic region of the membrane-bound bacterial cell wall synthesis enzyme and the plasma membrane. In the present study, a total of 20 new amphiphilic compounds were systematically designed and the relationship between molecular hydrophobicity and the antibacterial activity by targeting at PGT was demonstrated. The *in vitro* lipid II transglycosylation inhibitory effects (IC<sub>50</sub>) against *E. coli* PBP1b and MICs of the compounds were investigated. Optimized results including MIC values of 6 µg/mL for MSSA, MRSA, *B. subtilis* and 12 µg/mL for *E. coli* were obtained with an isatin derivative **5m** which has a molecular mass of 335 g/mol.

### 1. Introduction

The World Health Organization's recent surveillance data on antibiotic resistance revealed high levels of resistance in a number of serious bacterial infections across many countries [1]. The development of antimicrobial resistance occurs so quickly that it was estimated by 2050 the number of death caused by antibiotic resistance will exceed that caused

by cancer [2]. Thus, there is an urgent need to develop the next generation antibiotics based on new drug targets or therapeutic mechanisms.

The peptidoglycan glycosyltransferase (PGT) that transfers the disaccharide-peptide of lipid II to the growing glycan chain in bacterial cell wall synthesis is regarded as a potential new drug target for new antibiotic development [3]. The PGT domain of penicillin-binding protein is anchored on the outer surface of the bacterial cell membrane by a transmembrane helix (Fig. 1) [4-6]. Lipid II, the substrate of PGT, is a large amphiphilic molecule containing a hydrophilic disaccharide-peptide head and a hydrophobic undecaprenyl diphosphate tail for its anchoring to the bacterial cell membrane during polymerization [7-9]. Moenomycin A (MoeA), the well-known inhibitor for PGT activity, is also an amphiphilic molecule consisting of a hydrophilic pentasaccharide head and a hydrophobic C<sub>25</sub>-lipid moiety (Fig. 2) [10, 11]. However, the poor pharmacokinetic properties of MoeA prevents its direct utilization as antibiotic for human, and no PGT inhibitors are available for clinical trial or used currently as antimicrobial agents [12]. Nonetheless, previous understanding on the chemistry and biological functions of MoeA [10, 12] and its analogues provide helpful information for rational design of PGT inhibitors [13-15]. Recently, a small molecule-based inhibitor adopting tryptamine as the main molecular scaffold has been reported [16].

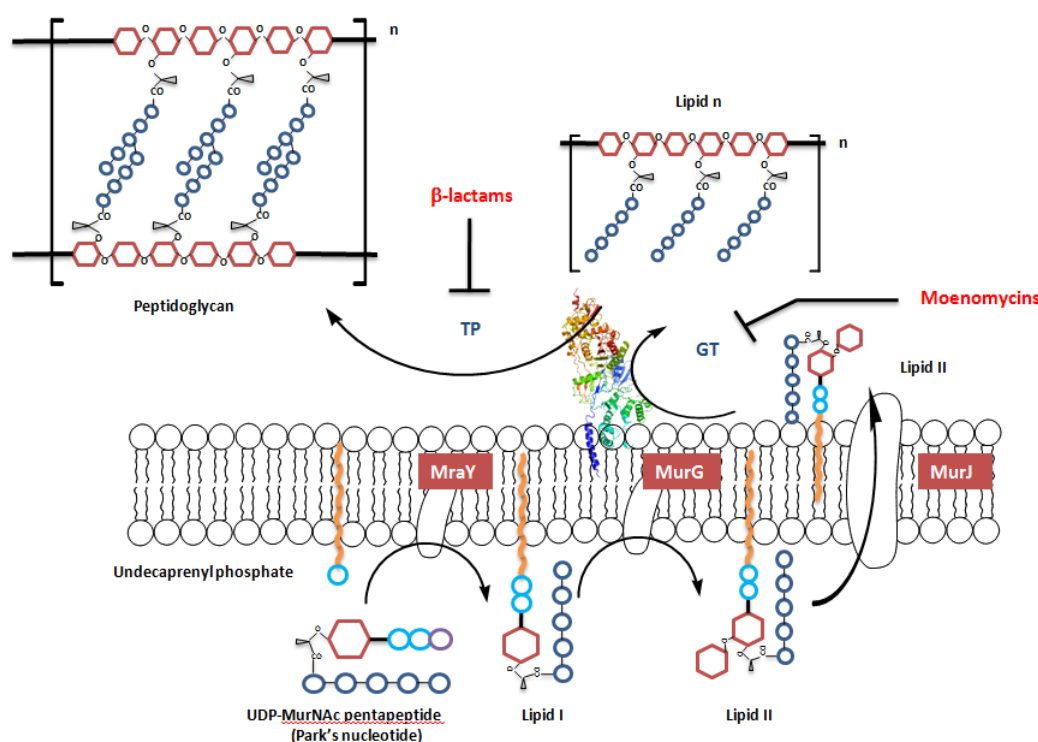


Fig. 1. The bacterial peptidoglycan biosynthesis. *E. coli* lipid II and PBP1b (PDB ID: 3VMA) were adopted in this figure.

The active site of PGT is hydrophilic in nature, which interacts with the disaccharide-peptide unit of lipid II or the pentasaccharide moiety of MoeA, while the adjacent surface is hydrophobic, allowing it to immerse in the membrane surface [5]. The structure of PGT also revealed an exposed hydrophobic region close to the active site, which most likely engages in the interaction with the lipid chains of the substrate while it goes into the active site [5]. We therefore reason that an effective inhibitor of PGT is likely to be amphiphilic in nature and its hydrophobicity has to be designed in a well-balanced manner in order to maximize the interaction. As shown in Fig. 2, a small molecular fragment of guanidine-tagged isatin is selected to design an effective PGT inhibitor due to its known antibacterial and moderate PGT inhibitory activities [17-19], and a non-polar group (R) with adjustable length can be linked to the nitrogen atom of  $\gamma$ -lactam to tune its hydrophobicity. In this study, a new series of isatin-based amphiphilic PGT inhibitors were synthesized and their Quantitative Structure-Activity Relationship with respect to the substituent (R group) of the molecules was studied.

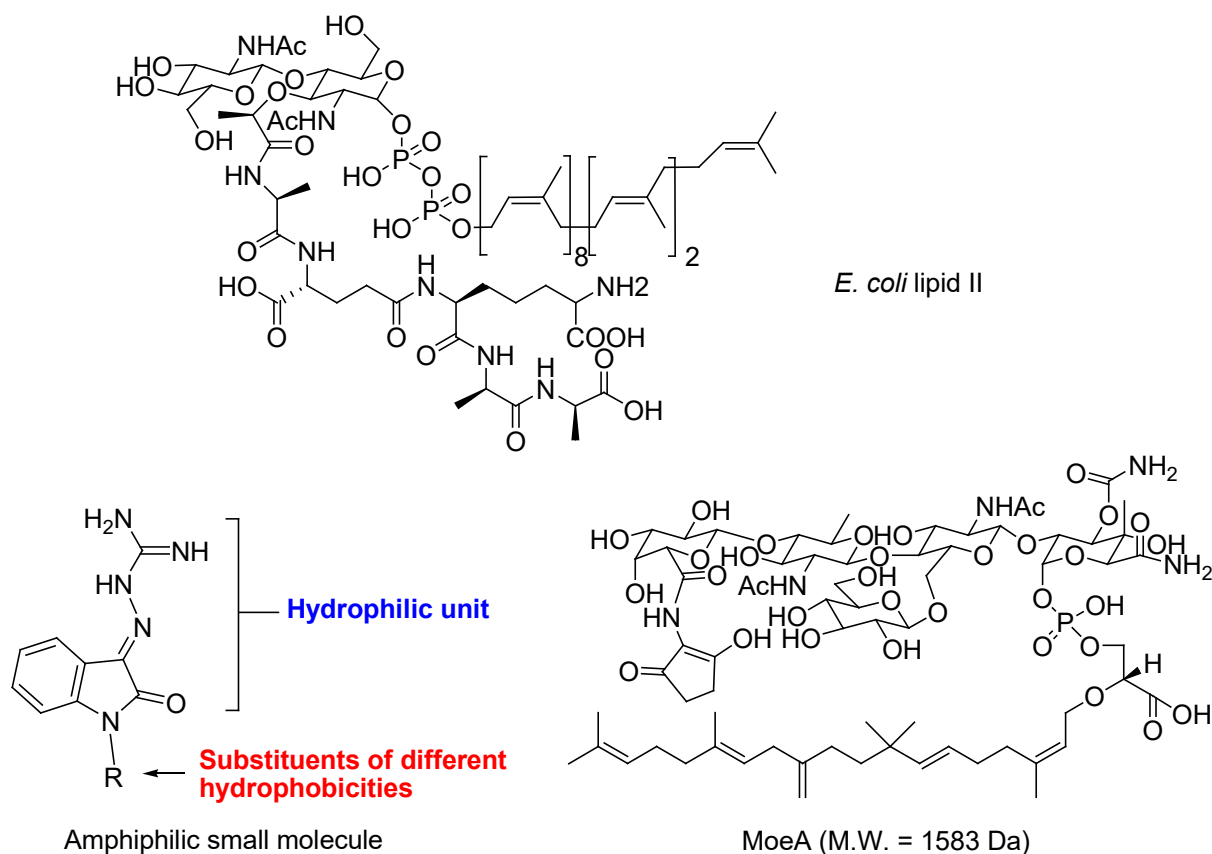


Fig. 2. Chemical structures of *E. coli* lipid II, MoeA and a guanidine-tagged isatin amphiphilic derivative.

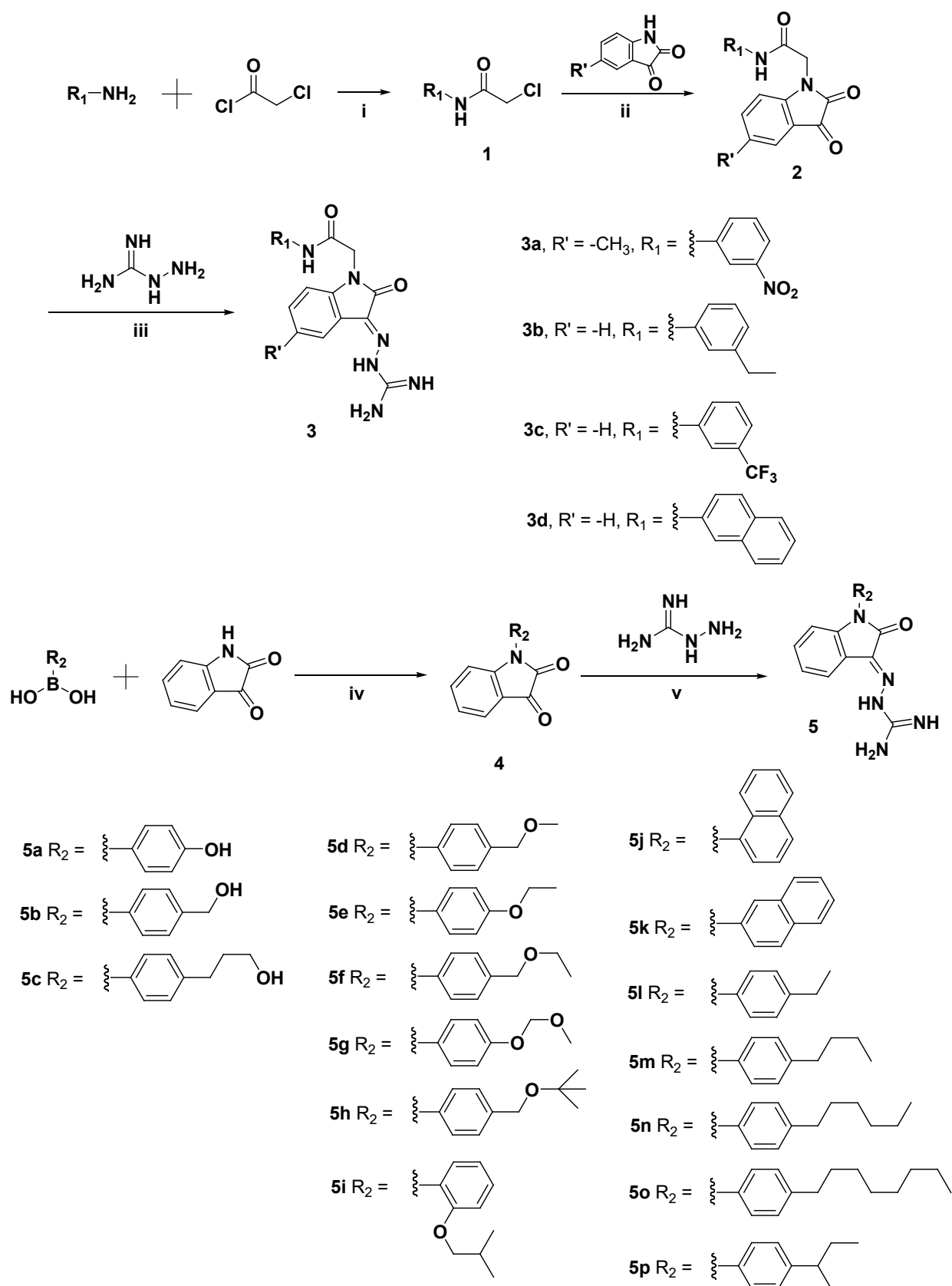
## 2. Results and discussions

### 2.1 Synthesis of inhibitors

Our previous study on isatin derivatives [19] as PGT inhibitors identified compound **3d** as a relatively potent inhibitor. We reasoned that the effectiveness of **3d** could be caused by a good balance of hydrophilicity and hydrophobicity between the polar aminoguanidine group and the non-polar naphthyl group. In order to explore the molecular hydrophilicity influence in the structure–activity relationship of PGT inhibitors in-depth, twenty new amphiphilic isatin-based inhibitors were systematically designed by regulating the hydrophobicity of the molecules via R group modifications. These small-molecular based inhibitors were synthesized through two different synthetic routes as shown in Scheme 1. For inhibitor **3a-3c**, they were synthesized similar to **3d** as previously reported [19] by reacting the primary amines with chloroacetyl chloride in acetonitrile to yield **1**, followed by the reaction with isatin or 5-methylisatin in DMF with potassium carbonate to form **2**. Compounds **3a-3d** were obtained by reacting **2** with aminoguanidine HCl in acetic acid as the solvent under reflux conditions. The compounds were purified by flash column chromatography and isolated with 52–61% yields.

Inhibitors **5a-5p** were synthesized by the Chan-Evans-Lam coupling reaction [20-22]. The intermediates **4** with a desirable substituent ( $R_2$  group) were prepared through the reaction of phenylboronic acids and isatin with  $Cu(OAc)_2$  as the catalyst. Compound **4** was reacted with aminoguanidine in acetic acid at room temperature to give **5a-5p**. The yields of **5a-5c** were very low in the reaction with aminoguanidine because esterification of acetic acid with the hydroxyl groups of **4** also occurred under reflux condition. However, this side reaction can be reduced significantly when the reaction is taken place under room temperature for 4 h. The isolated yields for the compound were 29-36 %, which is comparable with their analogues **5d-5p** (35-56 % yields).

As shown in Fig. 2, the overall hydrophobicity of the inhibitors can be tuned by varying the substituent (R group), which is able to maximize the interactions with PGT and to achieve higher inhibitory potency. In this series of compounds, 20 new inhibitors were systematically designed to acquire different hydrophobicity, in terms of averaged calculated LogP (cLogP) values estimated with four different reported calculation methods [23-26]. The averaged cLogP values of the compounds ranged from -1.9 to 4.4. The molecular structure and cLogP values are listed in Table 1 and S2. In general, compounds with the substituent R containing a terminal hydroxyl group showed lower averaged cLogP values, while those compounds possessing a terminal alkoxyl group showed medium averaged cLogP values whereas higher averaged cLogP values of compounds were obtained with a terminal alkyl group of different chain lengths.



Scheme 1. Synthetic routes of isatin derivatives. (i) MeCN, 3h; (ii) DMF,  $K_2CO_3$ , 80 °C, 12 h; (iii) acetic acid / reflux, 2 h; (iv)  $Cu(OAc)_2$ ,  $Et_3N$ ,  $CH_2Cl_2$ , 48 – 72 h; (v) acetic acid / room temperature, 4h.

## 2.2 Antimicrobial susceptible testing and their structure-activity relationship

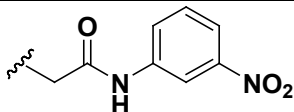
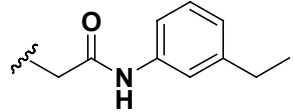
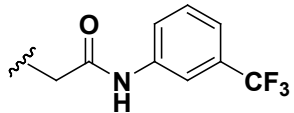
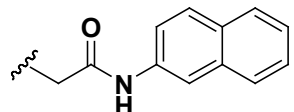
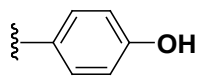
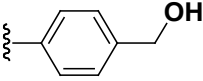
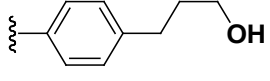
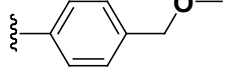
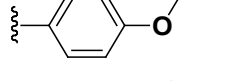
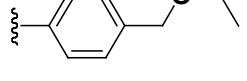
To study the structure-activity relationship between the R group (Fig. 2) of the isatin derivatives and their antibacterial potencies, their antibacterial activities targeting PGT were examined with Gram-positive *S. aureus*, *B. subtilis* and Gram-negative *E. coli*, including the methicillin-resistant *S. aureus* strain (ATCC BAA-41). The MIC results and averaged cLogP values are listed in Table 1. Starting with compounds with methanediylamidyl linkage conserved (**3a-3d**, Scheme 1), **3a** with a terminal *m*-nitrobenzyl group and its R' group replaced from hydro group to methyl group did not further improve the antibacterial activities compared to its parent molecule (R' = H), suggested that the R' of **3a** may not be a promising position for further modifications. However, **3c** showed slight improvement to the antibacterial activity on the 3 strains (24 µg/mL on *S. aureus*; 12 µg/mL on *B. subtilis* and 48 µg/mL on *E. coli*) while **3d** showed even better potencies on *S. aureus* (12 µg/mL), the rigid non-polar naphthyl group of **3d** should play an important role on the enhanced activities.

In compounds **5a-5p**, the substituent groups (R<sub>2</sub>) can be further categorized as polar hydroxyl (**5a – 5c**), polar alkoxyl (**5d – 5i**) and non-polar (**5j – 5p**) substituent groups (see Scheme 1), to offer a wide range of hydrophobicity for bioactivity comparison. MIC results (Table 1) showed that all compounds with polar hydroxyl and alkoxyl groups (except **5i**) had no significant antibacterial activities against both Gram-positive and Gram-negative bacteria. These results may indicate that both the hydroxyl and alkoxyl groups in the substituent cannot achieve a well-balanced hydrophobicity for the amphiphilic inhibitors. Interestingly, the antibacterial potencies increased significantly when we adopted non-polar side groups (**5j – 5p**). Considering **5j** and **5k**, both are naphthyl substituents, but **5k** (*m, p*-naphthyl) was 1-fold more potent than **5j** (*o, m*-naphthyl) against the two Gram-positive bacteria (*S. aureus* and *B. subtilis*). This may suggest that the branch at *para*-position of the phenyl ring was more potent than that at *ortho*-position. For **5l – 5p**, the compounds were analogues with different length of alkyl chains extended from the *ortho*-position of the phenyl ring of the substituent R<sub>2</sub>. **5l** with a 4-ethylphenyl substituent showed only moderate MICs, which are similar to that of **3a** and **5j**. However, when increasing the alkyl chain length (**5m**: *n* = 4), the antibacterial activities against Gram-positive bacteria were found improved drastically, MICs against *S. aureus* and *B. subtilis* were both lowered to 6 µg/mL. Interestingly, **5m** also showed good antibacterial activity against *E. coli* (12 µg/mL).

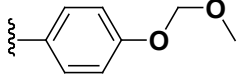
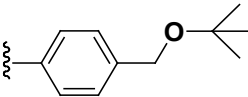
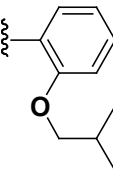
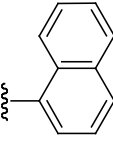
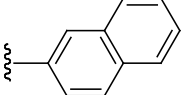
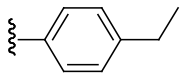
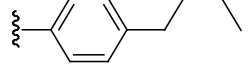
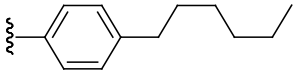
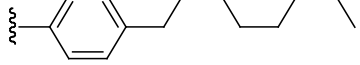
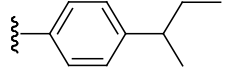
An attempt to further enhance the antibacterial activities by increasing the alkyl chain length from butyl to hexyl and octyl group, however, did not further improve the MIC against *S.*

*aureus*. These compounds even showed weaker activities against *E. coli* (MIC = 48 µg/mL for **5n** and > 96 µg/mL for **5o** compared to 12 µg/mL for **5m**) and the trend is obviously different from that of *S. aureus*. Similar observation has also been for MoeA, which showed excellent antibacterial activities against *S. aureus* and *B. subtilis* but no observable activity against *E. coli* because the high molecular mass MoeA cannot pass through the periplasmic region of the Gram negative bacteria [27]. We therefore postulated that the highly hydrophobic compounds (**5n** and **5o**) may behave in a similar manner as MoeA in that they may mainly stay within the outer membrane rather than diffusing into the periplasmic space. On the other hand, the much smaller periplasmic space between the inner membrane and the peptidoglycan layer in Gram-positive bacteria (*S. aureus* and *B. subtilis*) represents a much lower hindrance to the entrance of hydrophobic compounds. Based on the isatin-based compounds examined in this report, a suitable cLogP range of 2.3–4.4 was found for the PGT inhibitors.

**Table 1.** MIC values ( $\mu\text{g/mL}$ ) and averaged cLogP values of the small molecular inhibitors.

Compound	R group	<i>S. aureus</i> (ATCC 29213)	<i>S. aureus</i> (ATCC BAA-41)	<i>B. subtilis</i> 168	<i>E. coli</i> (ATCC 25922)	Averaged cLogP
3a		48	48	24	96	-1.90
3b		48	48	24	>96	1.53
3c		24	24	12	48	1.94
3d		12	12	12	> 96	1.85
5a		> 96	> 96	96	> 96	1.08
5b		> 96	> 96	> 96	> 96	1.10
5c		> 96	> 96	> 96	> 96	1.76
5d		> 96	> 96	> 96	> 96	1.64
5e		96	> 96	24	96	1.94
5f		> 96	> 96	96	> 96	2.00



<b>5g</b>		> 96	> 96	96	> 96	1.59
<b>5h</b>		96	96	48	> 96	2.39
<b>5i</b>		24	48	12	> 96	2.49
<b>5j</b>		48	48	24	48	2.38
<b>5k</b>		24	24	12	48	2.36
<b>5l</b>		48	48	12	48	2.20
<b>5m</b>		6	6	6	12	2.97
<b>5n</b>		6	6	6	48	3.69
<b>5o</b>		6	6	6	> 96	4.40
<b>5p</b>		6	6	3	48	2.90
<b>MoeA</b>	Not available	< 0.75	< 0.75	1.5	> 96	Not determined
<b>Ampicillin</b>	Not available	< 0.75	> 96	< 0.75	6	Not determined

### 2.3 Lipid II-based *in vitro* transglycosylation assay

To study the inhibitory effects of the new inhibitors against PGT, fluorescent lipid II-based transglycosylation inhibition assays were conducted using purified *E. coli* PBP1b [28] as the targeting enzyme. The reaction rate of transglycosylation was fast in Triton X-100 buffered solution and about 35 % lipid II (substrate) was consumed within 5 min (Fig. S3). Five inhibitors (**5d**, **5e**, **5l**, **5m** and **5o**) were selected for the inhibitory assays (Table 2). Interestingly, the IC<sub>50</sub> of the compounds are highly correlated to their MIC values.

**5d** has an extraordinary high IC<sub>50</sub> of 2156.1  $\mu$ M, indicated that it is virtually not a PGT inhibitor. This result is also consistent to its MIC values of > 96  $\mu$ g/mL obtained against 3 selected bacteria species, meaning that it has no observable antibacterial activities. A similar analogue **5e**, however, showed a more than 10-fold decrease in IC<sub>50</sub> (203.4  $\mu$ M). The difference of *in vitro* activities is reflected in the MIC value of *B. subtilis*, which was lowered to 24  $\mu$ g/mL. **5e** is practically not effective against *S. aureus* and *E. coli*. **5l**, **5m** and **5o** are analogues with non-polar substituents of different alkyl chain length ( $n = 2, 4$  and  $8$ , respectively). The IC<sub>50</sub> of **5l** is 125.2  $\mu$ M which is slightly lower than that of **5e**, at the same time its MIC values showed a 1-fold decrease against the 3 selected bacteria species; the IC<sub>50</sub> of **5m** is reduced to 82.8  $\mu$ M and its MICs were also significantly lowered to 6 mg/mL for *S. aureus* and *B. subtilis* and 12  $\mu$ g/mL for *E. coli* respectively. These results support that the inhibition effect of the compounds on PGT is closely related to their antibacterial activities.

Increase in the alkyl chain length of the compounds in general enhances the PGT inhibitory activity. Although **5o** has the lowest IC<sub>50</sub> (12.4  $\mu$ M) among the compounds, its antibacterial activities against Gram-positive bacteria did not further improve compared with that of **5m**. On the other hand, the MIC value against Gram-negative *E. coli* dropped significantly (> 96  $\mu$ g/mL). This inconsistency might be explained by its too high hydrophobicity (cLogP = 4.4). Its diffusion to the PGT target is hindered by the outer membrane of the Gram-negative bacteria. As a result, the antibacterial activity against *E. coli* is compromised regardless of its stronger PGT inhibition ability. The cytotoxicity of two representative compounds **3d** and **5m** was evaluated against human fibroblast cells (Detroit 551). Their IC<sub>50</sub> values were found to be 2.2 and 1.9  $\mu$ g/mL, respectively.

**Table 2.** *In-vitro* lipid II transglycosylation inhibitory constants (IC<sub>50</sub>) against *E. coli* PBP1b and MICs of some compounds.

Compound	IC <sub>50</sub> (μM)	<i>S. aureus</i> (ATCC BAA-41)	<i>B. subtilis</i> 168	<i>E. coli</i> (ATCC 25922)
<b>5d</b>	2156.1	> 96	> 96	> 96
<b>5e</b>	203.4	96	24	96
<b>5l</b>	125.2	48	12	48
<b>5m</b>	82.8	6	6	12
<b>5o</b>	12.4	6	6	> 96
Vancomycin*	1.01	N.D.	N.D.	N.D.

\*A positive control measurement with a reported value of 0.38 μM using a modified lipid II substrate [29].

## 2.4 Molecular modelling

From the results obtained, we reason that the small amphiphilic inhibitor **5m** is able to mimic certain properties of MoeA, in which the hydrophilic unit could bind to the active-site pocket of PGT whereas the alkyl chain could interact with the hydrophobic transmembrane region of the enzyme. The binding pose between *E. coli* PBP1b and **5m** was thus investigated by molecular docking using AutoDock Vina [30]. One of the interaction modes depicted in Fig. 3 showed that the hydrophilic guanidyl moiety (shown in blue-violet) is able to bind to the active site pocket of PGT, the same region occupied by the phosphate group of MoeA (shown in cyan), the well-known inhibitor of PGT. In addition, the hydrophobic unit of **5m** (4-butylphenyl group) points to the direction of the transmembrane domain of PBP1b. Detailed interaction between **5m** and individual residues of PGT are shown in Fig. S4.

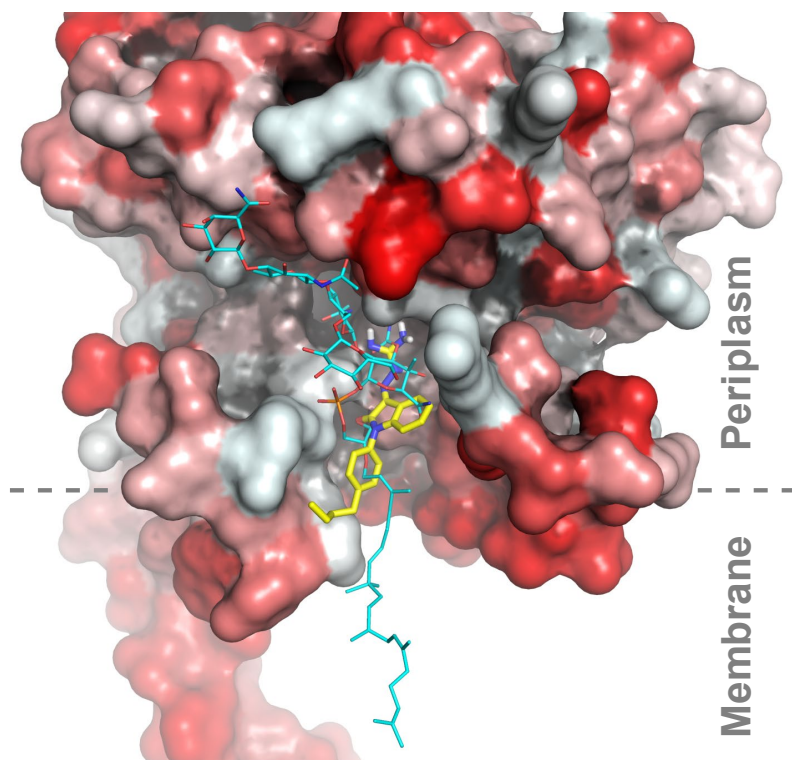


**Fig. 3.** Binding pose between MoeA (skeleton shown in cyan), **5m** (skeleton shown in yellow) and *E. coli* PBP1b model. The hydrophobic regions and hydrophilic regions of the PBP1b model were indicated in red and grey, respectively. One of the best interaction modes of **5m** bound with the hydrophilic active-site pocket (indicated in grey) of PGT was calculated (see Fig. S4 for details). The guanidyl moiety of **5m** overlapped with the phosphate moiety of MoeA, suggested that they competed the same active site pocket. The hydrophobic moiety of **5m** was pointing downward and in similar direction as transmembrane domain.

### 3. Conclusion

We demonstrated an amphiphilic approach to design potent inhibitors targeting at PGT. Our results showed that using guanidine-tagged isatin as the core scaffold accompanied by a hydrophobic group can lead to PGT inhibitors with broad-spectrum antibacterial activities against both Gram-positive and Gram-negative bacteria. The antibacterial activities of the amphiphilic inhibitors can be tuned by adjusting the overall hydrophobicity of the molecules. MICs of 6  $\mu\text{g/mL}$  for MSSA, MRSA and *B. subtilis* and 12  $\mu\text{g/mL}$  for *E. coli* (12  $\mu\text{g/mL}$ ) were obtained with an inhibitor **5m** of averaged cLogP value 2.97. Our findings suggest that an effective inhibitor of PGT should be amphiphilic in nature consisting of a hydrophilic moiety to interact with the active site of the enzyme and a hydrophobic group to interact with the transmembrane region of the enzyme as well as the plasma membrane which will assist the inhibitor molecule to approach the active-site pocket of PGT. Nevertheless, in order to maintain bioavailability, the hydrophobicity of the inhibitor molecule should not be too high to prevent it

from entering the bacterial cell. The molecular design of an effective PGT inhibitor should be a well balance of the hydrophilicity and hydrophobicity of the amphiphilic molecule.

#### 4. Acknowledgments

This work was supported by the General Research Fund of the Hong Kong Research Grants Council (PolyU 153338/16P), the Innovation and Technology Commission, the Ministry of Science and Technology of China, and The Hong Kong Polytechnic University. We gratefully acknowledged the support of the University Research Facilities on Life Sciences and Chemical and Environmental Analysis of The Hong Kong Polytechnic University. KYW acknowledged the support from the Patrick S.C. Poon endowed professorship.

### 5. Experimental

#### 5.1 Chemicals

Phenylboric acid derivatives, isatin, 5-methylisatin and aminoguanidine HCl were purchased from Aldrich. Dansyl-chloride was purchased from Sigma-Aldrich. Cell culture media were purchased from Oxoid; bacteria strains were purchased from American Type Culture Collection (ATCC). Moenomycin A (MoeA) was purified from flavomycin purchased from International Laboratory as described [31].

#### 5.2 Synthetic procedures for the new isatin-based inhibitors

Compounds **3a** – **3d** were obtained by following the reported procedures [19].

General procedures for the synthesis of compound **5a** – **5p**: To a mixture of phenylboronic acid (0.30 mmol), isatin (0.33 mmol), copper(II) acetate (0.30 mmol) and triethylamine (125  $\mu$ L) in dichloromethane (10 mL), dried molecular sieve (4 $\text{\AA}$ ) was added. The mixture was then allowed to react with stirring for 60 h at room temperature. Excessive isatin was removed by silica gel chromatography using a mobile phase of ethyl acetate: petroleum ether = 1:4. Some vacuum dried product (0.15 mmol) was further reacted with aminoguanidine HCl salt (0.27 mmol) with acetic acid (20 mL) as the solvent. The reaction mixture was allowed to stir for 2 h at room temperature. The crude products were precipitated by the addition of diethyl ether (200 mL) into the reaction mixture and were collected by filtration. The pure product was isolated as a yellowish solid after the purification with silica gel chromatography using a mobile phase of methanol: dichloromethane = 1: 4.

**5.2.1 (E)-2-(3-(2-carbamimidoylhydrazineylidene)-5-methyl-2-oxoindolin-1-yl)-N-(3-nitrophenyl)acetamide (3a):** The reaction was taken place for 23 h. Isolated yield 52 %. <sup>1</sup>H NMR (400 MHz, CD<sub>3</sub>OD) δ: 2.40 (s, 3H, Ar-CH<sub>3</sub>), 4.73 (s, 2H), 6.97 (d, *J* = 8.1 Hz, 1H), 7.31 (d, *J* = 7.6 Hz, 1H), 7.59 (t, *J* = 8.2 Hz, 1H), 7.66 (s, 1H), 7.92 (d, *J* = 8.1 Hz, 1H), 8.02 (d, *J* = 8.1 Hz, 1H), 8.61 (s, 1H). <sup>13</sup>C NMR (125 MHz, CD<sub>3</sub>OD) δ: 21.01, 30.74, 44.00, 110.76, 115.50, 119.88, 120.40, 123.28, 126.63, 131.10, 134.02, 134.88, 138.66, 140.63, 142.83, 149.88, 162.79, 167.60. HRMS calculated for C<sub>18</sub>H<sub>18</sub>N<sub>7</sub>O<sub>4</sub>: *m/z*: 396.1415 [M+H]<sup>+</sup>, found 396.1405.

**5.2.2 (E)-2-(3-(2-carbamimidoylhydrazineylidene)-2-oxoindolin-1-yl)-N-(3-ethylphenyl)acetamide (3b):** The reaction was taken place for 23 h. Isolated yield 56 %. <sup>1</sup>H NMR (400 MHz, CD<sub>3</sub>OD) δ: 1.23 (t, *J* = 7.6 Hz, 3H), 2.64 (q, *J* = 7.6 Hz, 2H), 4.71 (s, 2 H), 7.00 (d, *J* = 8.1 Hz, 1H), 7.09 (d, *J* = 8.0 Hz, 1H), 7.23 (q, *J* = 7.5 Hz, 2H), 7.38 - 7.43 (m, 2H), 7.51 (t, *J* = 7.9, 1H), 7.82 (d, *J* = 7.5 Hz, 1H). <sup>13</sup>C NMR (125 MHz, CD<sub>3</sub>OD) δ: 16.05, 29.86, 43.60, 111.01, 112.31, 118.62, 120.64, 122.97, 124.12, 124.82, 125.28, 129.90, 133.76, 139.21, 144.57, 146.49, 157.67, 162.80, 166.82. HRMS calculated for C<sub>19</sub>H<sub>21</sub>N<sub>6</sub>O<sub>2</sub>: *m/z*: 365.1721 [M+H]<sup>+</sup>; found 365.1732.

**5.2.3 (E)-2-(3-(2-carbamimidoylhydrazineylidene)-2-oxoindolin-1-yl)-N-(3-(trifluoromethyl)phenyl)acetamide (3c):** The reaction was taken place for 23 h. Isolated yield 61 %. <sup>1</sup>H NMR (400 MHz, CD<sub>3</sub>OD) δ: 4.75 (s, 2H), 7.10 (d, *J* = 8.0 Hz, 1H), 7.23 (t, *J* = 7.6 Hz, 1H), 7.43 – 7.45 (m, 1H), 7.49 - 7.57 (m, 2H), 7.78-7.84 (m, 2H), 8.01 (s, 1H). <sup>13</sup>C NMR (125 MHz, CD<sub>3</sub>OD) δ: 43.65, 111.02, 117.49, 120.37, 121.90, 122.90, 124.24, 124.88, 130.93, 132.14, 132.40, 133.73, 138.64, 140.18, 145.19, 157.67, 162.80, 167.27. HRMS calculated for C<sub>18</sub>H<sub>16</sub>F<sub>3</sub>N<sub>6</sub>O<sub>2</sub>: *m/z*: 405.1281 [M+H]<sup>+</sup>, found 405.1289.

**5.2.4 (E)-2-(3-(2-carbamimidoylhydrazineylidene)-2-oxoindolin-1-yl)-N-(naphthalen-2-yl)acetamide (3d):** The reaction was taken place for 23 h. Isolated yield 62 %. <sup>1</sup>H NMR (400 MHz, CD<sub>3</sub>OD) δ: 4.78 (s, 2H), 7.13 (d, *J* = 7.9 Hz, 1H), 7.24 (t, *J* = 7.6 Hz, 1H), 7.41 - 7.54 (m, 3H), 7.59 (d, *J* = 8.9, 1H), 7.77-7.87 (m, 4H), 8.20 (s, 1H). <sup>13</sup>C NMR (125 MHz, CD<sub>3</sub>OD) δ: 43.68, 111.06, 118.01, 120.40, 121.00, 122.88, 124.84, 126.28, 127.63, 128.57, 128.63, 129.76, 132.29, 133.72, 135.18, 136.74, 139.86, 145.29, 147.29, 162.83, 167.07. HRMS calculated for C<sub>21</sub>H<sub>19</sub>N<sub>6</sub>O<sub>2</sub>: *m/z*: 387.1564 [M+H]<sup>+</sup>, found 387.1573.

**5.2.5 (E)-2-(1-(4-hydroxyphenyl)-2-oxoindolin-3-ylidene)hydrazine-1-carboximidamide (5a):**

The reaction was taken place for 64 h. Isolated yield 32 %.  $^1\text{H}$  NMR (400 MHz,  $\text{CD}_3\text{OD}$ )  $\delta$ : 6.83 (d,  $J = 8.0$  Hz, 1H), 7.00 (d,  $J = 8.8$  Hz, 2H), 7.21 (t,  $J = 7.6$  Hz, 1H), 7.28 (d,  $J = 8.8$  Hz, 2H), 7.44 (t,  $J = 7.6$  Hz, 1H), 7.84 (d,  $J = 7.2$  Hz, 1H).  $^{13}\text{C}$  NMR (125 MHz,  $\text{CD}_3\text{OD}$ )  $\delta$ : 111.54, 117.40, 120.27, 122.87, 124.89, 125.45, 129.17, 133.57, 138.84, 146.60, 157.68, 159.30, 162.17. HRMS calculated for  $\text{C}_{15}\text{H}_{14}\text{N}_5\text{O}_2$ :  $m/z$ : 296.1142  $[\text{M}+\text{H}]^+$ , found 296.1161.

*5.2.5 (E)-2-(1-(4-(hydroxymethyl)phenyl)-2-oxoindolin-3-ylidene)hydrazine-1-*

*carboximidamide (5b)*: The reaction was taken place for 64 h. Isolated yield 29 %.  $^1\text{H}$  NMR (400 MHz,  $\text{CD}_3\text{OD}$ )  $\delta$ : 4.73 (s, 2H), 6.90 (d,  $J = 8.0$  Hz, 1H), 7.24 (t,  $J = 7.5$  Hz, 1H), 7.43 - 7.50 (m, 3H), 7.58 - 7.62 (m, 2H), 7.86 (d,  $J = 7.4$  Hz, 1H).  $^{13}\text{C}$  NMR (125 MHz,  $\text{CD}_3\text{OD}$ )  $\delta$ : 64.52, 111.49, 120.53, 122.92, 125.03, 127.63, 129.18, 133.22, 133.42, 138.52, 143.88, 145.92, 157.95, 161.85. HRMS calculated for  $\text{C}_{16}\text{H}_{16}\text{N}_5\text{O}_2$ :  $m/z$ : 310.1299  $[\text{M}+\text{H}]^+$ , found 310.1301.

*5.2.7 (E)-2-(1-(4-(3-hydroxypropyl)phenyl)-2-oxoindolin-3-ylidene)hydrazine-1-*

*carboximidamide (5c)*: The reaction was taken place for 64 h. Isolated yield 36 %.  $^1\text{H}$  NMR (400 MHz,  $\text{CD}_3\text{OD}$ )  $\delta$ : 1.92 (quin,  $J = 7.1$  Hz, 2H), 2.82 (t,  $J = 7.6$  Hz, 2H), 3.64 (t,  $J = 6.2$  Hz, 2H), 6.90 (d,  $J = 8.0$  Hz, 1H), 7.24 (t,  $J = 7.6$  Hz, 1H), 7.40 - 7.49 (m, 5H), 7.86 (d,  $J = 7.2$  Hz, 1H).  $^{13}\text{C}$  NMR (125 MHz,  $\text{CD}_3\text{OD}$ )  $\delta$ : 32.80, 35.35, 62.10, 111.53, 120.35, 123.02, 125.03, 127.60, 130.91, 131.95, 133.54, 138.65, 144.65, 146.07, 157.62, 161.92. HRMS calculated for  $\text{C}_{18}\text{H}_{20}\text{N}_5\text{O}_2$ :  $m/z$ : 338.1612  $[\text{M}+\text{H}]^+$ , found 338.1614.

*5.2.8 (E)-2-(1-(4-(methoxymethyl)phenyl)-2-oxoindolin-3-ylidene)hydrazine-1-*

*carboximidamide (5d)*: The reaction was taken place for 64 h. Isolated yield 41 %.  $^1\text{H}$  NMR (400 MHz,  $\text{CD}_3\text{OD}$ )  $\delta$ : 3.46 (s, 3H), 4.58 (s, 2H), 6.91 (d,  $J = 8.4$  Hz, 1H), 7.24 (t,  $J = 7.6$ , 1H), 7.43 - 7.51 (m, 3H), 7.59 - 7.61 (m, 2H), 7.86 (d,  $J = 7.2$ , 1H).  $^{13}\text{C}$  NMR (125 MHz,  $\text{CD}_3\text{OD}$ )  $\delta$ : 58.59, 74.89, 111.51, 120.52, 122.96, 125.06, 127.62, 130.03, 133.44, 133.63, 138.50, 140.63, 145.84, 157.84, 161.82. HRMS calculated for  $\text{C}_{17}\text{H}_{18}\text{N}_5\text{O}_2$ :  $m/z$ : 324.1455  $[\text{M}+\text{H}]^+$ , found 324.1453.

*5.2.9 (E)-2-(1-(4-ethoxyphenyl)-2-oxoindolin-3-ylidene)hydrazine-1-carboximidamide (5e)*:

The reaction was taken place for 64 h. Isolated yield 42 %.  $^1\text{H}$  NMR (400 MHz,  $\text{CD}_3\text{OD}$ )  $\delta$ : 1.45 (t,  $J = 7.0$  Hz, 3H), 4.14 (q,  $J = 6.9$  Hz, 2H), 6.84 (d,  $J = 8.0$  Hz, 1H), 7.12 (d,  $J = 8.4$ , 2H), 7.22 (t,  $J = 7.6$  Hz, 1H), 7.38 - 7.45 (m, 3H), 7.84 (d,  $J = 7.2$ , 1H).  $^{13}\text{C}$  NMR (125 MHz,  $\text{CD}_3\text{OD}$ )  $\delta$ : 15.08, 64.94, 111.51, 116.58, 120.34, 122.88, 124.93, 126.56, 129.11, 133.54,

138.77, 146.44, 157.73, 160.69, 162.11. HRMS calculated for  $C_{17}H_{18}N_5O_2$ :  $m/z$ : 324.1455  $[M+H]^+$ , found 324.1454.

**5.2.10 (E)-2-(1-(4-(ethoxymethyl)phenyl)-2-oxoindolin-3-ylidene)hydrazine-1-carboximidamide (5f):** The reaction was taken place for 64 h. Isolated yield 41 %.  $^1H$  NMR (400 MHz,  $CD_3OD$ )  $\delta$ : 1.28 (t,  $J = 7.0$  Hz, 3H), 3.64 (q,  $J = 7.0$  Hz, 2H), 4.63 (s, 2H), 6.91 (d,  $J = 8.0$  Hz, 1H), 7.24 (t,  $J = 7.6$ , 1H), 7.43 - 7.51 (m, 3H), 7.59 - 7.61 (m, 2H), 7.86 (d,  $J = 7.8$ , 1H).  $^{13}C$  NMR (125 MHz,  $CD_3OD$ )  $\delta$ : 15.48, 67.09, 72.93, 111.57, 120.42, 123.02, 125.08, 127.61, 130.00, 133.52, 133.58, 138.67, 141.04, 145.98, 157.64, 161.91. HRMS calculated for  $C_{18}H_{20}N_5O_2$ :  $m/z$ : 338.1612  $[M+H]^+$ , found 338.1614.

**5.2.11 (E)-2-(1-(4-(methoxymethoxy)phenyl)-2-oxoindolin-3-ylidene)hydrazine-1-carboximidamide (5g):** The reaction was taken place for 64 h. Isolated yield 35 %.  $^1H$  NMR (400 MHz,  $CD_3OD$ )  $\delta$ : 3.52 (s, 3H), 5.29 (s, 2H), 6.86 (d,  $J = 8.0$  Hz, 1H), 7.20 - 7.28 (m, 3H), 7.40 - 7.46 (m, 3H), 7.84 (d,  $J = 7.6$ , 1H).  $^{13}C$  NMR (125 MHz,  $CD_3OD$ )  $\delta$ : 56.37, 95.54, 114.48, 118.39, 120.37, 122.90, 124.97, 127.78, 129.08, 133.50, 138.61, 146.21, 157.79, 158.85, 162.02. HRMS calculated for  $C_{17}H_{18}N_5O_3$ :  $m/z$ : 340.1404  $[M+H]^+$ , found 340.1407.

**5.2.12 (E)-2-(1-(4-(tert-butoxymethyl)phenyl)-2-oxoindolin-3-ylidene)hydrazine-1-carboximidamide (5h):** The reaction was taken place for 64 h. Isolated yield 42 %.  $^1H$  NMR (400 MHz,  $CD_3OD$ )  $\delta$ : 1.35 (s, 9H), 4.60 (s, 2H), 6.90 (d,  $J = 8.0$  Hz, 1H), 7.24 (t,  $J = 7.6$  Hz, 1H), 7.43 - 7.48 (m, 3H), 7.59 - 7.61 (m, 2H), 7.86 (d,  $J = 7.6$  Hz, 1H).  $^{13}C$  NMR (125 MHz,  $CD_3OD$ )  $\delta$ : 26.61, 63.29, 73.82, 110.23, 119.04, 121.68, 123.74, 126.16, 128.52, 131.81, 132.25, 137.34, 140.94, 144.69, 156.28, 160.57. HRMS calculated for  $C_{20}H_{24}N_5O_2$ :  $m/z$ : 366.1925  $[M+H]^+$ , found 366.1926.

**5.2.13 (E)-2-(1-(2-isobutoxyphenyl)-2-oxoindolin-3-ylidene)hydrazine-1-carboximidamide (5i):** The reaction was taken place for 64 h. Isolated yield 48 %.  $^1H$  NMR (400 MHz,  $CD_3OD$ )  $\delta$ : 0.79 [m, 6H], 1.85 [m, 1H], 3.79 [m, 2H], 6.59 (d,  $J = 8.0$  Hz, 1H), 7.14 - 7.26 (m, 3H), 7.40 - 7.41 (m, 2H), 7.54 (t,  $J = 8.0$  Hz, 1H), 7.84 (d,  $J = 7.2$  Hz, 1H).  $^{13}C$  NMR (125 MHz,  $CD_3OD$ )  $\delta$ : 19.25, 19.27, 29.36, 75.81, 111.97, 114.57, 120.09, 122.13, 122.54, 122.75, 124.81, 130.66, 132.29, 133.60, 138.58, 146.58, 156.250, 157.69, 162.30. HRMS calculated for  $C_{19}H_{22}N_5O_2$ :  $m/z$ : 352.1768  $[M+H]^+$ , found 352.1768.



5.2.14 (*E*)-2-(1-(naphthalen-1-yl)-2-oxoindolin-3-ylidene)hydrazine-1-carboximidamide (**5j**):

The reaction was taken place for 62 h. Isolated yield 55 %. <sup>1</sup>H NMR (400 MHz, CD<sub>3</sub>OD) δ: 6.42 (d, *J* = 7.9 Hz, 1H), 7.23 (t, *J* = 7.5 Hz, 1H), 7.34 (t, *J* = 7.4 Hz, 1H), 7.50 - 7.71 (m, 5H), 7.92 (d, *J* = 7.4 Hz, 1H), 8.06 (d, *J* = 8.2, 1H), 8.11 (d, *J* = 8.2, 1H). <sup>13</sup>C NMR (125 MHz, CD<sub>3</sub>OD) δ: 118.83, 120.46, 123.02, 123.58, 125.07, 126.97, 127.64, 128.05, 128.50, 129.86, 130.66, 131.01, 131.37, 133.67, 136.24, 138.63, 146.88, 157.74, 162.54. HRMS calculated for C<sub>19</sub>H<sub>16</sub>N<sub>5</sub>O: *m/z*: 330.1349 [M+H]<sup>+</sup>, found 330.1362.

5.2.15 (*E*)-2-(1-(naphthalen-2-yl)-2-oxoindolin-3-ylidene)hydrazine-1-carboximidamide (**5k**):

The reaction was taken place for 62 h. Isolated yield 50 %. <sup>1</sup>H NMR (400 MHz, CD<sub>3</sub>OD) δ: 6.90 (d, *J* = 7.9 Hz, 1H), 7.22 (t, *J* = 7.5 Hz, 1H), 7.40 (t, *J* = 7.7 Hz, 1H), 7.51 - 7.58 (m, 3H), 7.85 - 8.04 (m, 5H). <sup>13</sup>C NMR (125 MHz, CD<sub>3</sub>OD) δ: 111.68, 120.51, 123.03, 124.99, 125.15, 126.66, 128.11, 128.24, 128.99, 129.09, 130.89, 131.69, 133.60, 134.42, 135.02, 138.70, 146.06, 157.70, 162.06. HRMS calculated for C<sub>19</sub>H<sub>16</sub>N<sub>5</sub>O: *m/z*: 330.1349 [M+H]<sup>+</sup>, found 330.1364.

5.2.16 (*E*)-2-(1-(4-ethylphenyl)-2-oxoindolin-3-ylidene)hydrazine-1-carboximidamide (**5l**):

The reaction was taken place for 62 h. Isolated yield 55 %. <sup>1</sup>H NMR (400 MHz, CD<sub>3</sub>OD) δ: 1.29 (t, 3H, *J* = 7.6 Hz), 2.74 (q, 2H, *J* = 7.6 Hz), 6.84 (d, *J* = 8.0 Hz, 1H), 7.20 (t, *J* = 7.5 Hz, 1H), 7.35 - 7.43 (m, 5H), 7.84 (d, *J* = 7.5, 1H). <sup>13</sup>C NMR (125 MHz, CD<sub>3</sub>OD) δ: 16.08, 29.60, 111.58, 120.39, 122.95, 125.00, 127.64, 130.30, 131.85, 133.55, 138.73, 146.17, 146.69, 157.69, 161.96. HRMS calculated for C<sub>17</sub>H<sub>18</sub>N<sub>5</sub>O: *m/z*: 308.1506 [M+H]<sup>+</sup>, found 308.1521.

5.2.17 (*E*)-2-(1-(4-butylphenyl)-2-oxoindolin-3-ylidene)hydrazine-1-carboximidamide (**5m**):

The reaction was taken place for 62 h. Isolated yield 54 %. <sup>1</sup>H NMR (400 MHz, CD<sub>3</sub>OD) δ: 0.97 (t, 3H, *J* = 7.4 Hz), 1.40 (m, 2H), 1.65 (m, 2H), 2.70 (t, *J* = 7.5 Hz, 2H), 6.83 (d, *J* = 8.0 Hz, 1H), 7.20 (t, *J* = 7.6 Hz, 1H), 7.33 - 7.41 (m, 5H), 7.83 (d, *J* = 7.5 Hz, 1H). <sup>13</sup>C NMR (125 MHz, CD<sub>3</sub>OD) δ: 14.10, 23.16, 34.59, 36.10, 111.31, 120.18, 122.79, 124.83, 127.22, 130.57, 131.57, 133.20, 138.14, 144.90, 145.65, 157.53, 161.55. HRMS calculated for C<sub>19</sub>H<sub>22</sub>N<sub>5</sub>O: *m/z*: 336.1819 [M+H]<sup>+</sup>, found 336.1830.

5.2.18 (*E*)-2-(1-(4-hexylphenyl)-2-oxoindolin-3-ylidene)hydrazine-1-carboximidamide (**5n**):

The reaction was taken place for 62 h. Isolated yield 52 %. <sup>1</sup>H NMR (400 MHz, CD<sub>3</sub>OD) δ: 0.94 (t, 3H, *J* = 6.9 Hz), 1.38 (m, 6H), 1.70 (m, 2H), 2.74 (t, *J* = 7.7 Hz, 2H), 6.89 (d, *J* = 8.0 Hz, 1H), 7.23 (t, *J* = 7.5 Hz, 1H), 7.38-7.46 (m, 5H), 7.85 (d, *J* = 7.5, 1H). <sup>13</sup>C NMR (125 MHz,

CD<sub>3</sub>OD)  $\delta$ : 14.42, 23.69, 30.04, 32.62, 32.88, 36.62, 111.36, 122.54, 124.02, 124.80, 127.59, 130.81, 132.10, 133.48, 138.12, 143.41, 144.45, 145.13, 161.63. HRMS calculated for C<sub>21</sub>H<sub>26</sub>N<sub>5</sub>O: m/z: 364.2132 [M+H]<sup>+</sup>, found 364.2145.

**5.2.19 (E)-2-(1-(4-octylphenyl)-2-oxoindolin-3-ylidene)hydrazine-1-carboximidamide (5o):** The reaction was taken place for 62 h. Isolated yield 46 %. <sup>1</sup>H NMR (400 MHz, CD<sub>3</sub>OD)  $\delta$ : 0.90 (t, 3H, *J* = 6.7 Hz), 1.30 - 1.36 (m, 10H), 1.68 (m, 2H), 2.71 (t, *J* = 7.6, 2H), 6.85 (d, *J* = 8.0 Hz, 1H), 7.20 (t, *J* = 7.5 Hz, 1H), 7.38 - 7.42 (m, 5H), 7.83 (d, *J* = 7.4, 1H). <sup>13</sup>C NMR (125 MHz, CD<sub>3</sub>OD)  $\delta$ : 14.44, 23.72, 30.35, 30.41, 30.58, 32.64, 33.04, 36.61, 111.59, 120.36, 122.97, 125.01, 127.52, 130.85, 131.83, 133.57, 138.74, 145.29, 146.16, 157.63, 161.96. HRMS calculated for C<sub>23</sub>H<sub>30</sub>N<sub>5</sub>O: m/z: 392.2445 [M+H]<sup>+</sup>, found 392.2465.

**5.2.20 (E)-2-(1-(4-(sec-butyl)phenyl)-2-oxoindolin-3-ylidene)hydrazine-1-carboximidamide (5p):** The reaction was taken place for 62 h. Isolated yield 56 %. <sup>1</sup>H NMR (400 MHz, CD<sub>3</sub>OD)  $\delta$ : 0.90 (t, *J* = 7.4 Hz, 3H), 1.32 (d, *J* = 7.2 Hz, 3H), 1.70 (m, 2H), 2.74 (m, 1H), 6.90 (d, *J* = 8.0 Hz, 1H), 7.23 (t, *J* = 7.6 Hz, 1H), 7.41 - 7.47 (m, 5H), 7.86 (d, *J* = 7.2 Hz, 1H). <sup>13</sup>C NMR (125 MHz, CD<sub>3</sub>OD)  $\delta$ : 12.58, 22.32, 32.16, 42.84, 111.55, 120.44, 122.92, 124.98, 127.55, 129.49, 131.98, 133.46, 138.59, 146.04, 149.94, 157.80, 161.89. HRMS calculated for C<sub>19</sub>H<sub>22</sub>N<sub>5</sub>O: m/z: 366.1819 [M+H]<sup>+</sup>, found 366.1814.

### 5.3 Antimicrobial susceptible testing

To prepare fresh bacteria media, frozen stock bacterial strains were streaked on a TSA plate and incubated at 37 °C overnight. A single colony was picked and added to corresponding media and grew at 37 °C for 5 h at 250 rpm. Working bacterial culture solutions were prepared by further diluting 2  $\mu$ L of the grown media into 5 mL fresh media. The working bacterial culture solutions were used immediately. Minimum inhibitory concentrations (MICs) were conducted using broth micro-dilution method as described [19]. Three bacterial strains were used in this experiment: MSSA (ATCC 29213), MRSA (ATCC BAA-41), *B. subtilis* 168 and *E. coli* (ATCC 25922). MHB was the medium for *B. subtilis* and *E. coli*, CA-MHB was the medium for *S. aureus*.

### 5.4 Over-expression and purification of *E. coli* PBP1b

*E. coli* PBP1b (residues 58 - 604) was expressed and purified as described [5] without the second purification step (size exclusion). The (His)<sub>6</sub>-tag was retained after purification. The

final protein concentration was measured by Bradford assay using bovine serum albumin as reference protein.

### 5.5 Lipid II-based *in vitro* transglycosylation assay

Lipid II was prepared as described [32]. Dansyl fluorophore was attached to lipid II for spectroscopic detection (see structure and mass spectrum of dansyl-lipid II in Fig. S5) [33]. *E. coli* PBP1b and compounds were pre-incubated at 30 °C for 15 min in reaction buffer (50 mM HEPES pH 7.5, 200 mM NaCl, 10 mM CaCl<sub>2</sub>) with additional 0.04 % Triton X-100, 25 % DMSO and 1 U/μL muramidase. Dansyl-lipid II (working concentration 2 μM) was then added into reaction mixture and mixed well to initiate the reaction. The reaction was allowed to stand for 5 min at 30 °C, and MoeA (working concentration 15 μM) was added to quench the reaction. The mixtures were stored at -80 °C before HPLC analysis as described [33, 34]. 20 μL of samples were injected into an Agilent 1200 series equipped with a Supelco SAX1 anion-exchange column and eluted using a gradient of NH<sub>4</sub>OAc/MeOH (20 mM to 500 mM). Half maximal inhibitory concentrations (IC<sub>50</sub>) of selected compounds were calculated by GraphPad Prism 7 with the model:  $Y=1/(1+10^{((\text{LogIC}_{50}-X)*h)})$  (Y, normalized response; X, log[inhibitor]; h, hillslope). The Dose-response curve for *in vitro* transglycosylation inhibition assays were shown in Fig. S2. The isatin-based compounds were measured in triplicate while vancomycin (positive control) was measured in duplicate, and half maximal inhibitory concentrations (IC<sub>50</sub>) were calculated as described [16]. HPLC chromatograms of *in vitro* transglycosylation assay of **5m** were shown in Fig. S1.

### 5.6 Molecular modelling

The docking study was using a *E. coli* PBP1b model built based on a protein crystal structure of *E. coli* PBP1b (PBP ID: 3VMA [5]) with the missing residues 241-246 and 252-266 added by Modeller [35] and Coot with reference to other PGT crystal structures (PBP ID: 3FWL [5], 3NB6 [36], 2OQO [37] and 6FTB [38]). The missing tail of MoeA in 3VMA was replenished based on the MoeA ligand from 6FTB, and was adjusted to point into the membrane (cyan, Fig. 3 of the main text).

Molecular model of the PGT domain of *E. coli* PBP1b in the presence of **5m** was performed using AutoDock Vina [30]. The structure of **5m** was drawn and 3D coordinates were generated by ChemDraw Ultra 8.0. Energy of **5m** was minimized by Avogadro with Merck Molecular Force Field 94 (MMFF94) [39]. PBP1b and **5m** were treated by reported procedures [40], the interaction between the hydrocarbon moiety and membrane did not count. The best mode with

**5m** bound to active-site of PGT domain was selected for reporting. Results were shown in Fig. 3 and Fig. S4.

### 5.7 Cytotoxicity

Human fibroblast cells (Detroit 551) (American Type Culture Collection) were grown in Eagle's Minimum Essential Medium with 10% fetal bovine serum at 37°C in a humidified atmosphere of 5% CO<sub>2</sub> in the air. Cells were seeded at ~5000 cells per well in 96-well plates and allowed to settle overnight. The compounds were diluted into the growth medium with stated concentrations and the plates were incubated for 3 days. Quantitative cell proliferation assays were performed using the 3-(4,5-dimethylthiazol-2-yl)-2,5-diphenyltetrazolium bromide (MTT) reagent according to the instructions provided by the manufacturer. Three independent experiments were performed in triplicate.

## References

- [1] WHO report on surveillance of antibiotic consumption: 2016-2018 early implementation, (2018).
- [2] J. O'Neill, Tackling drug-resistant infections globally: final report and recommendations, The Review on Antimicrobial Resistance, (2016).
- [3] B. Ostash, S. Walker, Bacterial transglycosylase inhibitors, *Curr Opin Chem Biol*, 9 (2005) 459-466.
- [4] C.Y. Huang, H.W. Shih, L.Y. Lin, Y.W. Tien, T.J. Cheng, W.C. Cheng, C.H. Wong, C. Ma, Crystal structure of *Staphylococcus aureus* transglycosylase in complex with a lipid II analog and elucidation of peptidoglycan synthesis mechanism, *Proc Natl Acad Sci U S A*, 109 (2012) 6496-6501.
- [5] M.T. Sung, Y.T. Lai, C.Y. Huang, L.Y. Chou, H.W. Shih, W.C. Cheng, C.H. Wong, C. Ma, Crystal structure of the membrane-bound bifunctional transglycosylase PBP1b from *Escherichia coli*, *Proc Natl Acad Sci U S A*, 106 (2009) 8824-8829.
- [6] A.L. Lovering, L.H. de Castro, D. Lim, N.C.J. Strynadka, Structural insight into the transglycosylation step of bacterial cell-wall biosynthesis, *Science*, 315 (2007) 1402-1405.
- [7] X.Y. Ye, M.C. Lo, L. Brunner, D. Walker, D. Kahne, S. Walker, Better substrates for bacterial transglycosylases, *J Am Chem Soc*, 123 (2001) 3155-3156.
- [8] L.Y. Huang, S.H. Huang, Y.C. Chang, W.C. Cheng, T.J. Cheng, C.H. Wong, Enzymatic synthesis of lipid II and analogues, *Angew Chem Int Ed Engl*, 53 (2014) 8060-8065.
- [9] Y. Qiao, V. Srisuknimit, F. Rubino, K. Schaefer, N. Ruiz, S. Walker, D. Kahne, Lipid II overproduction allows direct assay of transpeptidase inhibition by beta-lactams, *Nat Chem Biol*, 13 (2017) 793-798.
- [10] J.G. Taylor, X. Li, M. Oberthur, W. Zhu, D.E. Kahne, The total synthesis of moenomycin A, *J Am Chem Soc*, 128 (2006) 15084-15085.
- [11] Y. Rebets, T. Lupoli, Y. Qiao, K. Schirner, R. Villet, D. Hooper, D. Kahne, S. Walker, Moenomycin resistance mutations in *Staphylococcus aureus* reduce peptidoglycan chain length and cause aberrant cell division, *ACS Chem Biol*, 9 (2014) 459-467.
- [12] B. Ostash, S. Walker, Moenomycin family antibiotics: chemical synthesis, biosynthesis, and biological activity, *Nat Prod Rep*, 27 (2010) 1594-1617.

- [13] T.J.R. Cheng, M.T. Sung, H.Y. Liao, Y.F. Chang, C.W. Chen, C.Y. Huang, L.Y. Chou, Y.D. Wu, Y. Chen, Y.S.E. Cheng, C.H. Wong, C. Ma, W.C. Cheng, Domain requirement of moenomycin binding to bifunctional transglycosylases and development of high-throughput discovery of antibiotics, *P Natl Acad Sci USA*, 105 (2008) 431-436.
- [14] C.M. Gampe, H. Tsukamoto, E.H. Doud, S. Walker, D. Kahne, Tuning the moenomycin pharmacophore to enable discovery of bacterial cell wall synthesis inhibitors, *J Am Chem Soc*, 135 (2013) 3776-3779.
- [15] J. Zuegg, C. Muldoon, G. Adamson, D. McKeveney, G. Le Thanh, R. Premraj, B. Becker, M. Cheng, A.G. Elliott, J.X. Huang, M.S. Butler, M. Bajaj, J. Seifert, L. Singh, N.F. Galley, D.I. Roper, A.J. Lloyd, C.G. Dowson, T.J. Cheng, W.C. Cheng, D. Demon, E. Meyer, W. Meutermans, M.A. Cooper, Carbohydrate scaffolds as glycosyltransferase inhibitors with in vivo antibacterial activity, *Nat Commun*, 6 (2015) 7719.
- [16] I. Sosic, M. Anderluh, M. Sova, M. Gobec, I.M. Rascan, A. Derouaux, A. Amoroso, M. Terrak, E. Breukink, S. Gobec, Structure-Activity Relationships of Novel Tryptamine-Based Inhibitors of Bacterial Transglycosylase, *J Med Chem*, 58 (2015) 9712-9721.
- [17] A. Medvedev, O. Buneeva, V. Glover, Biological targets for isatin and its analogues: Implications for therapy, *Biologics*, 1 (2007) 151-162.
- [18] S.K. Sridhar, M. Saravanan, A. Ramesh, Synthesis and antibacterial screening of hydrazones, Schiff and Mannich bases of isatin derivatives, *Eur J Med Chem*, 36 (2001) 615-625.
- [19] Y. Wang, F.Y. Chan, N. Sun, H.K. Lui, P.K. So, S.C. Yan, K.F. Chan, J. Chiou, S. Chen, R. Abagyan, Y.C. Leung, K.Y. Wong, Structure-based design, synthesis, and biological evaluation of isatin derivatives as potential glycosyltransferase inhibitors, *Chem Biol Drug Des*, 84 (2014) 685-696.
- [20] D.M.T. Chan, K.L. Monaco, R.P. Wang, M.P. Winters, New N- and O-arylations with phenylboronic acids and cupric acetate, *Tetrahedron Lett*, 39 (1998) 2933-2936.
- [21] D.A. Evans, J.L. Katz, T.R. West, Synthesis of diaryl ethers through the copper-promoted arylation of phenols with arylboronic acids. An expedient synthesis of thyroxine, *Tetrahedron Lett*, 39 (1998) 2937-2940.
- [22] P.Y.S. Lam, C.G. Clark, S. Saubern, J. Adams, M.P. Winters, D.M.T. Chan, A. Combs, New aryl/heteroaryl C-N bond cross-coupling reactions via arylboronic acid cupric acetate arylation, *Tetrahedron Lett*, 39 (1998) 2941-2944.
- [23] A. Daina, O. Michielin, V. Zoete, iLOGP: a simple, robust, and efficient description of n-octanol/water partition coefficient for drug design using the GB/SA approach, *J Chem Inf Model*, 54 (2014) 3284-3301.
- [24] T. Cheng, Y. Zhao, X. Li, F. Lin, Y. Xu, X. Zhang, Y. Li, R. Wang, L. Lai, Computation of octanol-water partition coefficients by guiding an additive model with knowledge, *J Chem Inf Model*, 47 (2007) 2140-2148.
- [25] S.A. Wildman, G.M. Crippen, Prediction of physicochemical parameters by atomic contributions, *J Chem Inf Comp Sci*, 39 (1999) 868-873.
- [26] I. Moriguchi, S. Hirono, Q. Liu, I. Nakagome, Y. Matsushita, Simple Method of Calculating Octanol Water Partition-Coefficient, *Chem Pharm Bull*, 40 (1992) 127-130.
- [27] E.R. Baizman, A.A. Branstrom, C.B. Longley, N. Allanson, M.J. Sofia, D. Gange, R.C. Goldman, Antibacterial activity of synthetic analogues based on the disaccharide structure of moenomycin, an inhibitor of bacterial transglycosylase, *Microbiol-Uk*, 146 (2000) 3129-3140.
- [28] W.L. Cheong, M.S. Tsang, P.K. So, W.H. Chung, Y.C. Leung, P.H. Chan, Fluorescent TEM-1 beta-lactamase with wild-type activity as a rapid drug sensor for in vitro drug screening, *Bioscience Rep*, 34 (2014) 523-533.
- [29] L. Chen, D. Walker, B. Sun, Y. Hu, S. Walker, D. Kahne, Vancomycin analogues active against vanA-resistant strains inhibit bacterial transglycosylase without binding substrate, *Proc Natl Acad Sci U S A*, 100 (2003) 5658-5663.

- [30] O. Trott, A.J. Olson, AutoDock Vina: improving the speed and accuracy of docking with a new scoring function, efficient optimization, and multithreading, *J Comput Chem*, 31 (2010) 455-461.
- [31] M. Adachi, Y. Zhang, C. Leimkuhler, B. Sun, J.V. LaTour, D.E. Kahne, Degradation and reconstruction of moenomycin A and derivatives: dissecting the function of the isoprenoid chain, *J Am Chem Soc*, 128 (2006) 14012-14013.
- [32] E. Breukink, H.E. van Heusden, P.J. Vollmerhaus, E. Swiezewska, L. Brunner, S. Walker, A.J.R. Heck, B. de Kruijff, Lipid II is an intrinsic component of the pore induced by nisin in bacterial membranes, *J Biol Chem*, 278 (2003) 19898-19903.
- [33] B. Schwartz, J.A. Markwalder, S.P. Seitz, Y. Wang, R.L. Stein, A kinetic characterization of the glycosyltransferase activity of *Eschericia coli* PBP1b and development of a continuous fluorescence assay, *Biochemistry-US*, 41 (2002) 12552-12561.
- [34] C.Y. Liu, C.W. Guo, Y.F. Chang, J.T. Wang, H.W. Shih, Y.F. Hsu, C.W. Chen, S.K. Chen, Y.C. Wang, T.J. Cheng, C. Ma, C.H. Wong, J.M. Fang, W.C. Cheng, Synthesis and evaluation of a new fluorescent transglycosylase substrate: lipid II-based molecule possessing a dansyl-C20 polyprenyl moiety, *Org Lett*, 12 (2010) 1608-1611.
- [35] B. Webb, A. Sali, Comparative Protein Structure Modeling Using MODELLER, *Curr Protoc Bioinformatics*, 54 (2016) 5 6 1-5 6 37.
- [36] S. Fuse, H. Tsukamoto, Y. Yuan, T.S. Wang, Y. Zhang, M. Bolla, S. Walker, P. Sliz, D. Kahne, Functional and structural analysis of a key region of the cell wall inhibitor moenomycin, *ACS Chem Biol*, 5 (2010) 701-711.
- [37] Y. Yuan, D. Barrett, Y. Zhang, D. Kahne, P. Sliz, S. Walker, Crystal structure of a peptidoglycan glycosyltransferase suggests a model for processive glycan chain synthesis, *Proc Natl Acad Sci U S A*, 104 (2007) 5348-5353.
- [38] A.S. Punekar, F. Samsudin, A.J. Lloyd, C.G. Dowson, D.J. Scott, S. Khalid, D.I. Roper, The role of the jaw subdomain of peptidoglycan glycosyltransferases for lipid II polymerization, *Cell Surf*, 2 (2018) 54-66.
- [39] M.D. Hanwell, D.E. Curtis, D.C. Lonie, T. Vandermeersch, E. Zurek, G.R. Hutchison, Avogadro: an advanced semantic chemical editor, visualization, and analysis platform, *J Cheminform*, 4 (2012) 17.
- [40] G.M. Morris, R. Huey, W. Lindstrom, M.F. Sanner, R.K. Belew, D.S. Goodsell, A.J. Olson, AutoDock4 and AutoDockTools4: Automated docking with selective receptor flexibility, *J Comput Chem*, 30 (2009) 2785-2791.

**Hydrophobic Substituents on Isatin Derivatives Enhance Their Inhibition against Bacterial  
Peptidoglycan Glycosyltransferase Activity**

Yong Wang<sup>‡a</sup>, Wing-Lam Cheong<sup>‡a</sup>, Zhiguang Liang<sup>a</sup>, Lok-Yan So<sup>a</sup>, Kin-Fai Chan<sup>a</sup>, Pui-Kin So<sup>a</sup>,  
Yu Wai Chen<sup>a</sup>, Wing-Leung Wong<sup>a</sup> and Kwok-Yin Wong<sup>\*,a</sup>

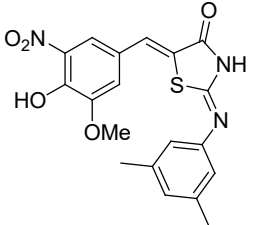
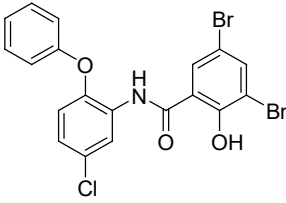
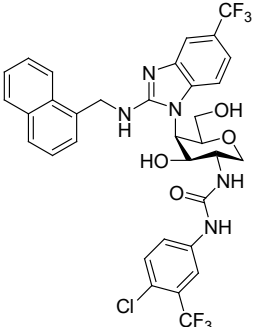
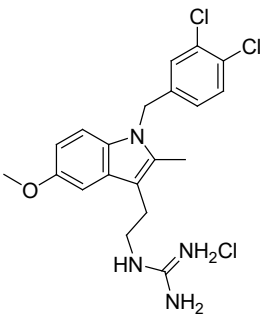
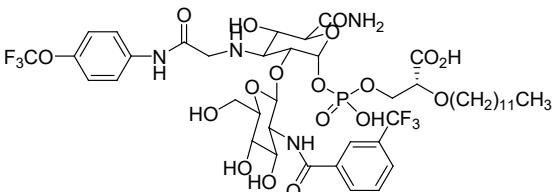
State Key Laboratory of Chemical Biology and Drug Discovery, Department of Applied Biology  
and Chemical Technology, The Hong Kong Polytechnic University, Hung Hom, Kowloon, Hong  
Kong, P. R. China.

<sup>‡</sup> The authors contributed equally to this work.

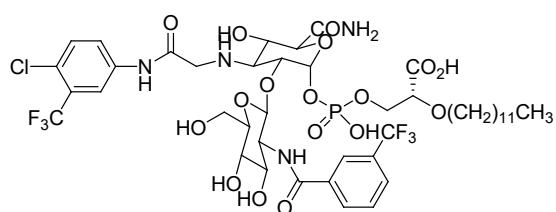
\* Corresponding author

E-mail: kwok-yin.wong@polyu.edu.hk

Table S1. List of some reported PGT binding compounds and the evaluation of their cLogP values and inhibitory potencies.

PGT binding compound	cLogP	MIC ( $\mu\text{g/mL}$ )		IC <sub>50</sub> ( $\mu\text{M}$ )
		<i>S. aureus</i> (ATCC 29213)	<i>E. coli</i> (ATCC 25922)	<i>E. coli</i> PBP1b
	2.98	16	NA	79
Reported by Daniel Kahne's group [1]				
	5.28	1	> 512	37.5
Reported by Chi-Huey Wong's group [2]				
	5.38	4 (ATCC 25923)	> 64	NA
Reported by Matthew A. Cooper's group [3]				
	3.92	4 (ATCC 25923)	32 (ATCC 8739)	39
Reported by Stanislav Gobec's group [4]				
	2.46	6.25	NA	NA



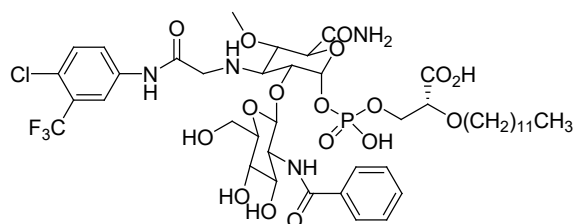


3.08

6.25-12.5

NA

NA



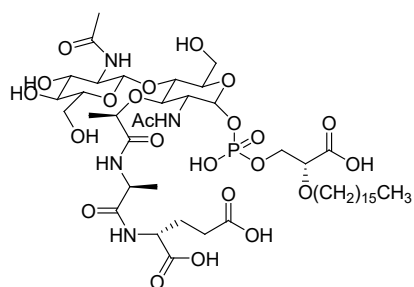
2.74

12.5

NA

NA

Reported by Robert C. Goldman's group [5]



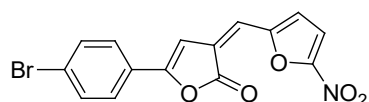
0.21

NA  
(128 for *B. subtilis* 168)

NA

NA

Reported by Mohammed Terrak's group [6]

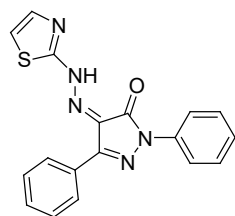


3.22

1.0

NA

34.00\*

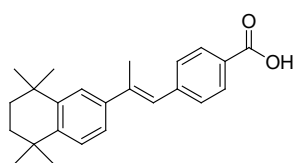


3.04

4.0

NA

3.70\*



5.77

&gt; 4.0

NA

9.30\*

Reported by Wei-Chieh Cheng's group [7]

\*IC<sub>50</sub> were calculated using lipid II-free fluorescence anisotropy assay

Table S2. Averaged cLogP values of the small molecular inhibitors.

Compound	iLOGP	XLOGP3	WLOGP	MLOGP	SILICOS-IT	Average <sup>a</sup>
<b>3a</b>	-11.22	1.39	0.92	0.29	-0.90	-1.90
<b>3b</b>	1.39	2.46	0.85	1.35	1.61	1.53
<b>3c</b>	1.14	2.54	2.46	1.73	1.81	1.94
<b>3d</b>	1.55	2.91	1.44	1.62	1.74	1.85
<b>5a</b>	0.78	1.96	0.88	1.11	0.69	1.08
<b>5b</b>	1.42	1.43	0.51	1.09	1.07	1.10
<b>5c</b>	2.06	2.25	1.10	1.57	1.84	1.76
<b>5d</b>	2.12	1.96	1.17	1.34	1.60	1.64
<b>5e</b>	2.29	2.65	1.57	1.60	1.60	1.94
<b>5f</b>	2.53	2.33	1.56	1.57	1.99	2.00
<b>5g</b>	2.21	2.23	1.15	1.22	1.15	1.59
<b>5h</b>	2.17	2.95	2.33	2.03	2.45	2.39
<b>5i</b>	2.33	3.62	2.21	2.07	2.21	2.49
<b>5j</b>	1.38	3.56	2.32	2.42	2.20	2.38
<b>5k</b>	1.28	3.56	2.32	2.42	2.20	2.36
<b>5l</b>	1.95	3.11	1.73	2.14	2.06	2.20
<b>5m</b>	2.73	4.19	2.51	2.61	2.84	2.97
<b>5n</b>	3.21	5.28	3.29	3.06	3.63	3.69
<b>5o</b>	3.65	6.36	4.07	3.49	4.43	4.40
<b>5p</b>	2.56	3.98	2.68	2.61	2.67	2.90

<sup>a</sup> Averaged cLogP values were calculated by SwissADME tool [8] as consensus cLogP<sub>o/w</sub> based on 4 different calculations: iLOGP [9]; XLOGP3 [10]; WLOGP [11]; MLOGP [12] and SILICOS-IT (version 1.0.2, 2013, <http://silicos-it.be.s3-website-eu-west-1.amazonaws.com/software/filter-it/1.0.2/filter-it.html>).

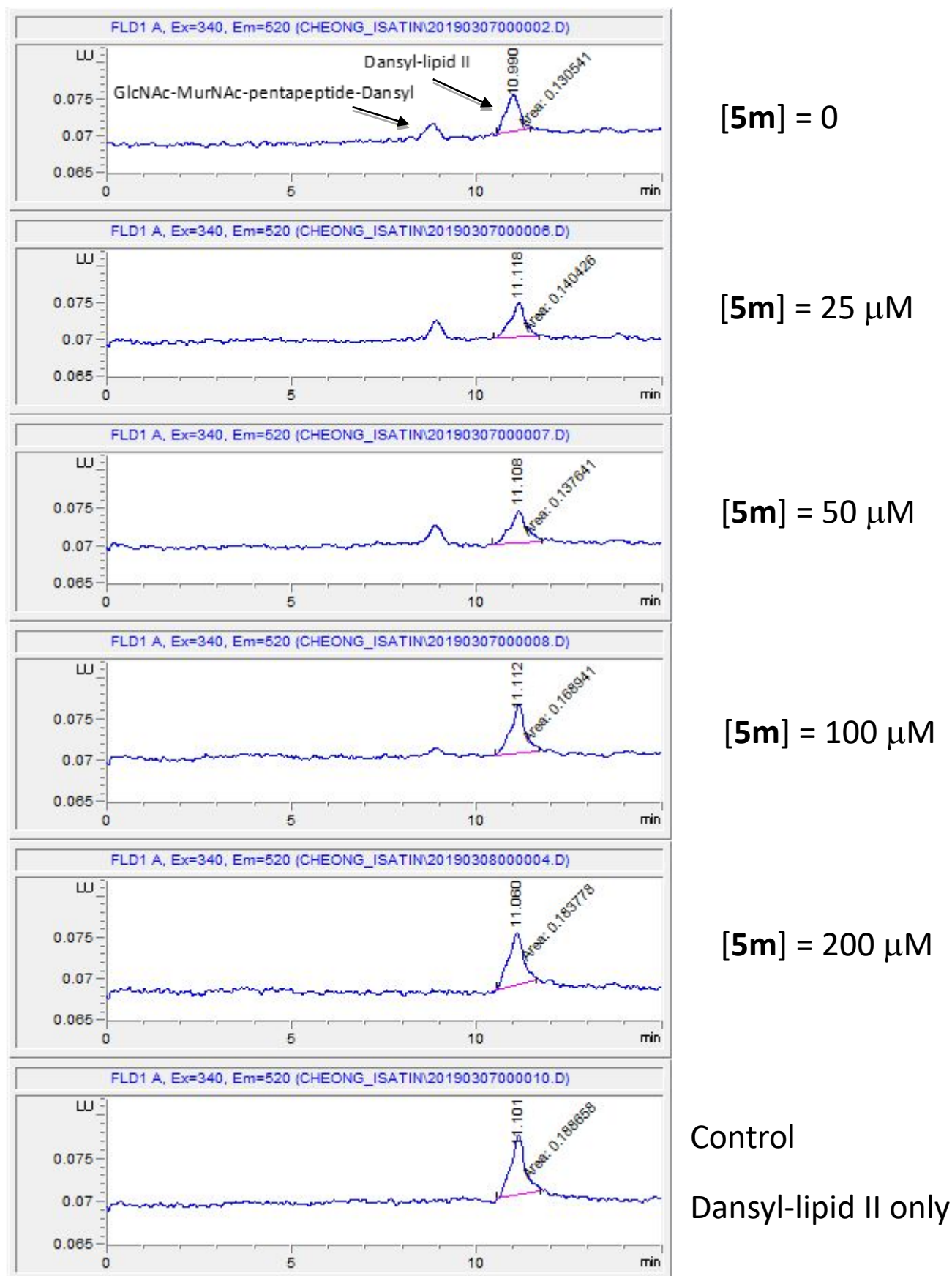
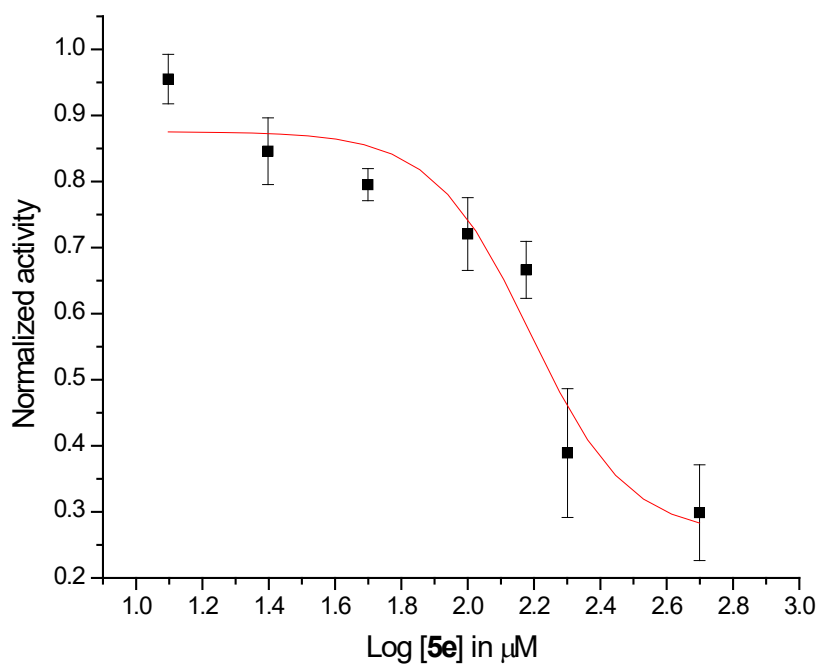
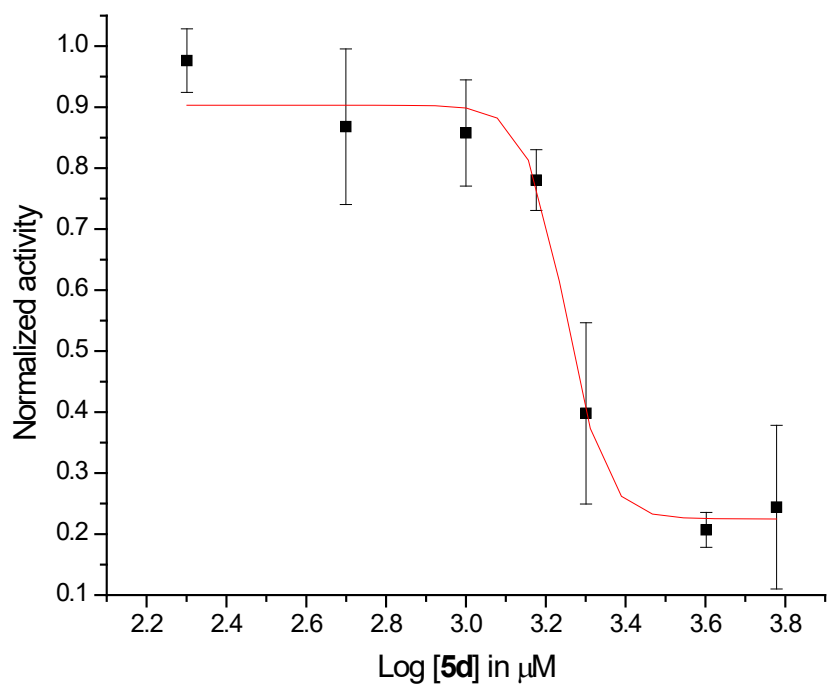
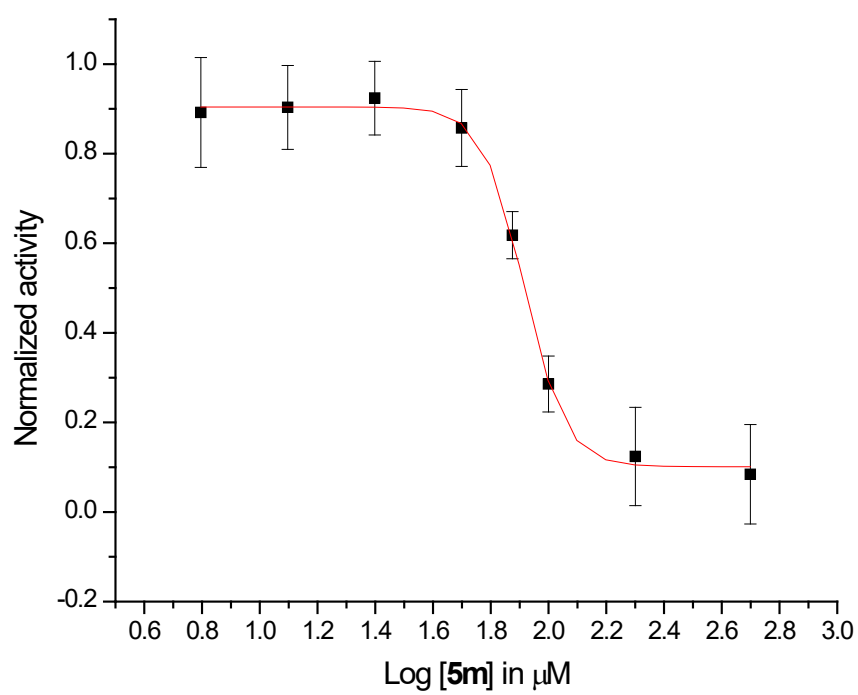
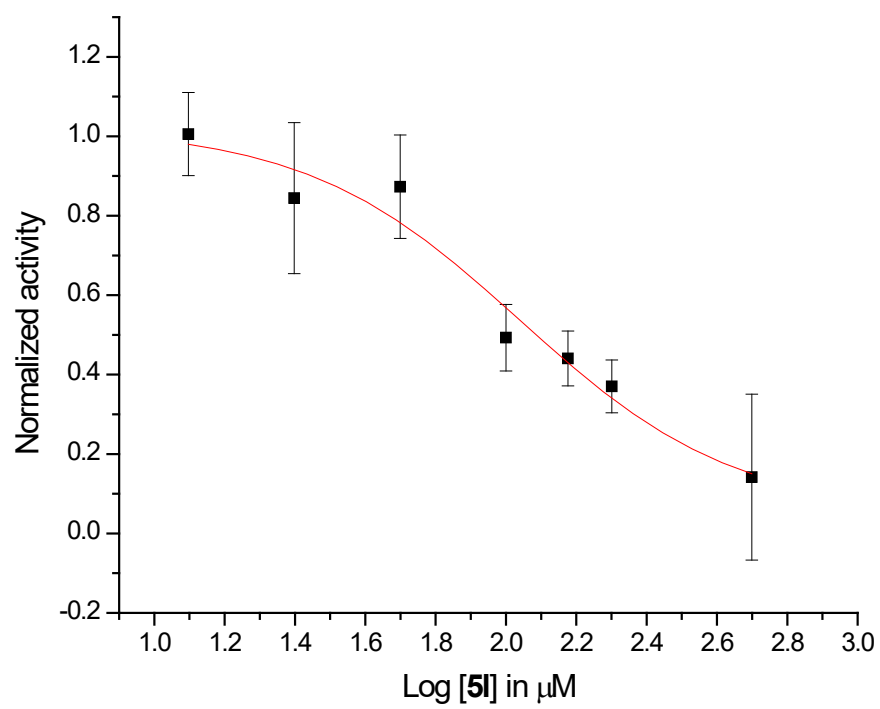


Fig. S1. HPLC chromatograms of *in vitro* transglycosylation assay in the presence of different concentrations of **5m**. *E. coli* PBP1b (200 nM) and dansyl-lipid II (2  $\mu$ M) was allowed to react in buffer (50 mM HEPES pH 7.5, 200 mM NaCl, 10 mM CaCl<sub>2</sub>, 0.04 % Triton X-100, 25 % DMSO and 1 U/ $\mu$ L muramidase) for 5 min. Reactions were quenched by adding 5  $\mu$ L of 300  $\mu$ M MoeA.





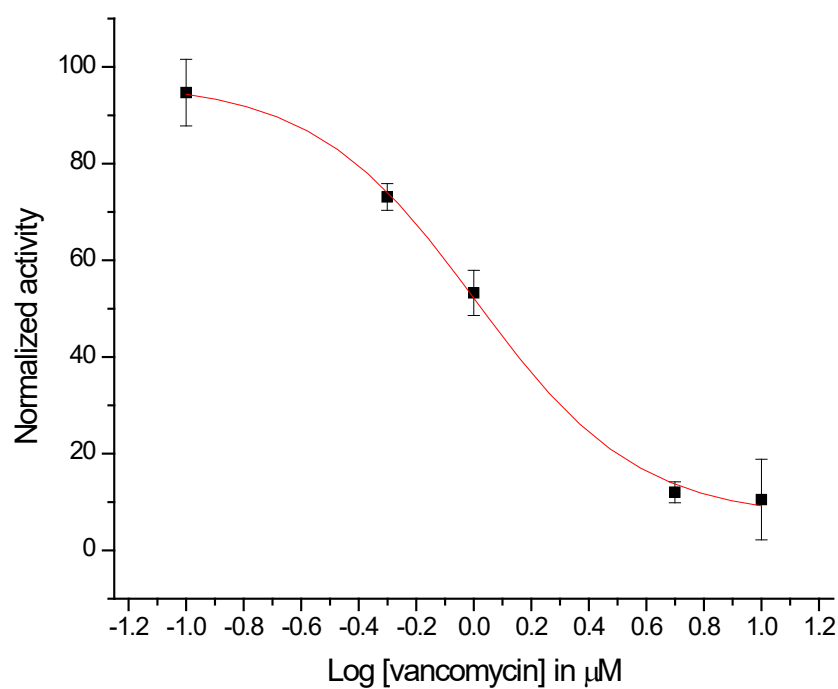
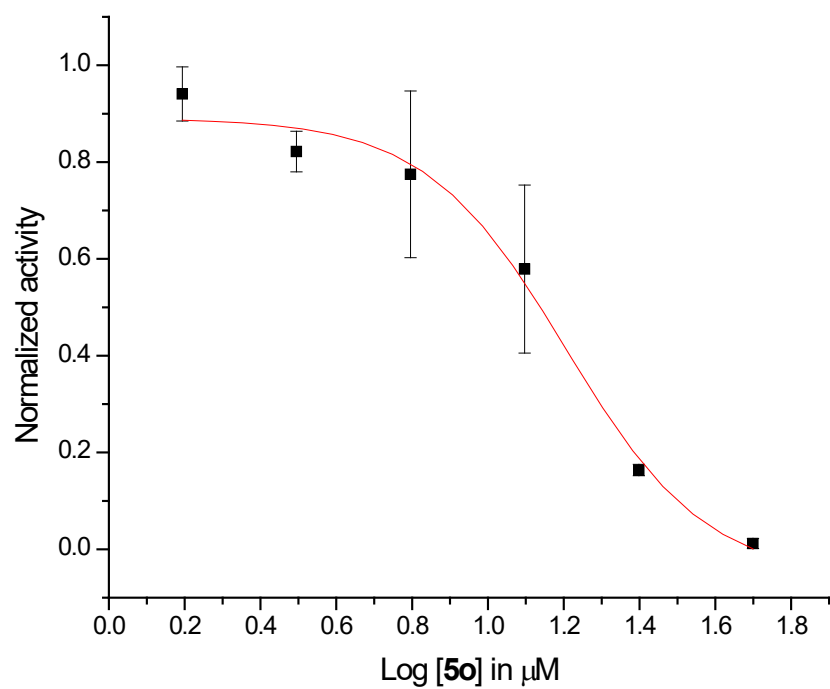


Fig. S2. Dose-response curve for *in vitro* transglycosylation inhibition assay in the presence of inhibitor (**5d**, **5e**, **5l**, **5m**, **5o**) and vancomycin (positive control), respectively. IC<sub>50</sub> of vancomycin was calculated to be  $1.01 \pm 0.11 \mu\text{M}$ , which was similar to reported value of  $0.38 \mu\text{M}$  using a modified lipid II substrate [13].

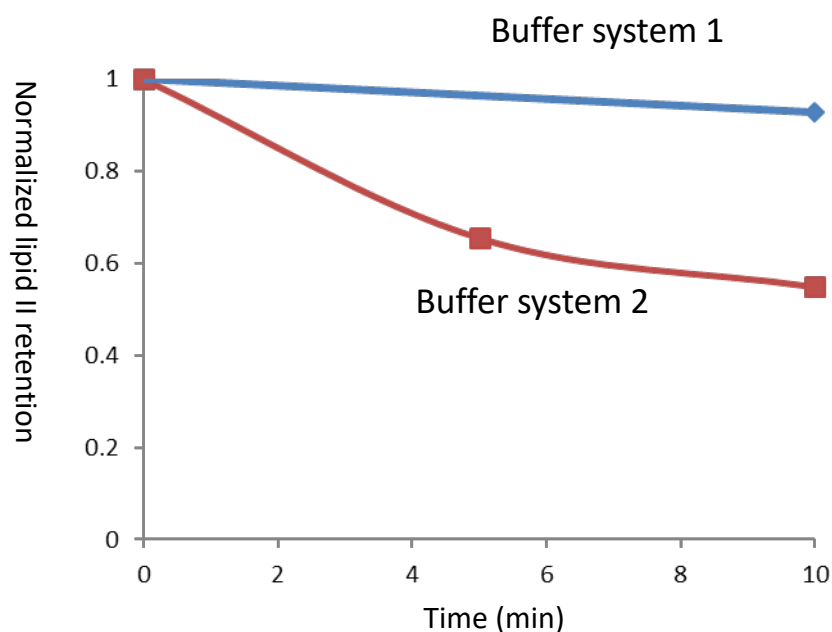
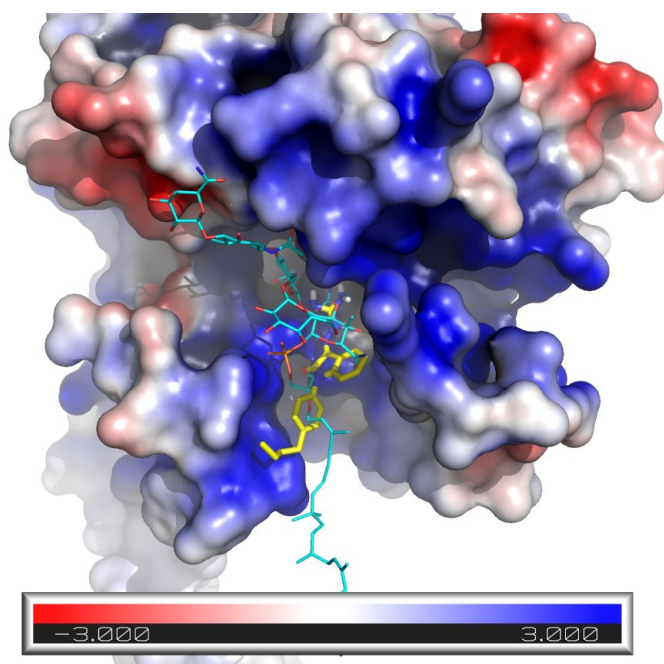


Fig. S3. Reaction rate study for *in vitro* transglycosylation inhibition assay using 2 different solvent systems. Buffer system 1: HEPES (50 mM, pH 7.5), NaCl (200 mM), CaCl<sub>2</sub> (10mM), with decyl PEG (0.085 %), DMSO (10 %), methanol (15 %) and muramidase (0.2 U/μL); buffer system 2: HEPES (50 mM, pH 7.5), NaCl (200 mM), CaCl<sub>2</sub> (10 mM) with Triton X-100 (0.04 %), DMSO (25 %) and muramidase (0.2 U/μL). A tangent line can be drawn at 5 min reaction time using buffer system 2, so it was selected as the reaction buffer in the transglycosylation inhibition assay.

(a)



(b)

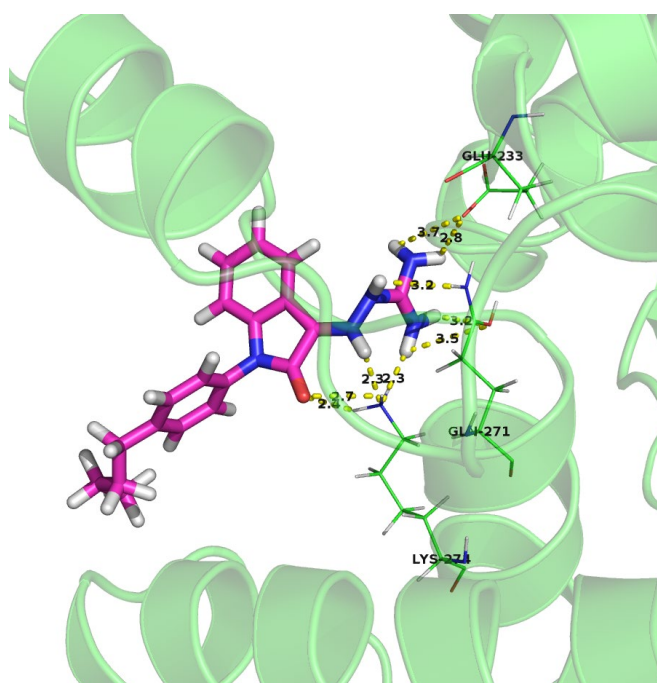


Fig. S4. (a) Electrostatic surface depiction of Fig. 3 calculated with the PyMOL APBS tools [14, 15]. The protein surface electrostatics potential map is coloured according to: red = -3 kT/e; white = 0 kT/e; blue = +3 kT/e; (b) proposed binding pose between **5m** (magenta and blue sticks) and *E. coli* PBP1b model (green) calculated by Autodock Vina [16]. The best binding mode showed an affinity of -6.4 kcal/mol. The hydrophilic moiety of **5m** showed hydrogen-bonding interactions between E233, Q271 and K274 of PGT while the hydrophobic moiety was pointing downward and in the similar direction as transmembrane domain, suggesting that the immersion of the hydrophobic moiety into plasma membrane.



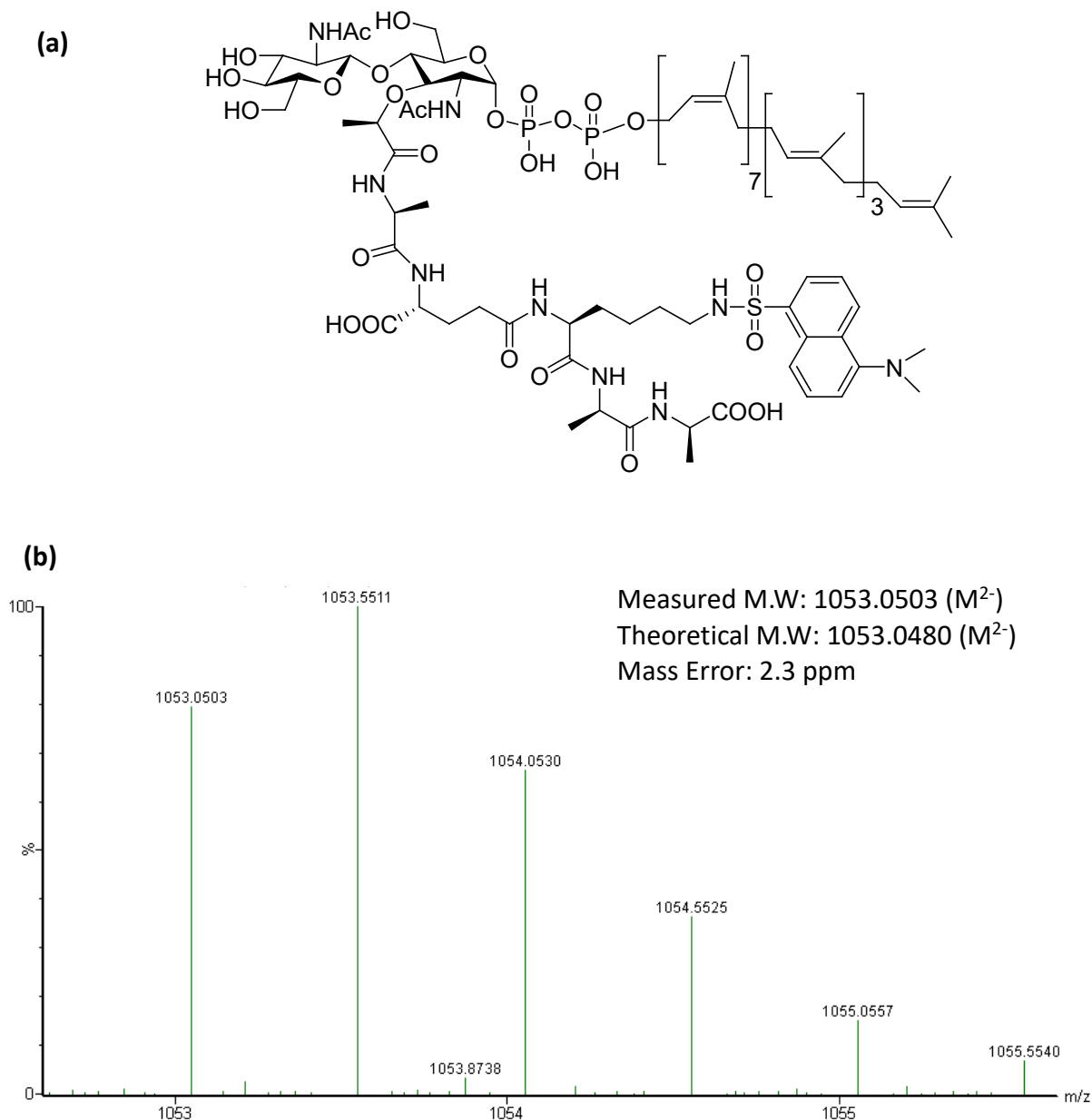
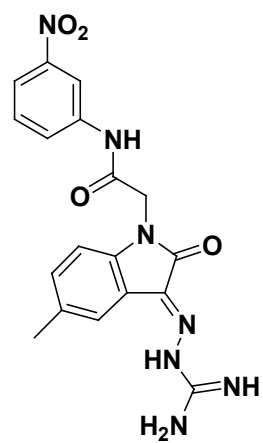


Fig. S5. (a) Structure of dansyl-lipid II prepared by reported procedures [17, 18]; and (b) high-resolution mass spectrum of purified dansyl-lipid II. The lipid II precursor, Park's nucleotide, was isolated from *S. aureus* culture (ATCC 29213), resulted in lysine as the third amino acid in the pentapeptide chain. Dansyl fluorophore was attached to the primary amino group of the lysine. HRMS calculated for  $C_{106}H_{167}N_9O_{28}P_2S$ :  $m/z$ : 1053.0480 [ $M-2H$ ] $^{2-}$ , found 1053.0503.

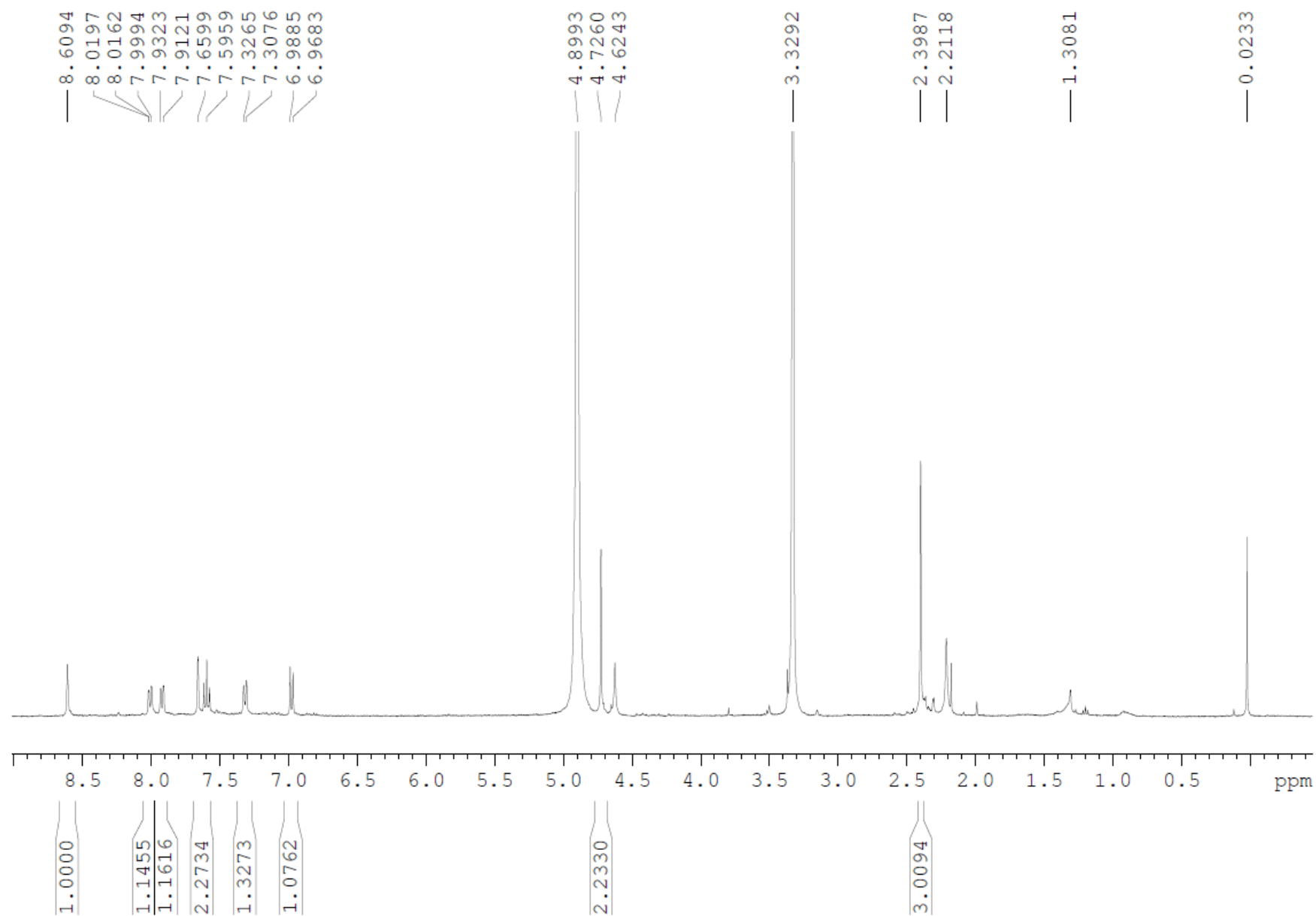
## References:

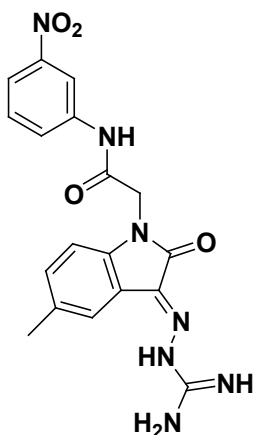
- [1] C.M. Gampe, H. Tsukamoto, E.H. Doud, S. Walker, D. Kahne, Tuning the moenomycin pharmacophore to enable discovery of bacterial cell wall synthesis inhibitors, *J Am Chem Soc*, 135 (2013) 3776-3779.
- [2] T.J.R. Cheng, Y.T. Wu, S.T. Yang, K.H. Lo, S.K. Chen, Y.H. Chen, W.I. Huang, C.H. Yuan, C.W. Guo, L.Y. Huang, K.T. Chen, H.W. Shih, Y.S.E. Cheng, W.C. Cheng, C.H. Wong, High-throughput identification of antibacterials against methicillin-resistant *Staphylococcus aureus* (MRSA) and the transglycosylase, *Bioorgan Med Chem*, 18 (2010) 8512-8529.
- [3] J. Zuegg, C. Muldoon, G. Adamson, D. McKeveney, G. Le Thanh, R. Premraj, B. Becker, M. Cheng, A.G. Elliott, J.X. Huang, M.S. Butler, M. Bajaj, J. Seifert, L. Singh, N.F. Galley, D.I. Roper, A.J. Lloyd, C.G. Dowson, T.J. Cheng, W.C. Cheng, D. Demon, E. Meyer, W. Meutermans, M.A. Cooper, Carbohydrate scaffolds as glycosyltransferase inhibitors with in vivo antibacterial activity, *Nat Commun*, 6 (2015) 7719.
- [4] I. Susic, M. Anderluh, M. Sova, M. Gobec, I.M. Rascan, A. Derouaux, A. Amoroso, M. Terrak, E. Breukink, S. Gobec, Structure-Activity Relationships of Novel Tryptamine-Based Inhibitors of Bacterial Transglycosylase, *J Med Chem*, 58 (2015) 9712-9721.
- [5] E.R. Baizman, A.A. Branstrom, C.B. Longley, N. Allanson, M.J. Sofia, D. Gange, R.C. Goldman, Antibacterial activity of synthetic analogues based on the disaccharide structure of moenomycin, an inhibitor of bacterial transglycosylase, *Microbiology*, 146 Pt 12 (2000) 3129-3140.
- [6] S. Dumbre, A. Derouaux, E. Lescrinier, A. Piette, B. Joris, M. Terrak, P. Herdewijn, Synthesis of modified peptidoglycan precursor analogues for the inhibition of glycosyltransferase, *J Am Chem Soc*, 134 (2012) 9343-9351.
- [7] T.J.R. Cheng, M.T. Sung, H.Y. Liao, Y.F. Chang, C.W. Chen, C.Y. Huang, L.Y. Chou, Y.D. Wu, Y. Chen, Y.S.E. Cheng, C.H. Wong, C. Ma, W.C. Cheng, Domain requirement of moenomycin binding to bifunctional transglycosylases and development of high-throughput discovery of antibiotics, *P Natl Acad Sci USA*, 105 (2008) 431-436.
- [8] A. Daina, O. Michielin, V. Zoete, SwissADME: a free web tool to evaluate pharmacokinetics, drug-likeness and medicinal chemistry friendliness of small molecules, *Sci Rep*, 7 (2017) 42717.
- [9] A. Daina, O. Michielin, V. Zoete, iLOGP: a simple, robust, and efficient description of n-octanol/water partition coefficient for drug design using the GB/SA approach, *J Chem Inf Model*, 54 (2014) 3284-3301.
- [10] T. Cheng, Y. Zhao, X. Li, F. Lin, Y. Xu, X. Zhang, Y. Li, R. Wang, L. Lai, Computation of octanol-water partition coefficients by guiding an additive model with knowledge, *J Chem Inf Model*, 47 (2007) 2140-2148.
- [11] S.A. Wildman, G.M. Crippen, Prediction of physicochemical parameters by atomic contributions, *J Chem Inf Comp Sci*, 39 (1999) 868-873.
- [12] I. Moriguchi, S. Hirono, Q. Liu, I. Nakagome, Y. Matsushita, Simple Method of Calculating Octanol Water Partition-Coefficient, *Chem Pharm Bull*, 40 (1992) 127-130.
- [13] L. Chen, D. Walker, B. Sun, Y. Hu, S. Walker, D. Kahne, Vancomycin analogues active against vanA-resistant strains inhibit bacterial transglycosylase without binding substrate, *Proc Natl Acad Sci U S A*, 100 (2003) 5658-5663.

- [14] T.J. Dolinsky, P. Czodrowski, H. Li, J.E. Nielsen, J.H. Jensen, G. Klebe, N.A. Baker, PDB2PQR: expanding and upgrading automated preparation of biomolecular structures for molecular simulations, *Nucleic Acids Res*, 35 (2007) W522-525.
- [15] N.A. Baker, D. Sept, S. Joseph, M.J. Holst, J.A. McCammon, Electrostatics of nanosystems: application to microtubules and the ribosome, *Proc Natl Acad Sci U S A*, 98 (2001) 10037-10041.
- [16] O. Trott, A.J. Olson, AutoDock Vina: improving the speed and accuracy of docking with a new scoring function, efficient optimization, and multithreading, *J Comput Chem*, 31 (2010) 455-461.
- [17] E. Breukink, H.E. van Heusden, P.J. Vollmerhaus, E. Swiezewska, L. Brunner, S. Walker, A.J.R. Heck, B. de Kruijff, Lipid II is an intrinsic component of the pore induced by nisin in bacterial membranes, *J Biol Chem*, 278 (2003) 19898-19903.
- [18] B. Schwartz, J.A. Markwalder, S.P. Seitz, Y. Wang, R.L. Stein, A kinetic characterization of the glycosyltransferase activity of *Eschericia coli* PBP1b and development of a continuous fluorescence assay, *Biochemistry-U S*, 41 (2002) 12552-12561.

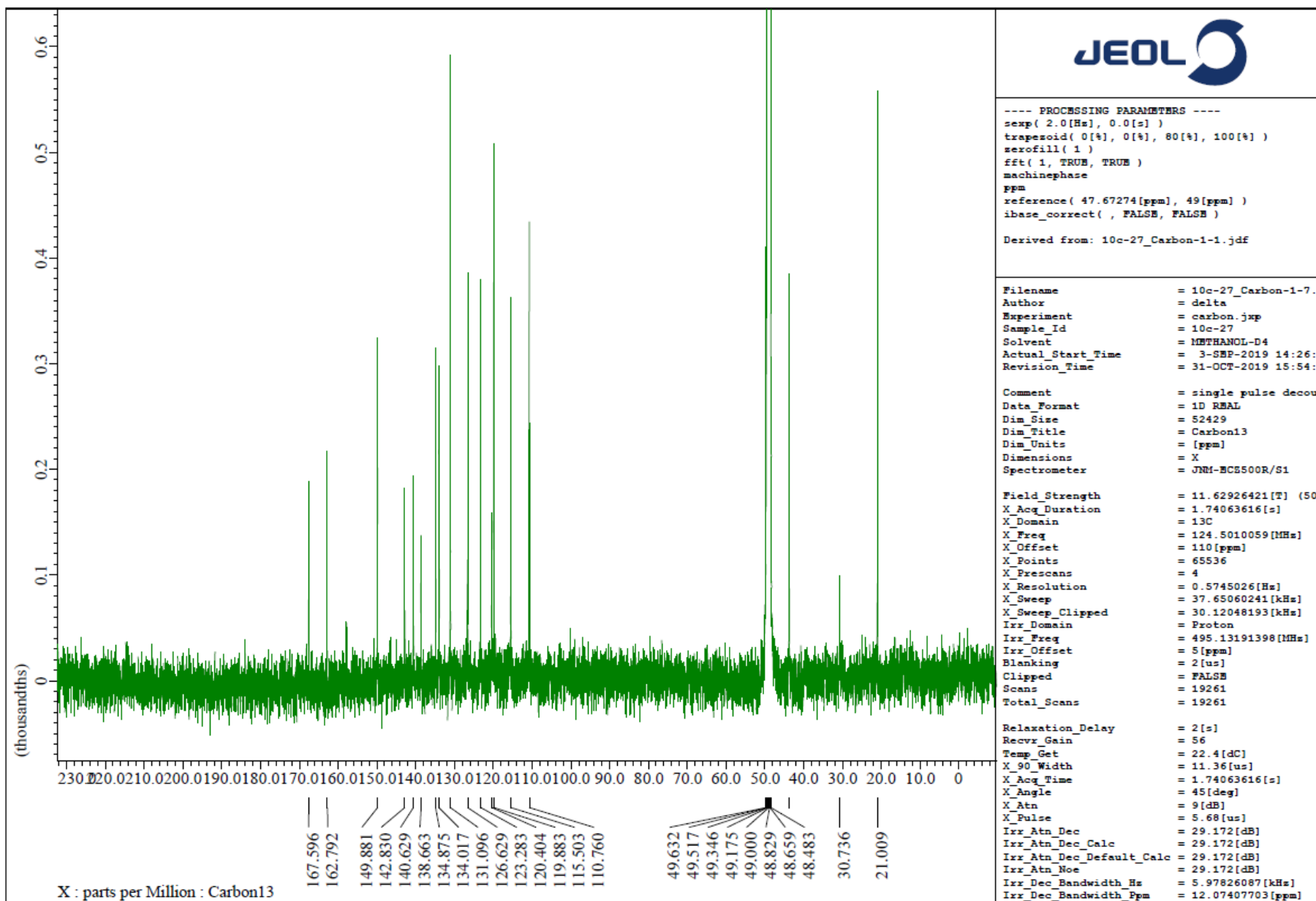


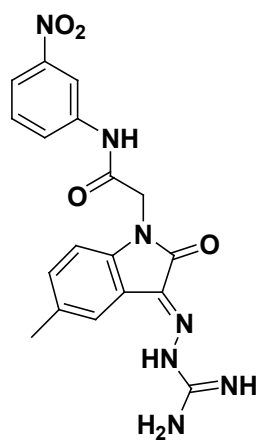
3a



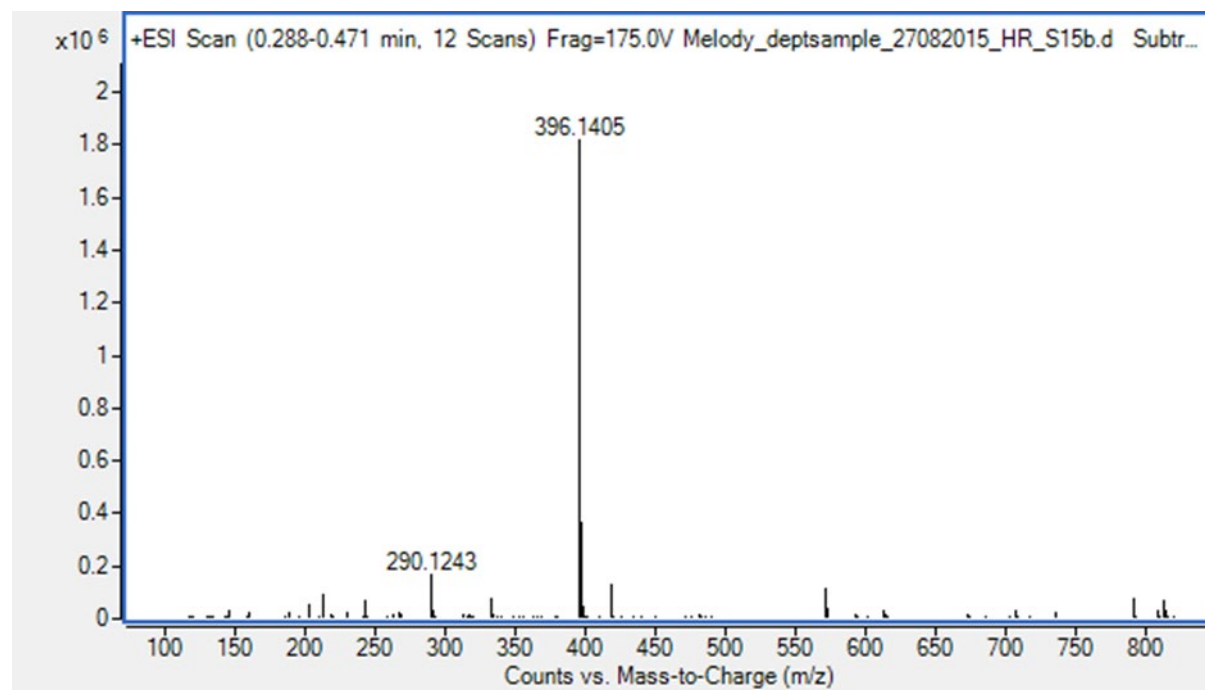


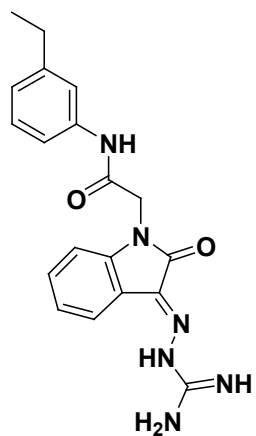
3a



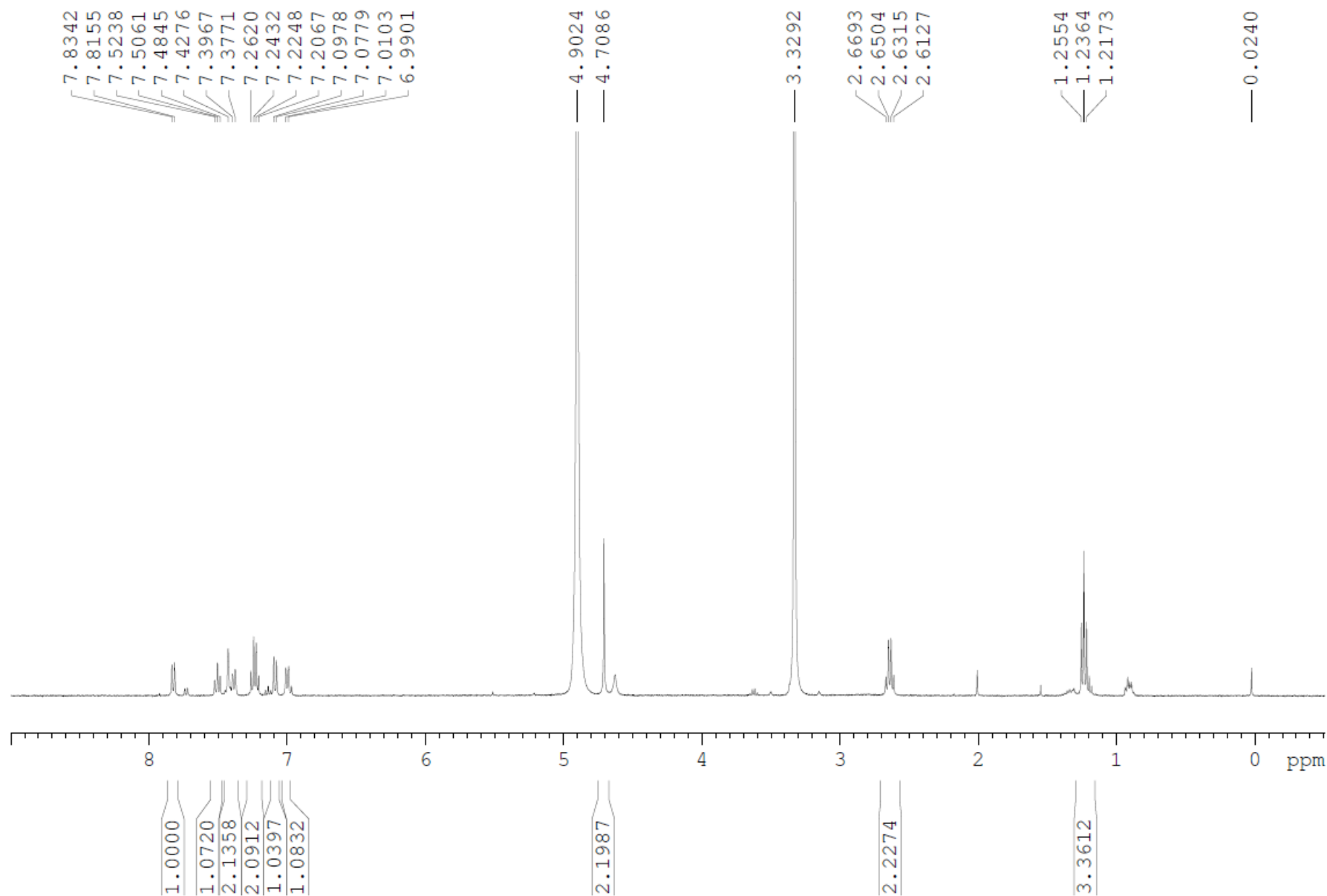


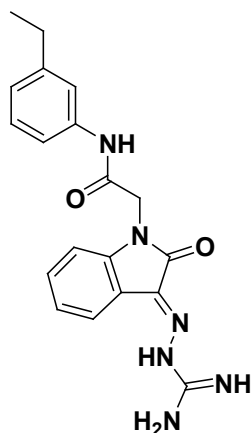
3a



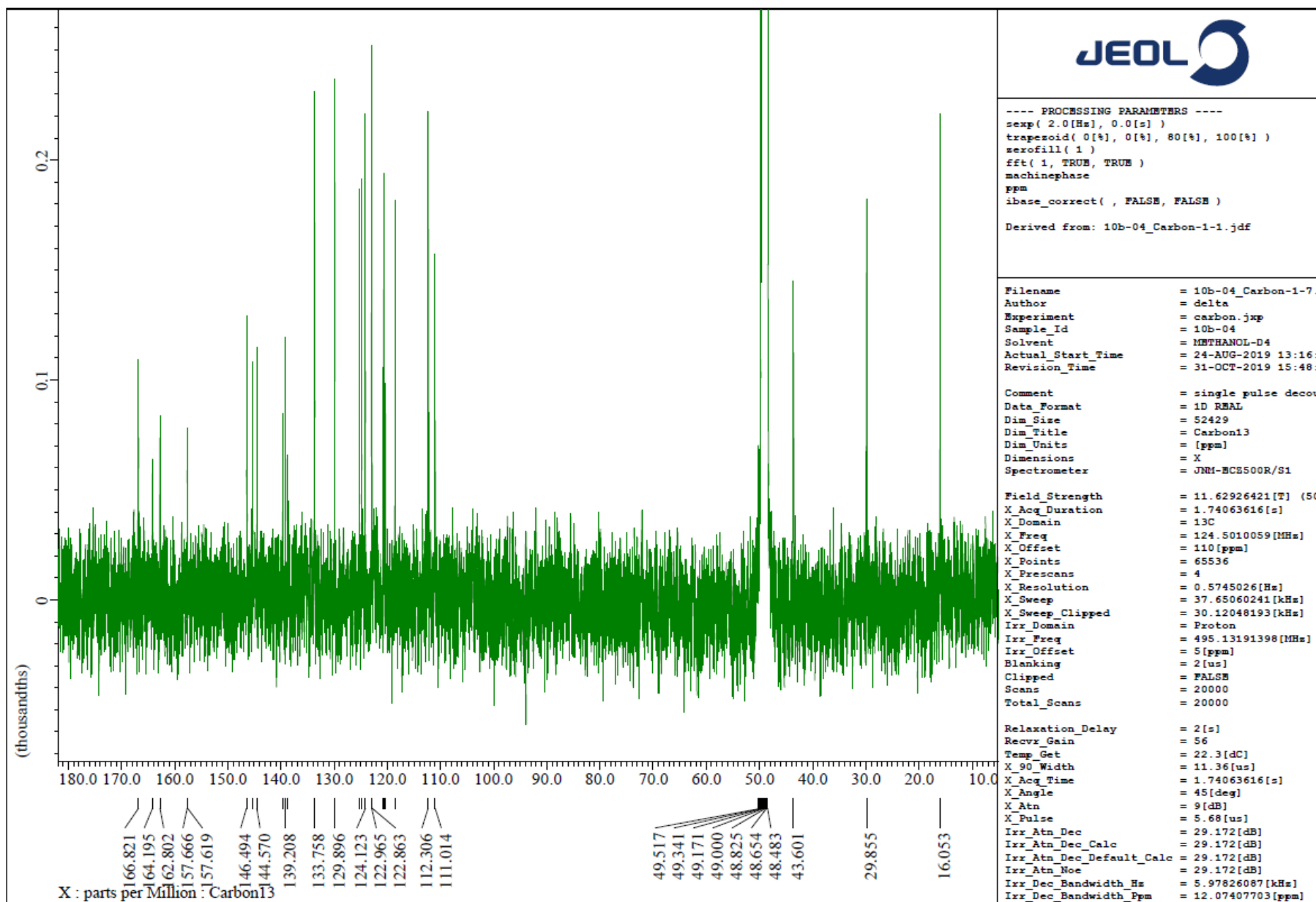


3b

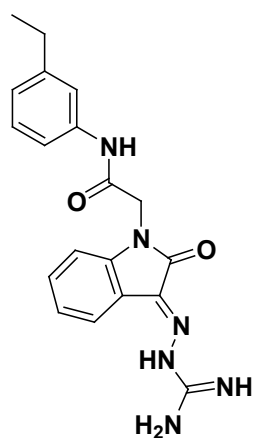




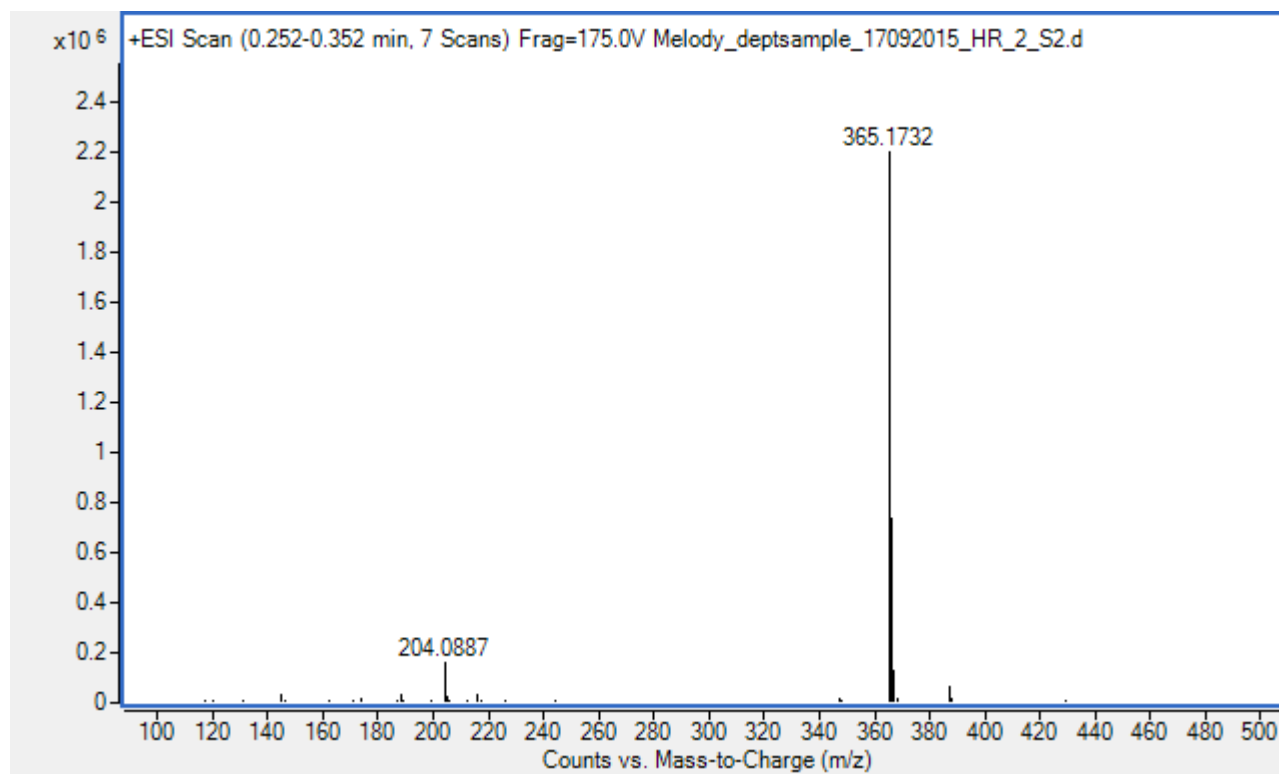
3b

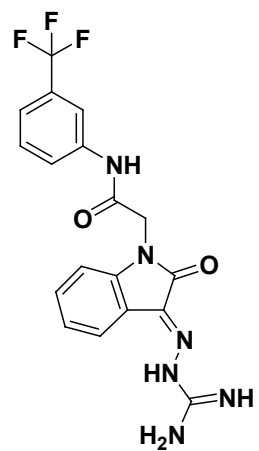




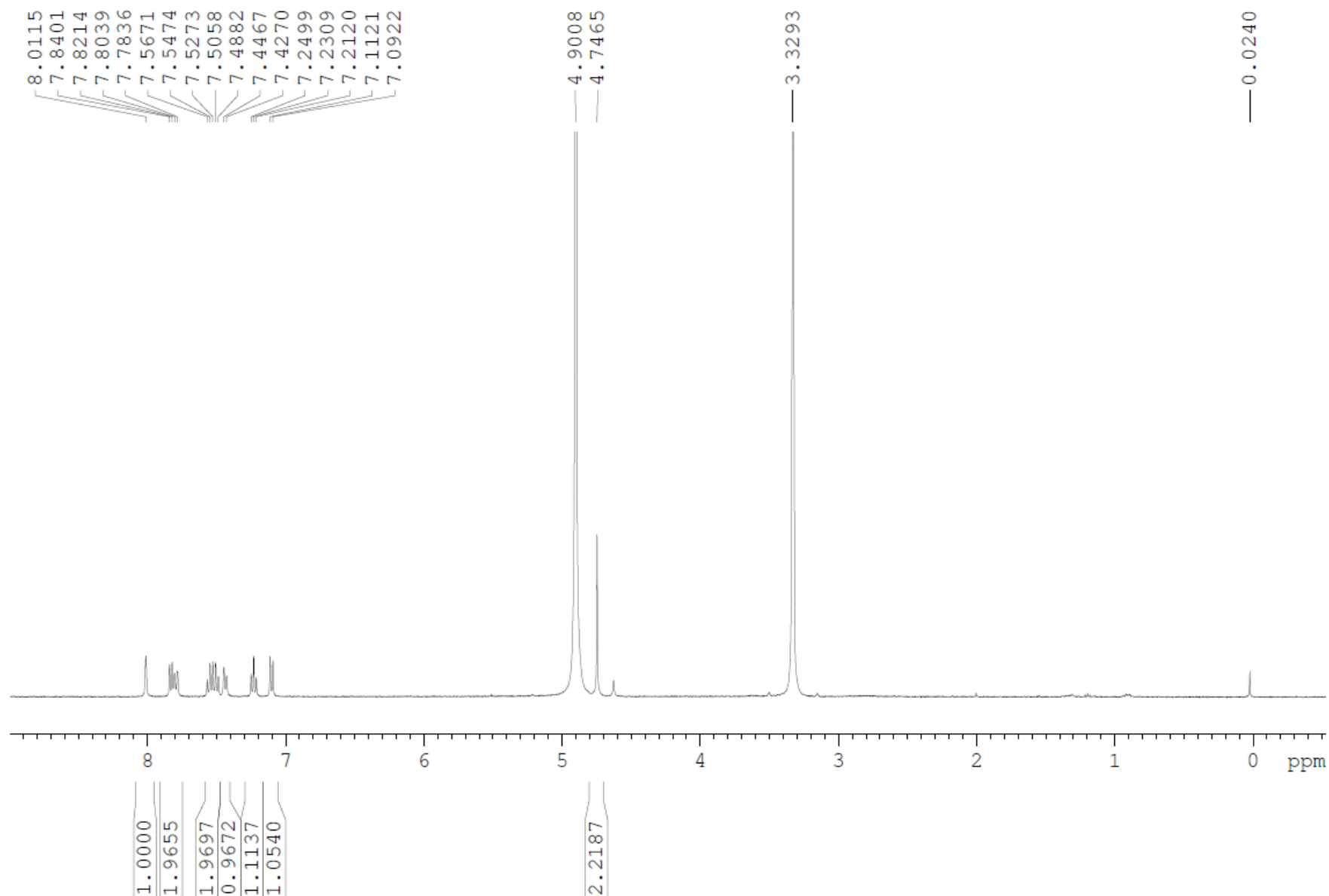


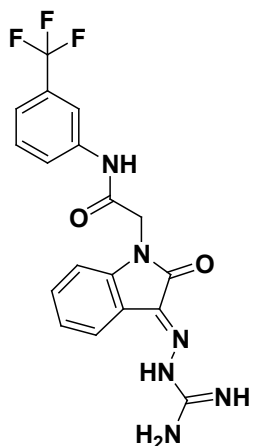
**3b**



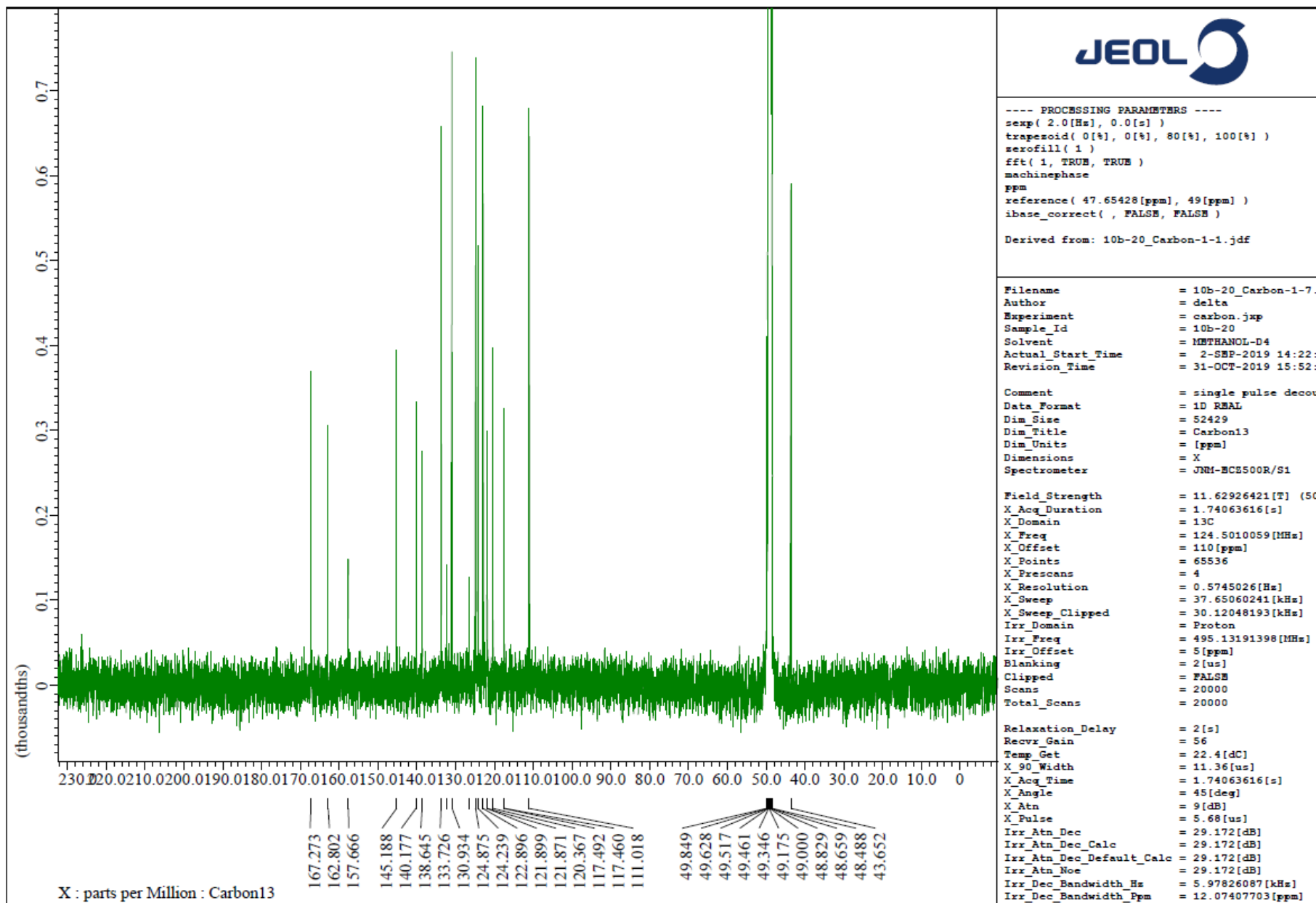


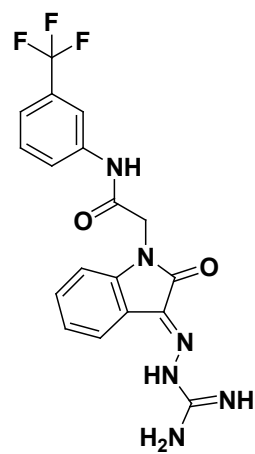
3c



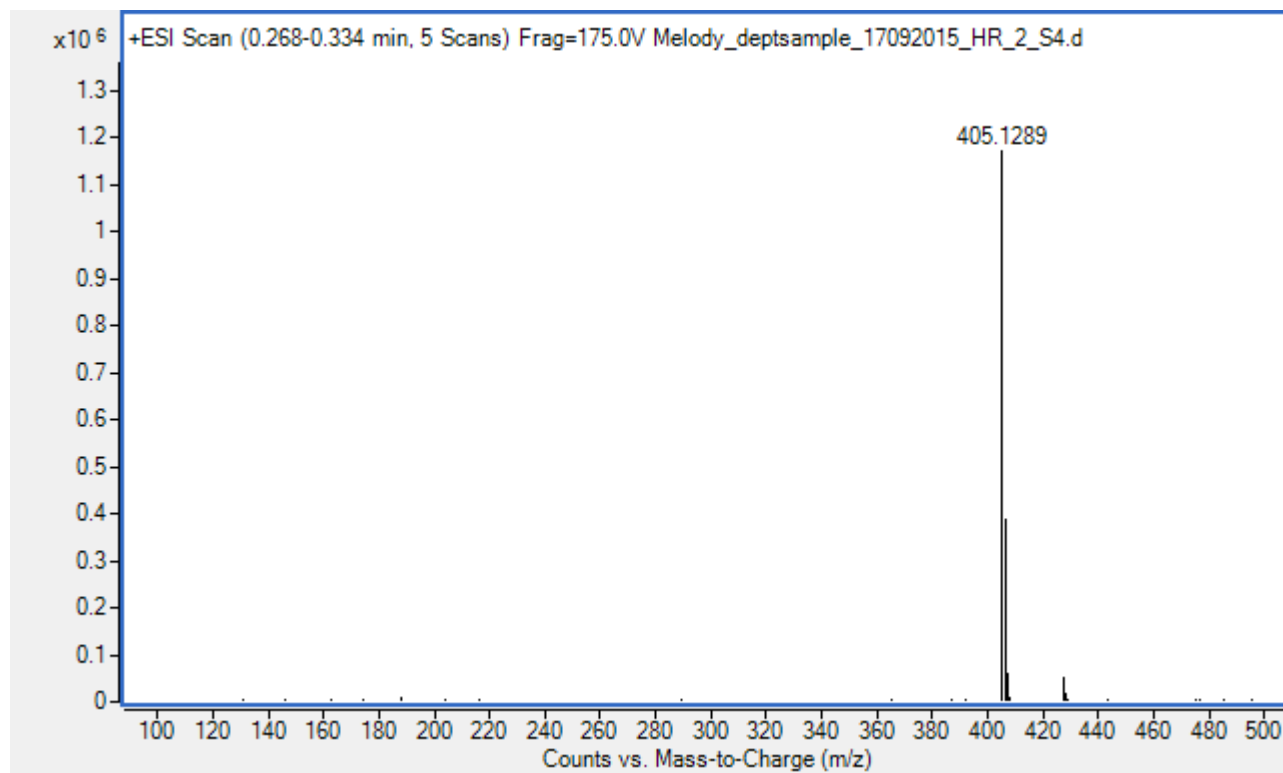


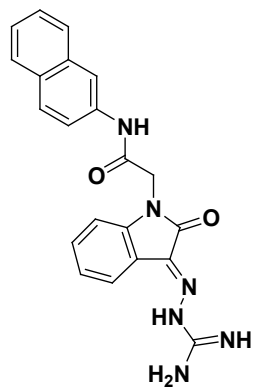
3c



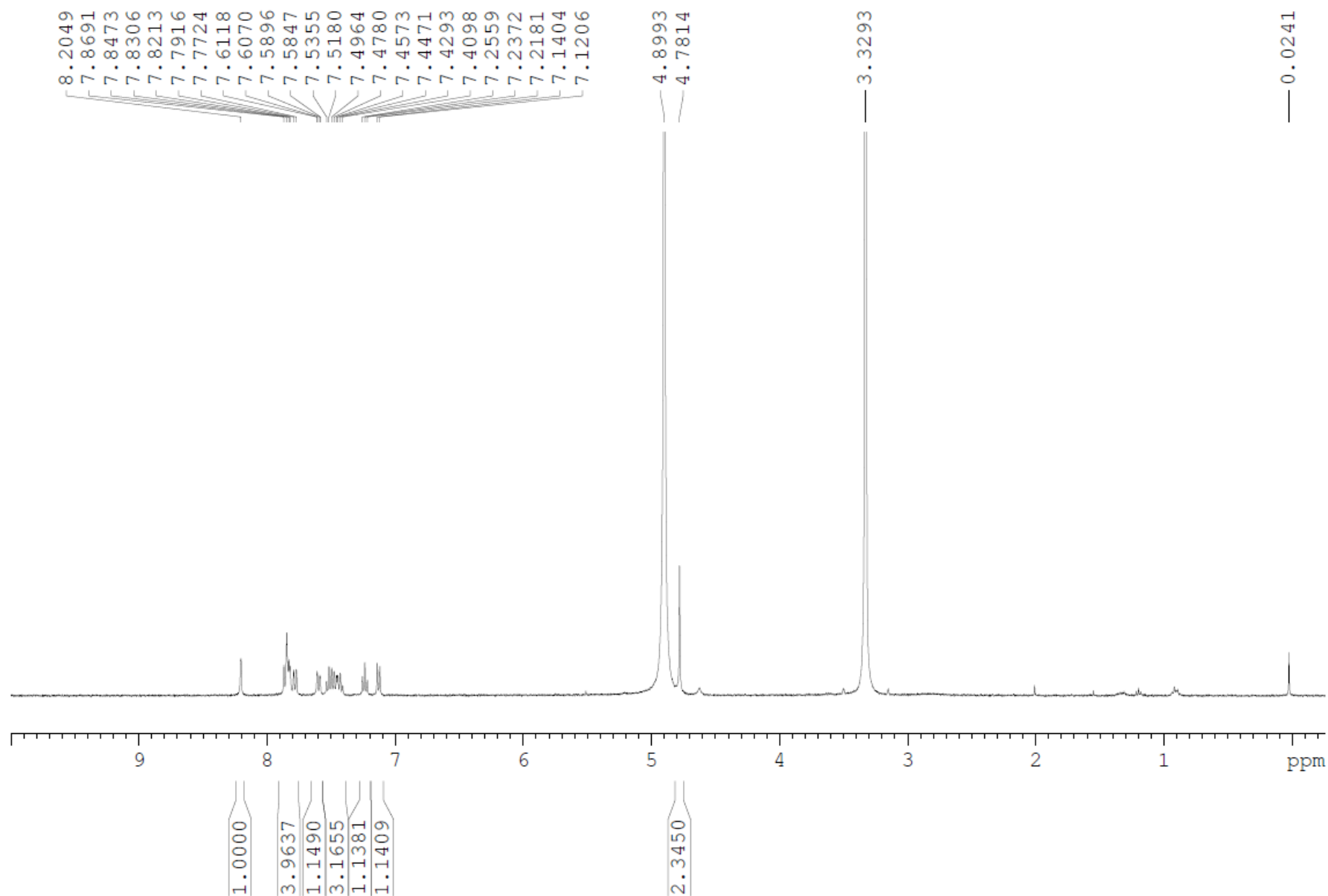


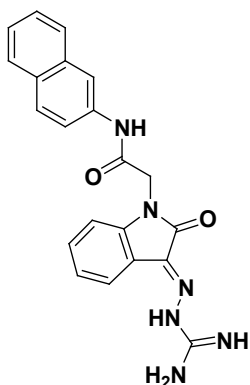
**3c**



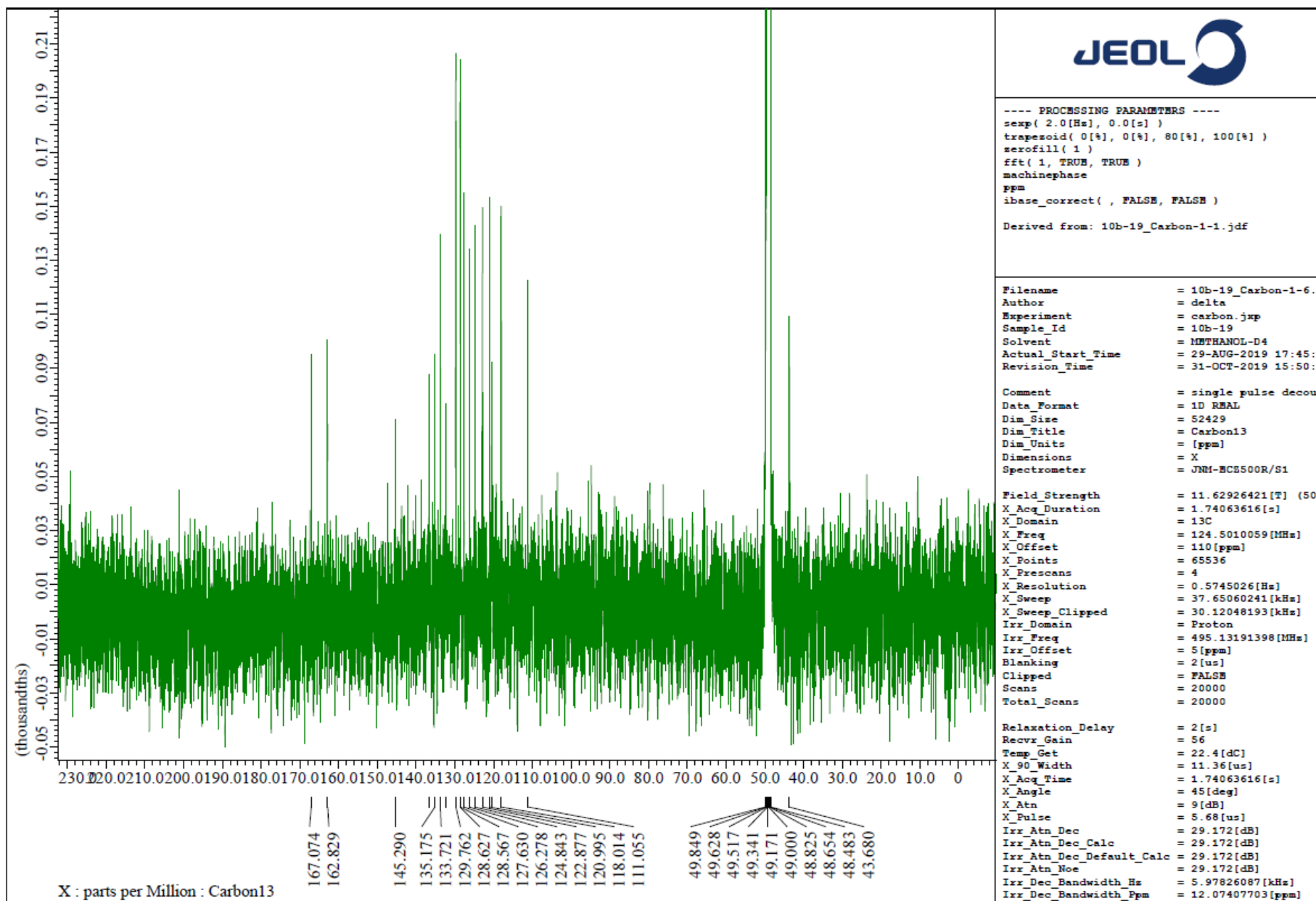


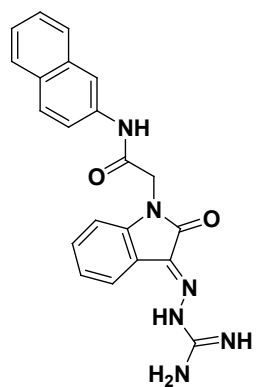
**3d**



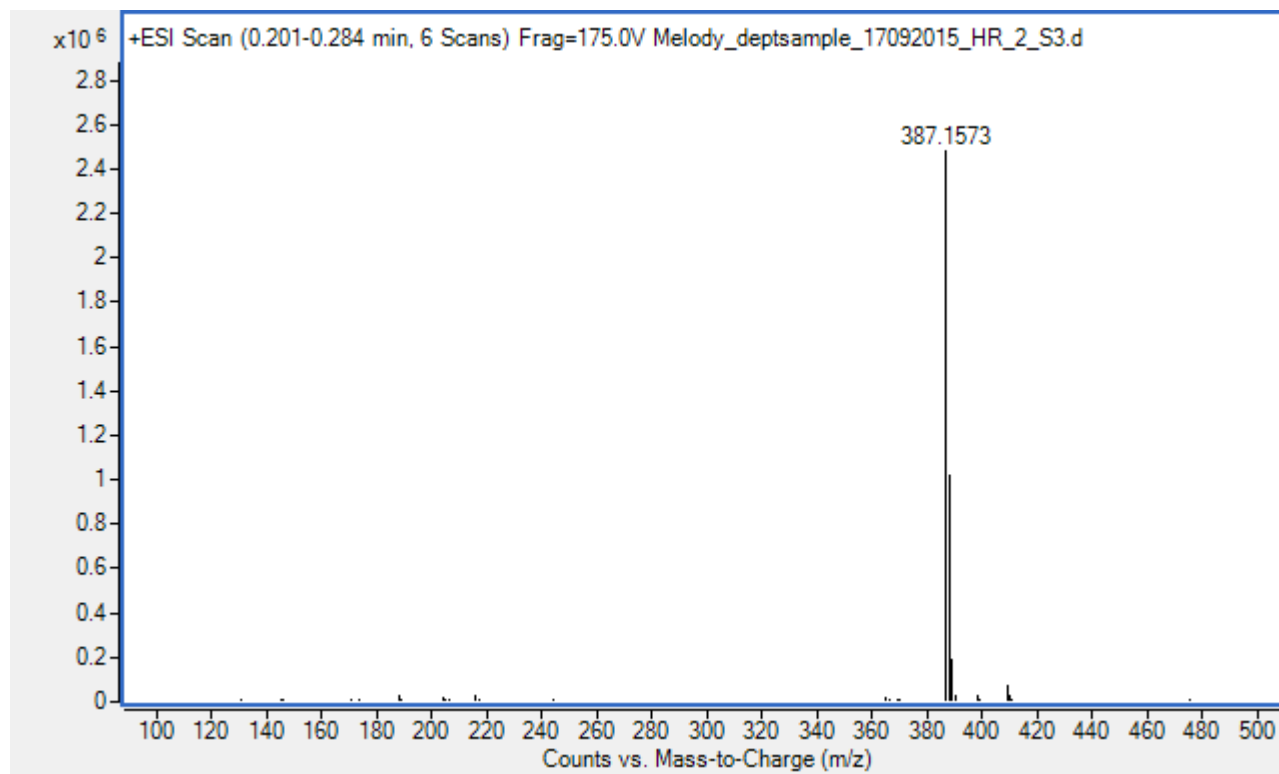


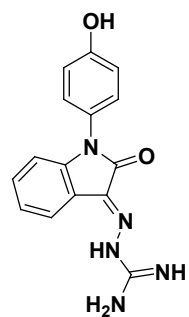
3d



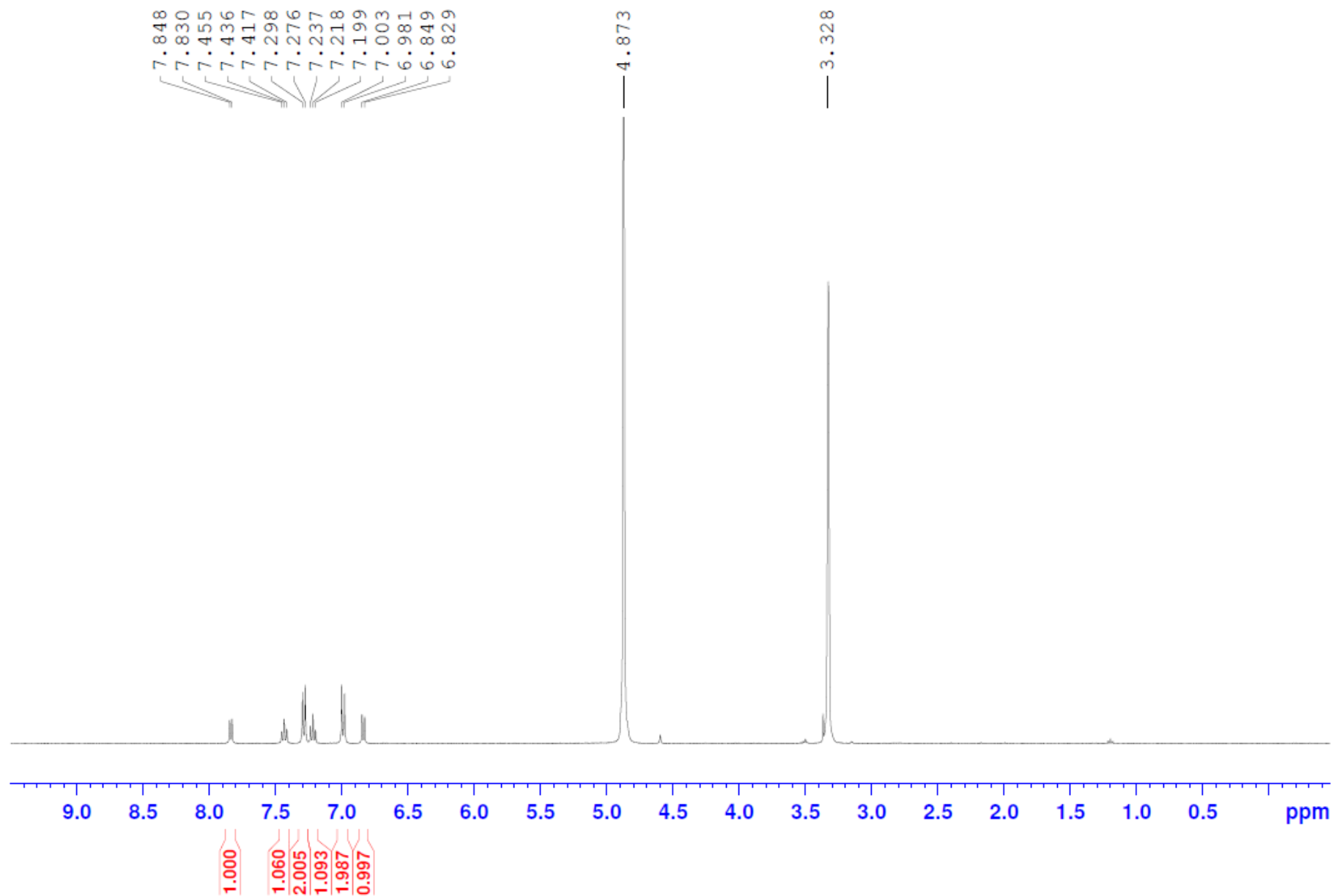


**3d**

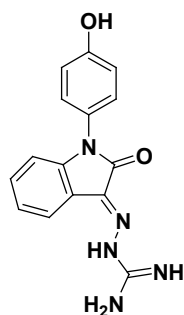




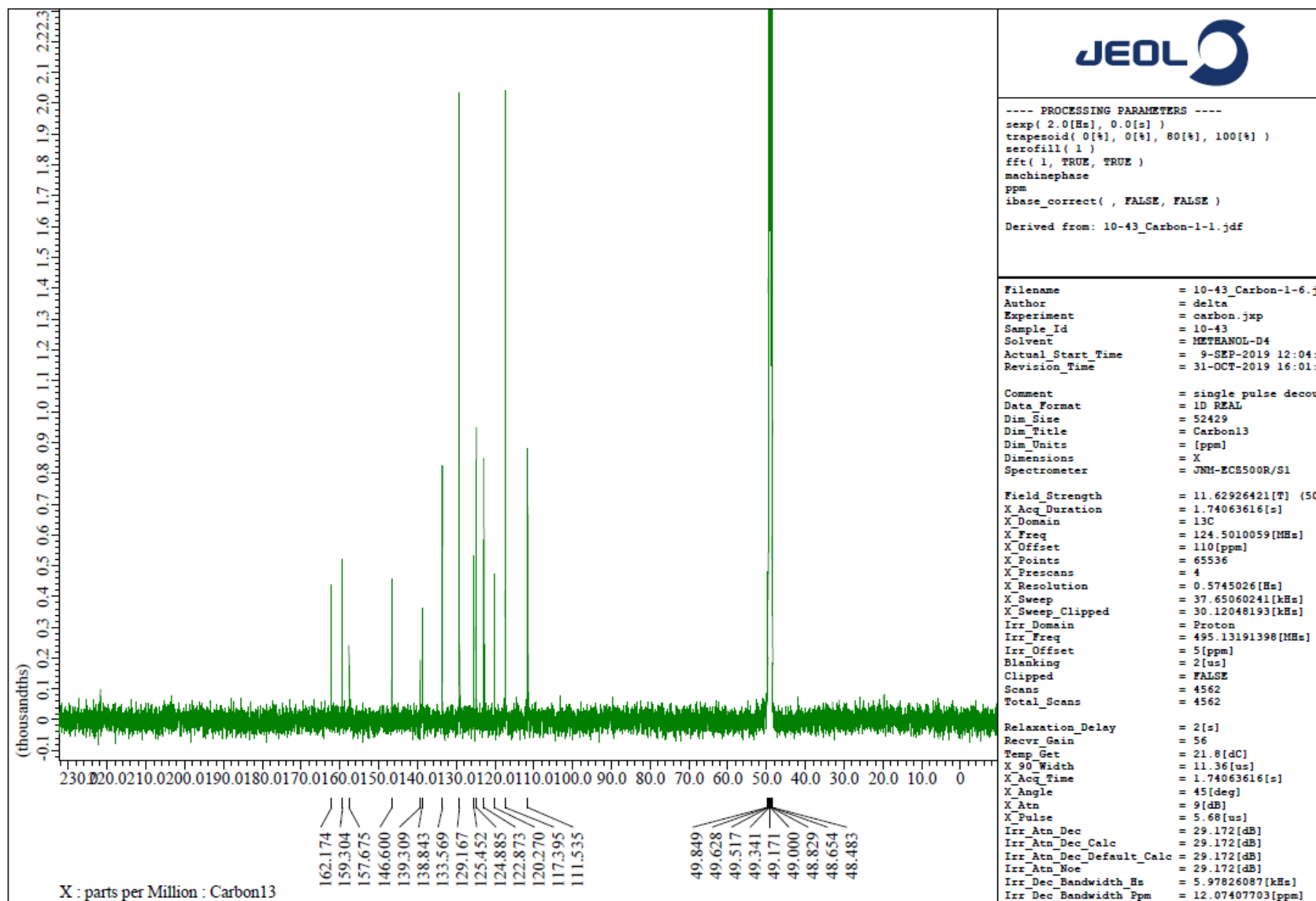
5a

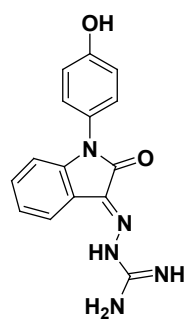




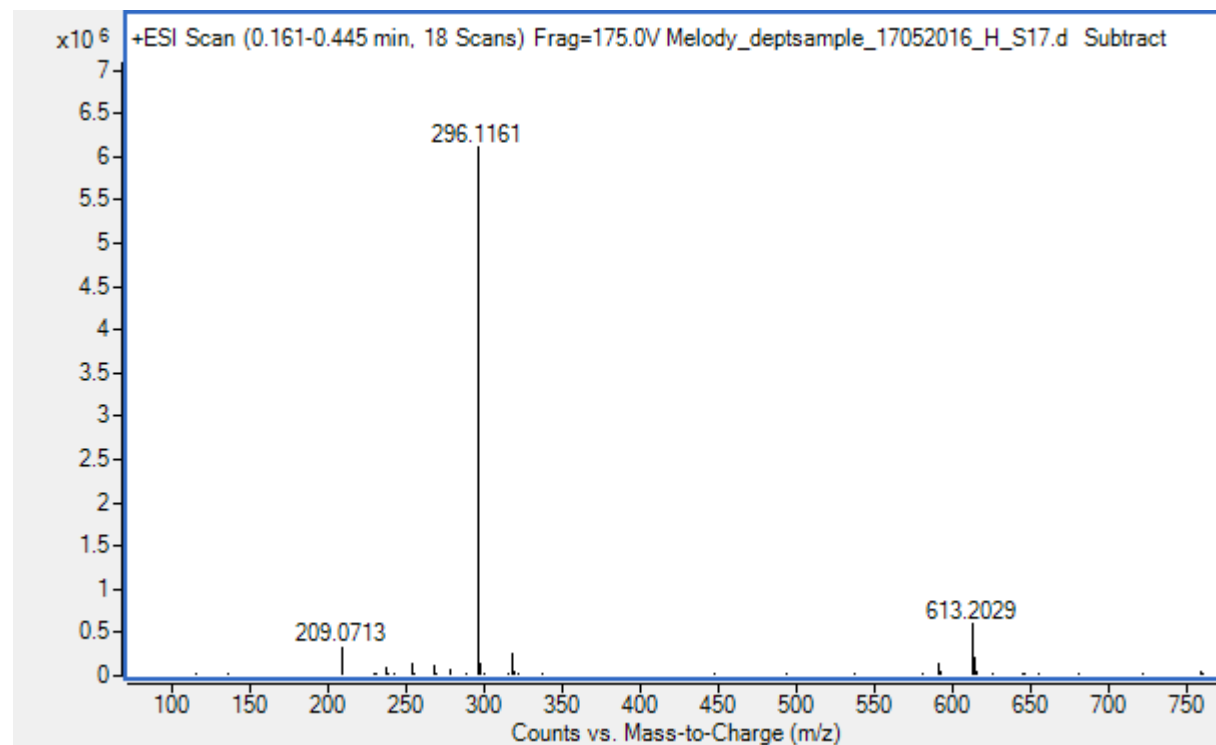


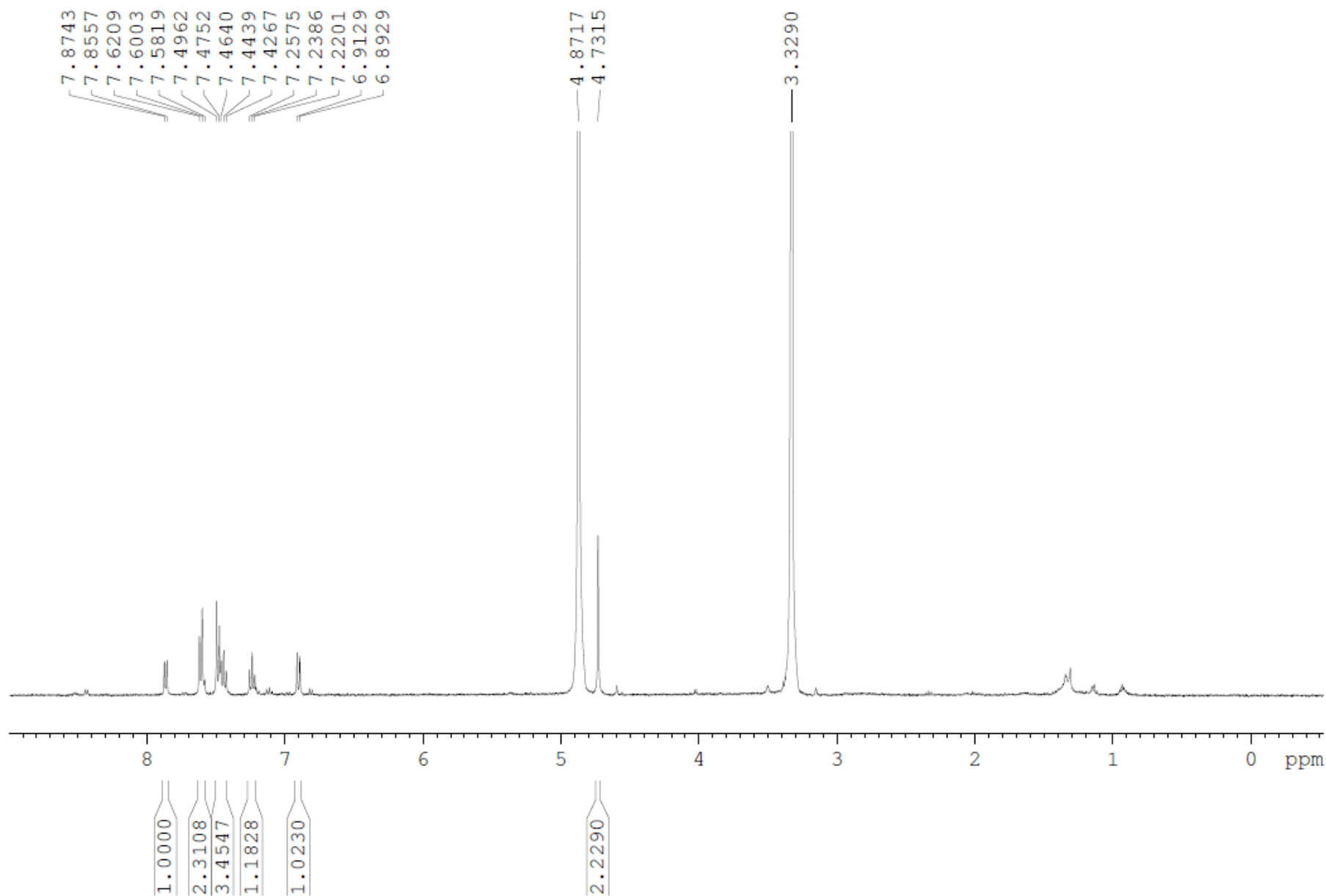
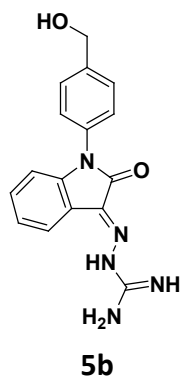
5a

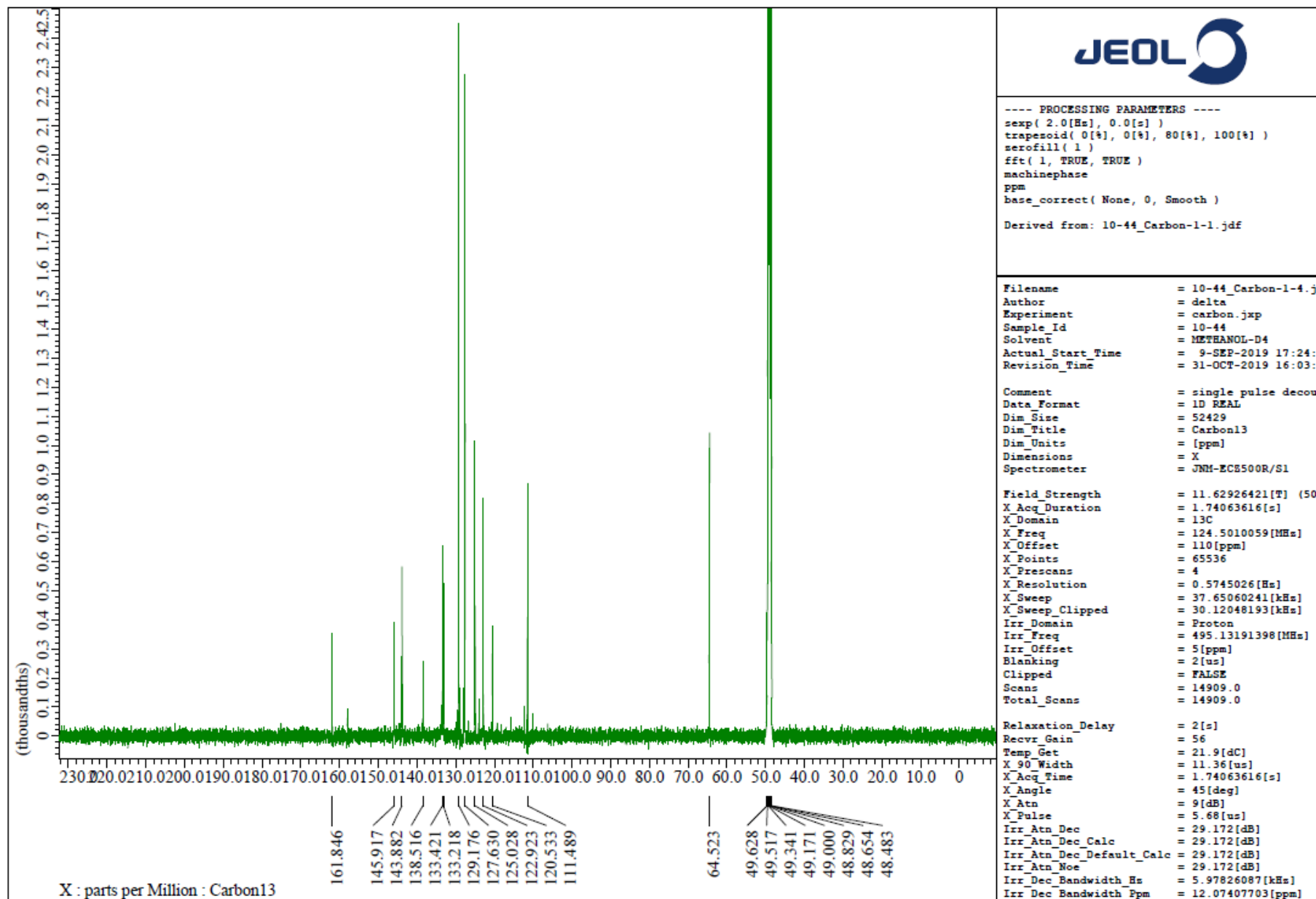
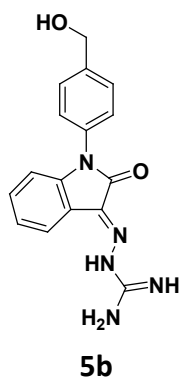


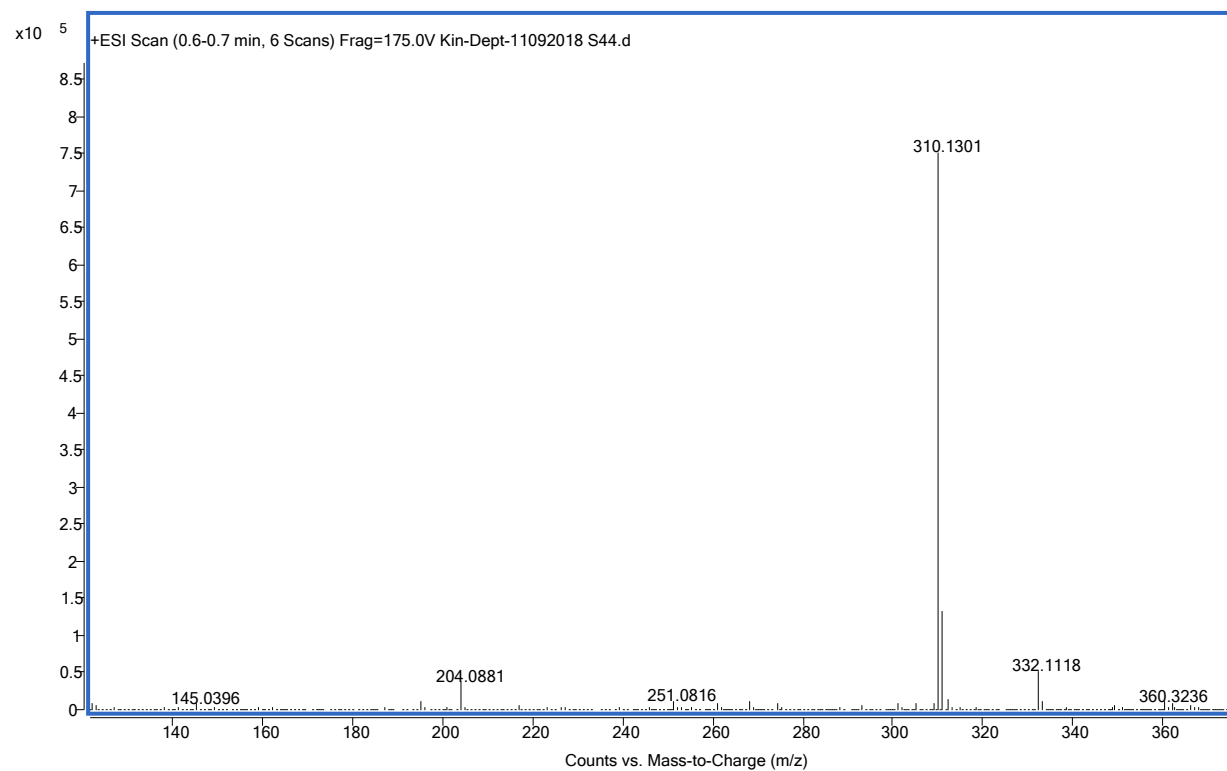
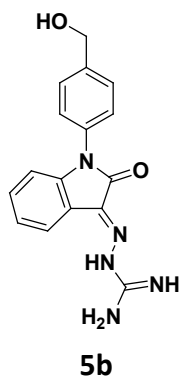


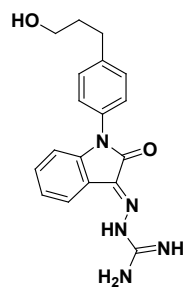
**5a**



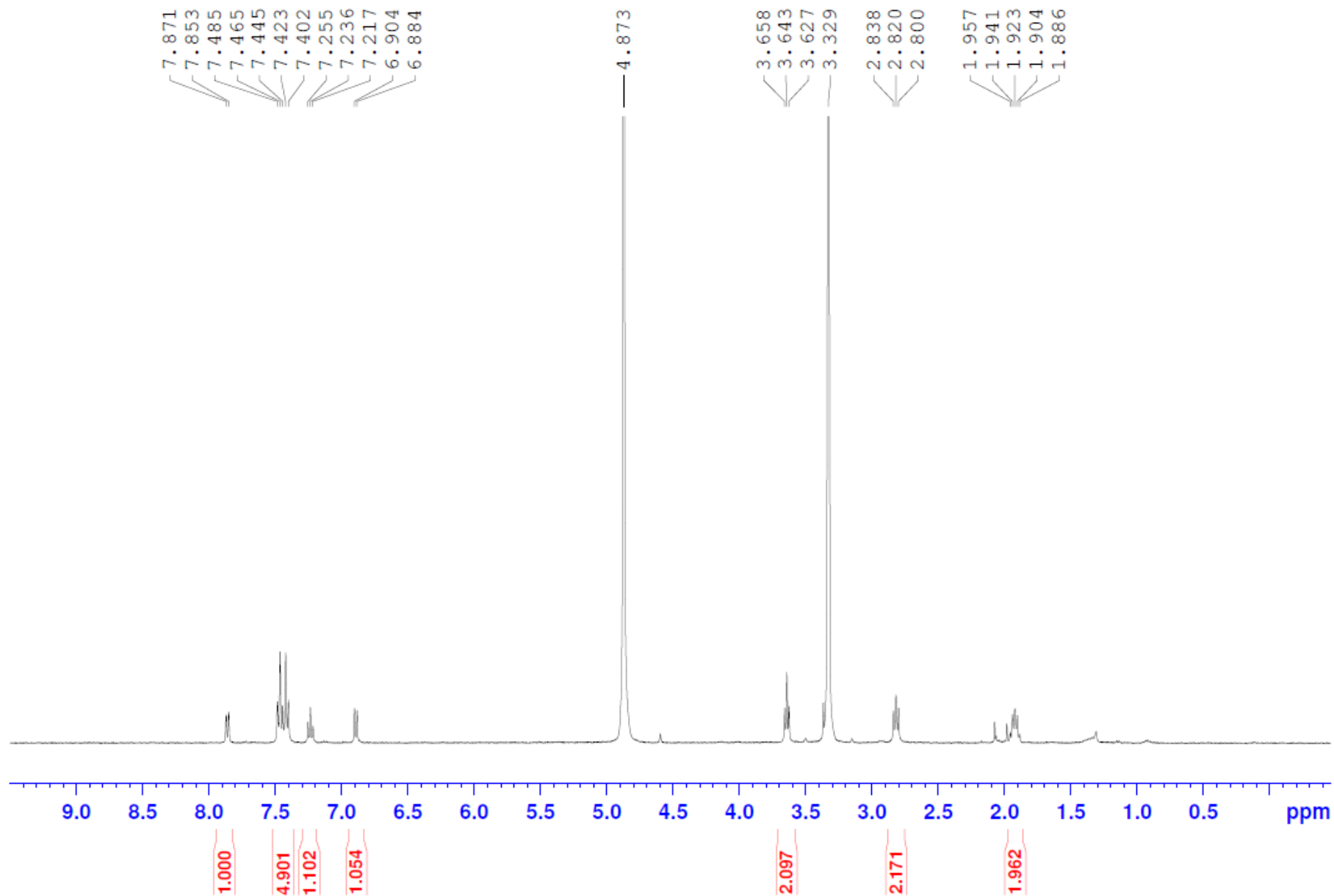


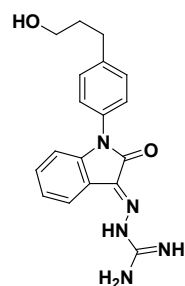




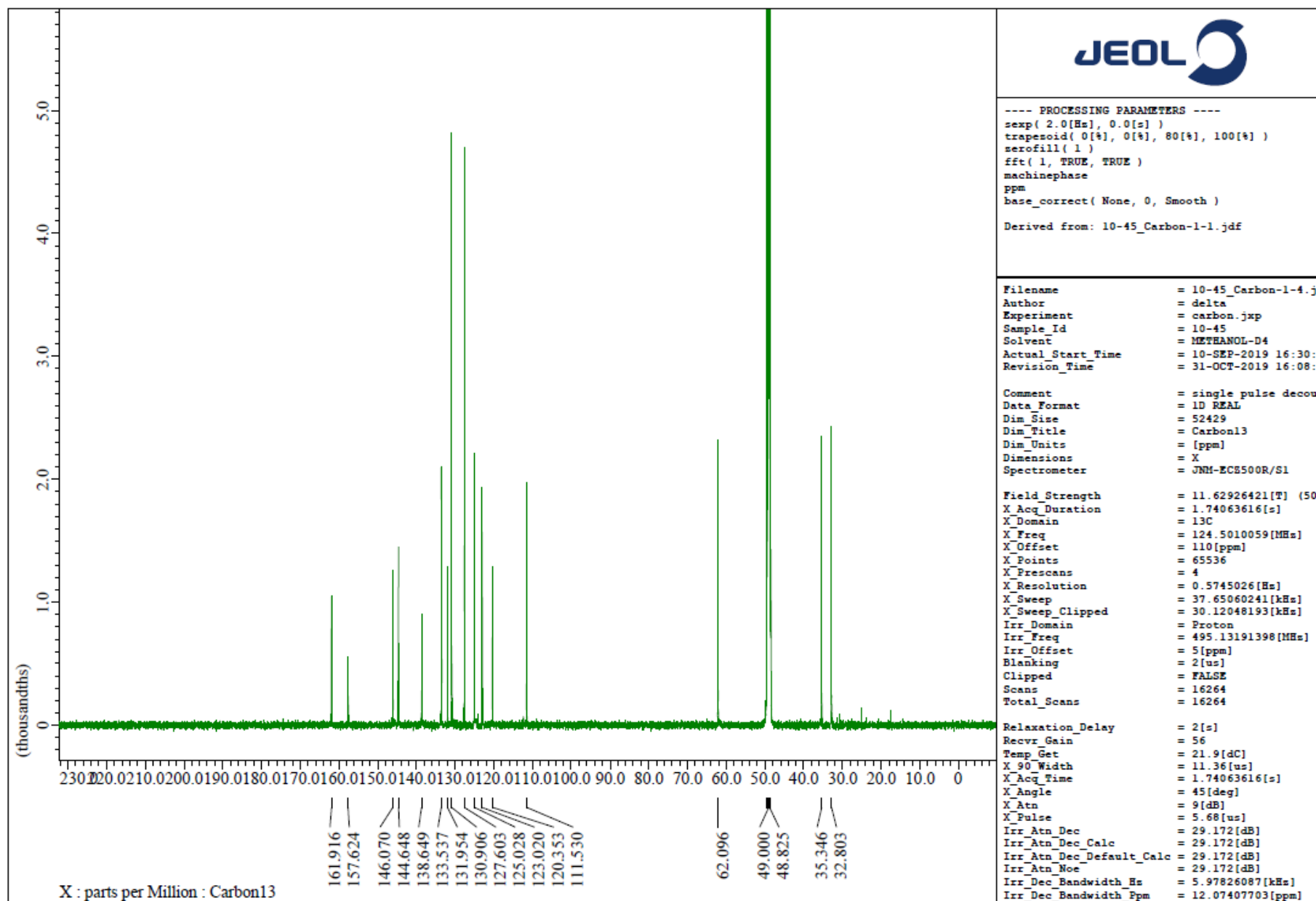


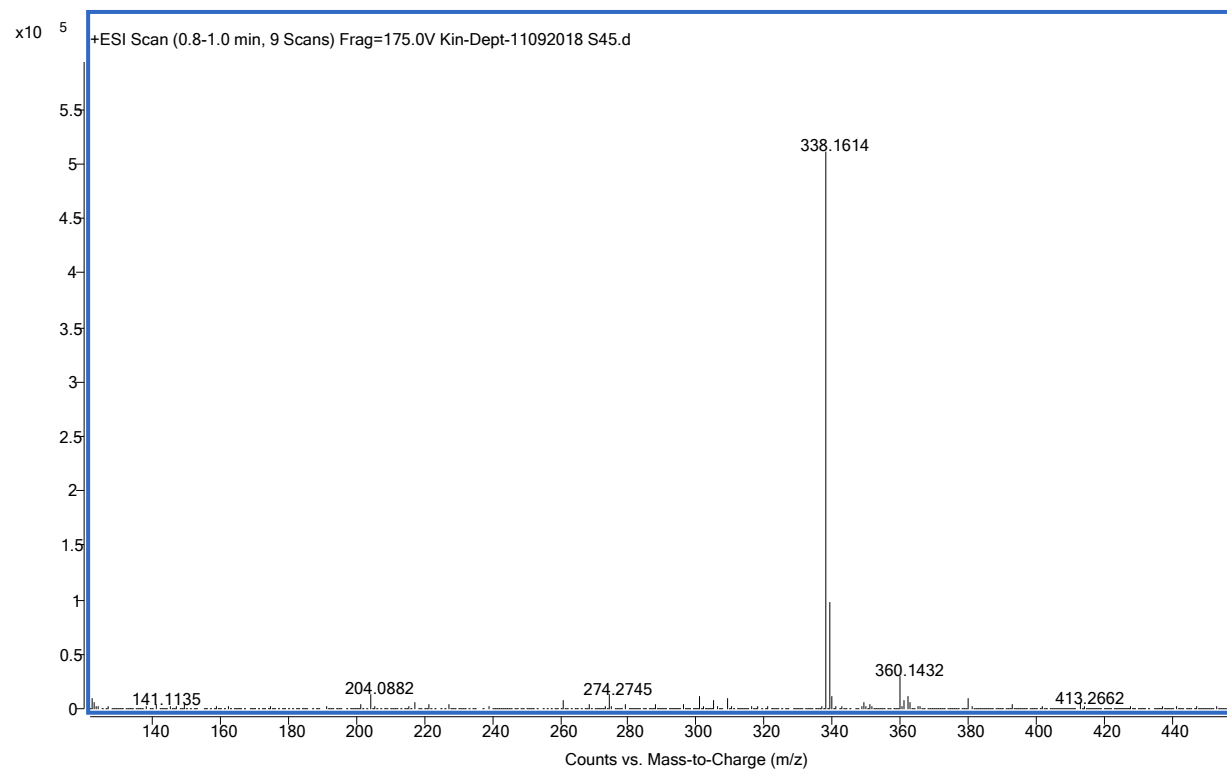
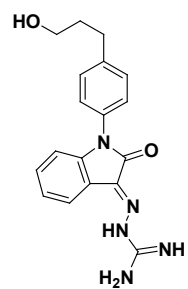
5c



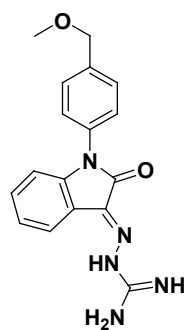


5c

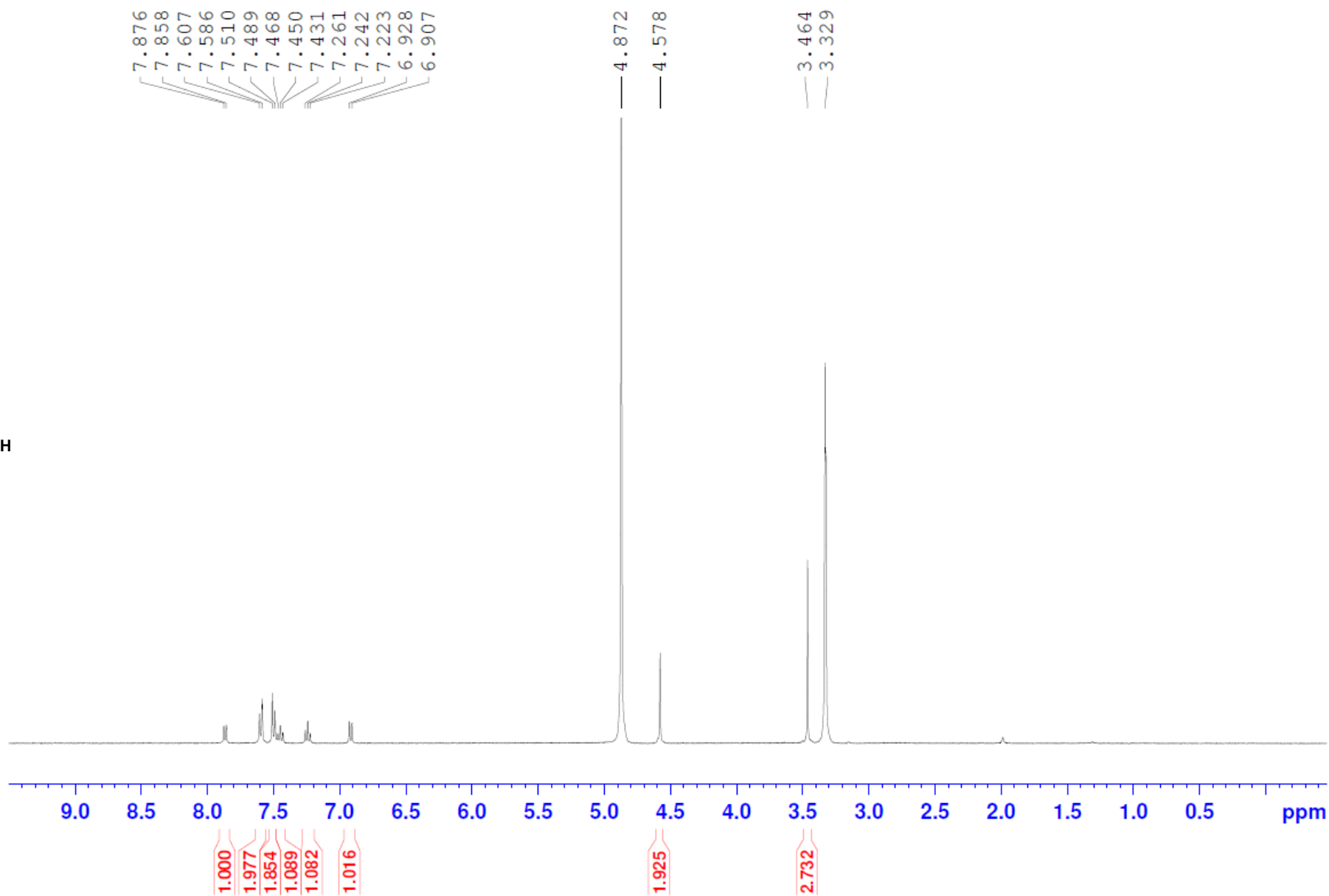


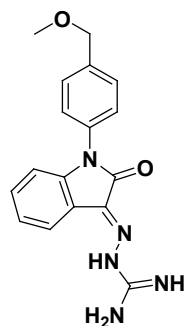




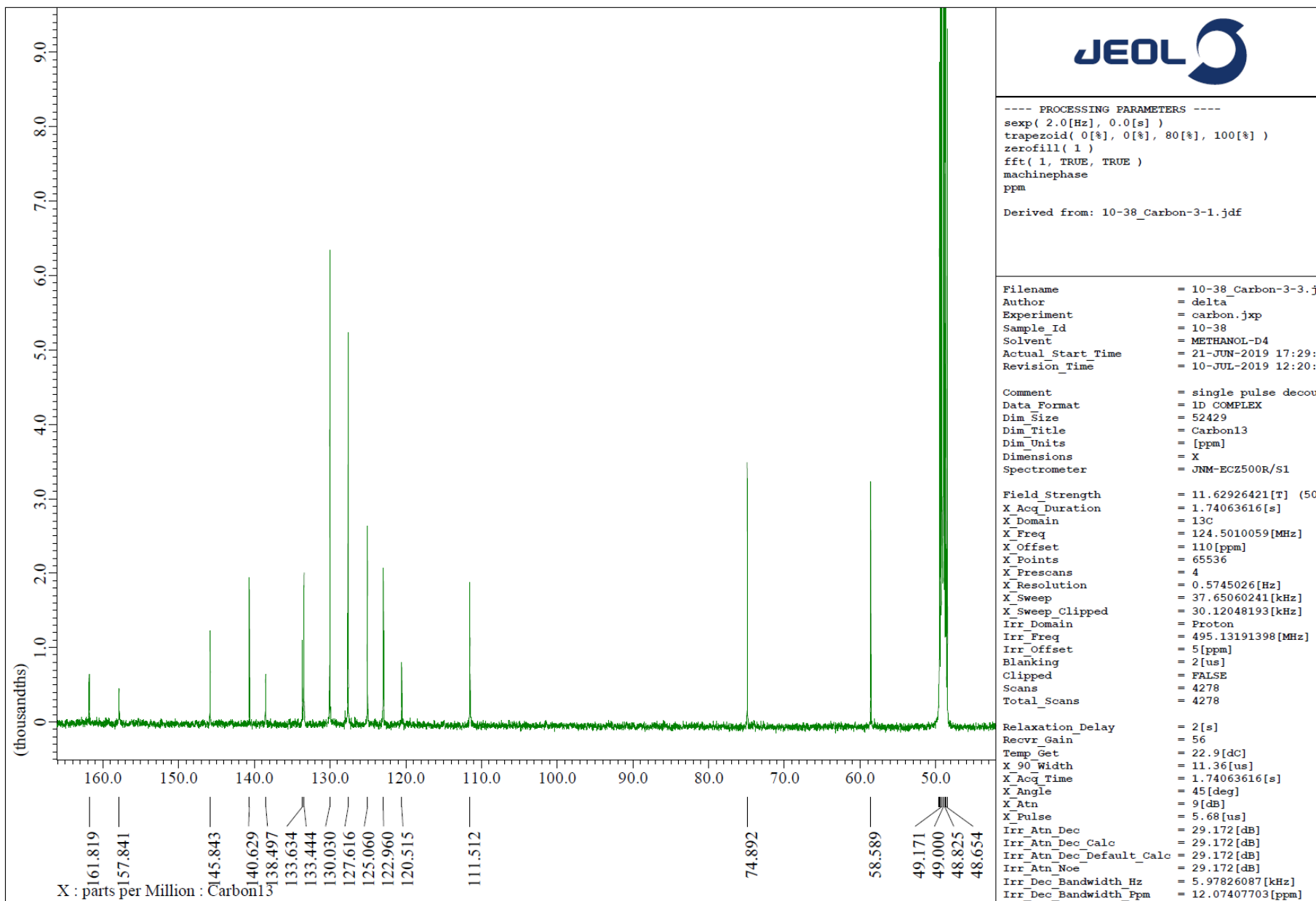


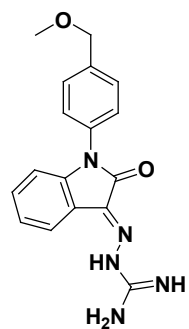
5d



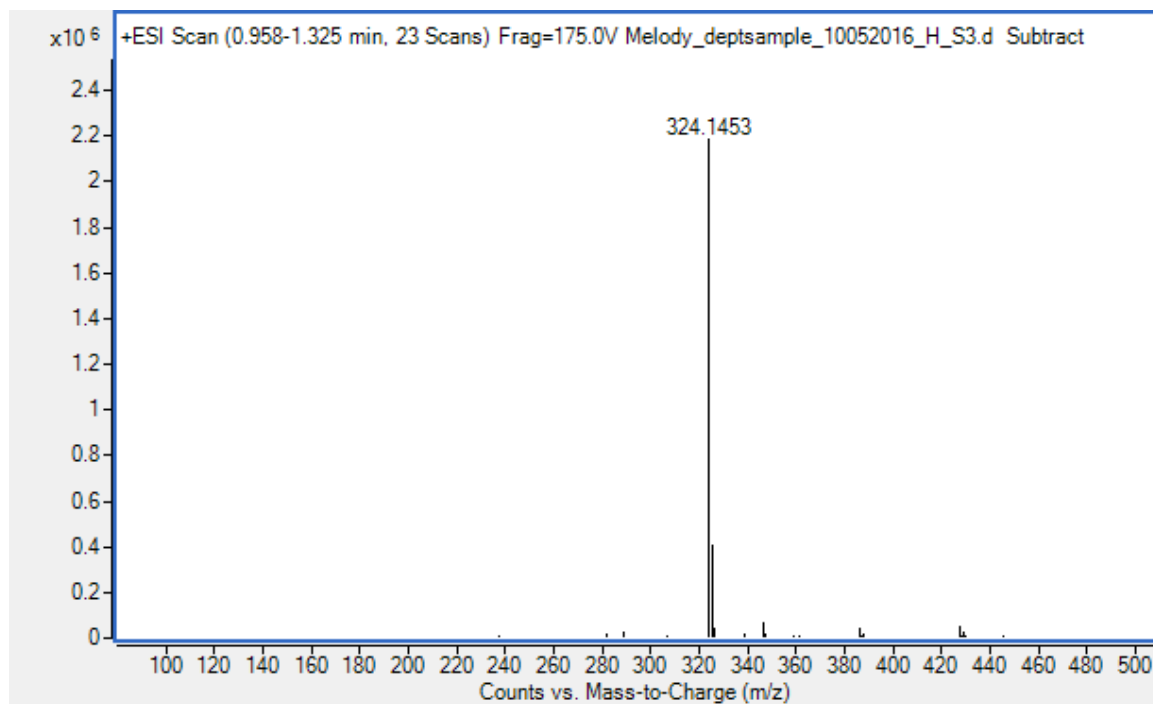


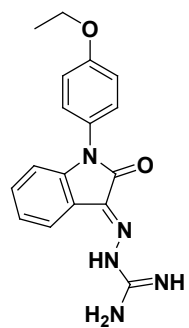
5d



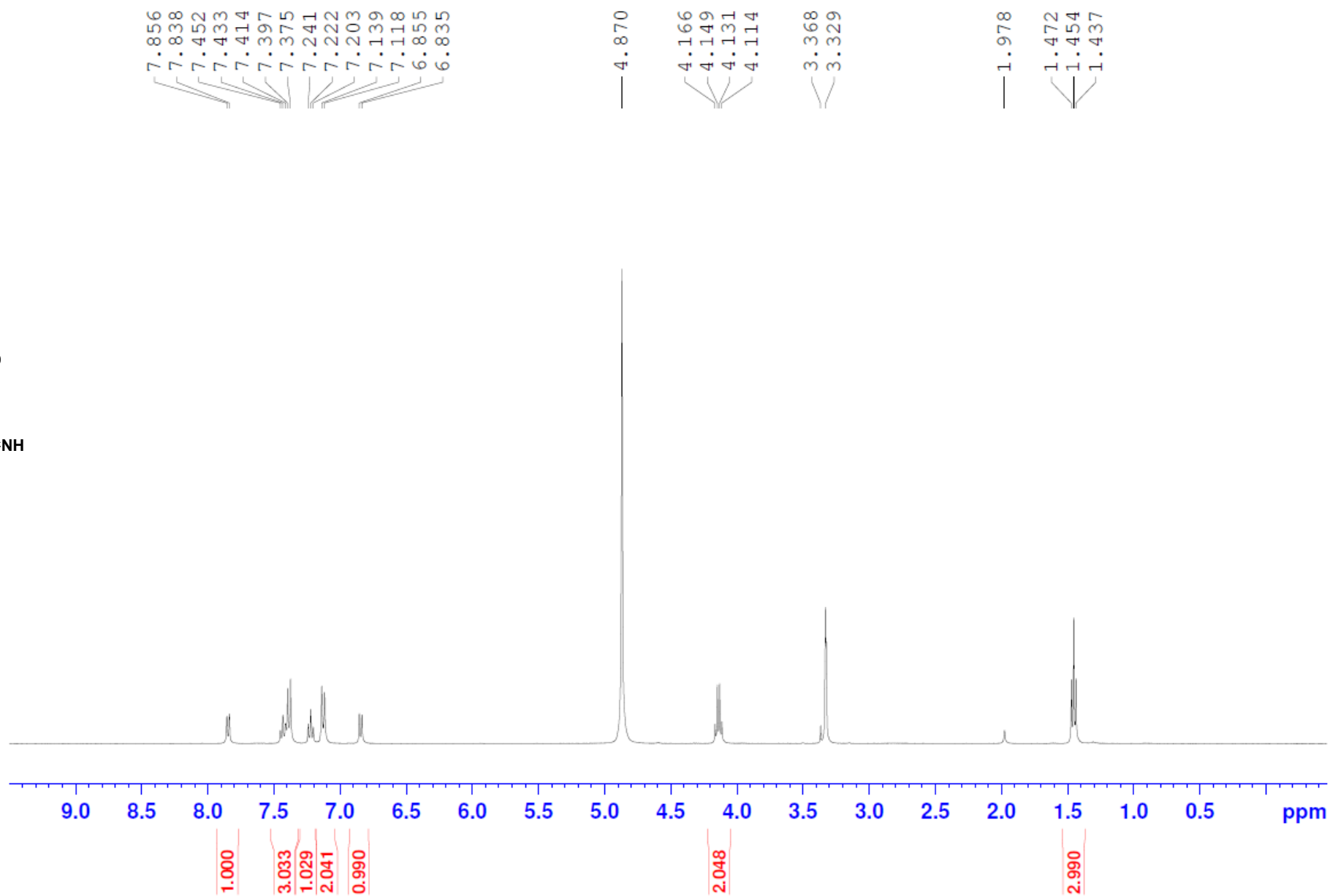


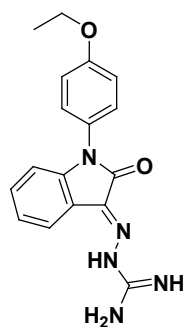
**5d**



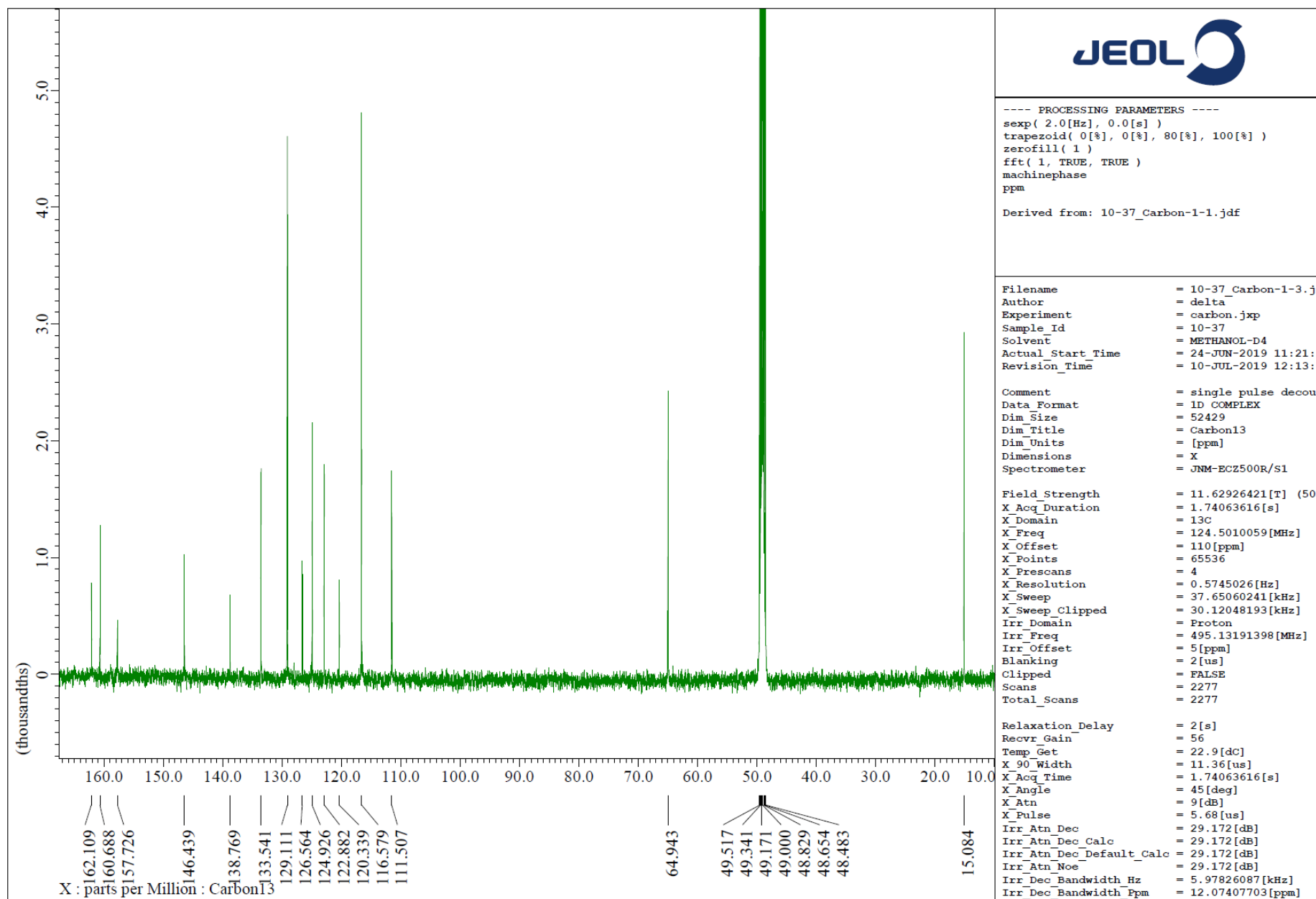


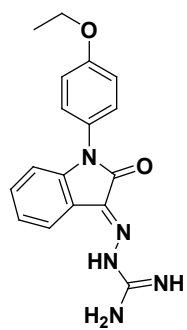
5e



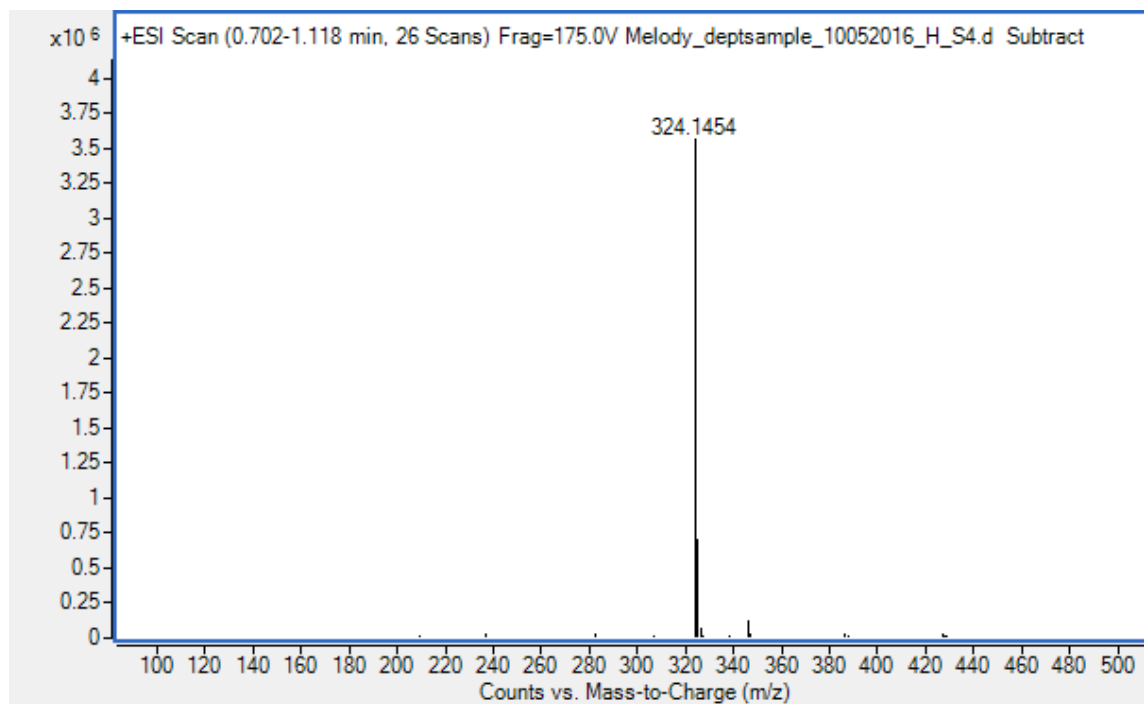


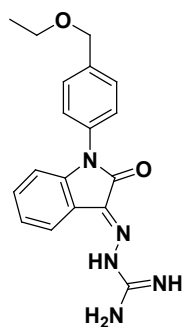
5e



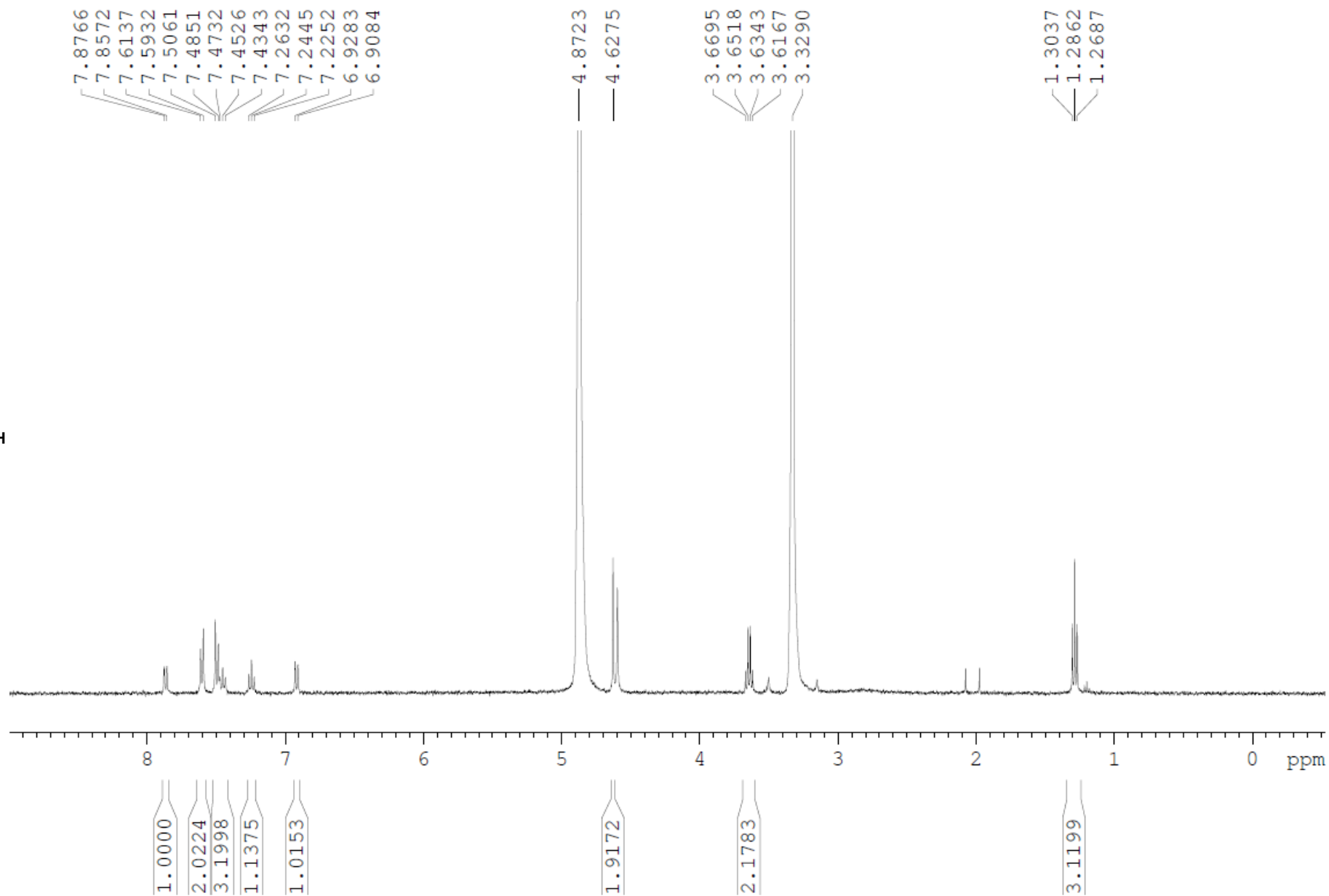


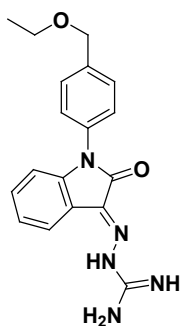
**5e**



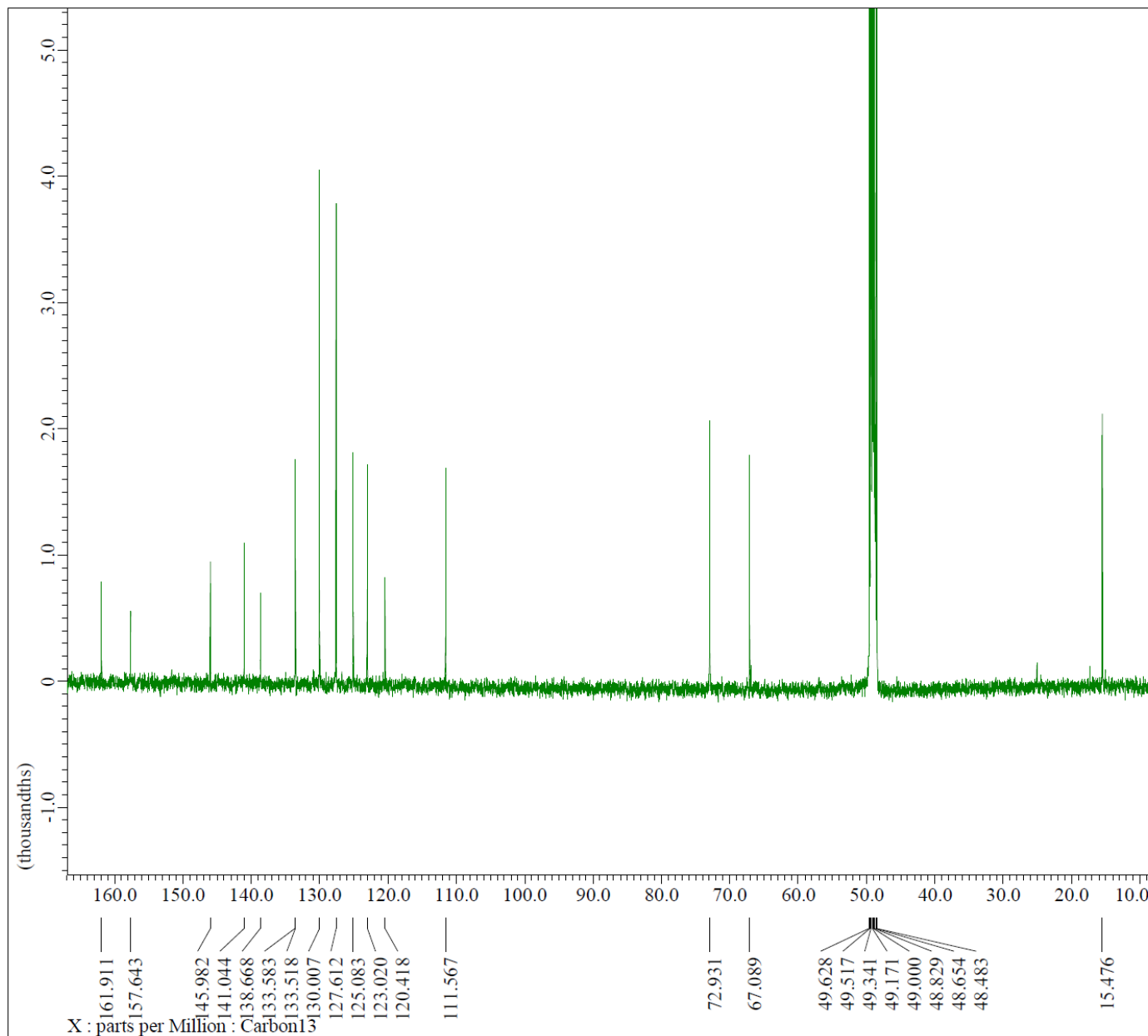


5f





5f



----- PROCESSING PARAMETERS -----  
 sexp( 2.0[Hz], 0.0[s] )  
 trapezoid( 0[%], 0[%], 80[%], 100[%] )  
 zerofill( 1 )  
 fft( 1, TRUE, TRUE )  
 machinephase  
 ppm

Derived from: 10-39\_Carbon-1-1.jdf

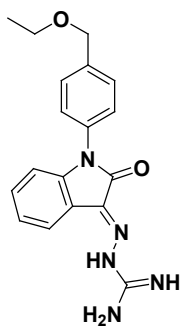
Filename = 10-39\_Carbon-1-3.j  
 Author = delta  
 Experiment = carbon.jxp  
 Sample\_Id = 10-39  
 Solvent = METHANOL-D4  
 Actual\_Start\_Time = 24-JUN-2019 13:57:  
 Revision\_Time = 10-JUL-2019 12:22:

Comment = single pulse decou  
 Data\_Format = 1D COMPLEX  
 Dim\_Size = 52429  
 Dim\_Title = Carbon13  
 Dim\_Units = [ppm]  
 Dimensions = X  
 Spectrometer = JNM-ECZ500R/S1

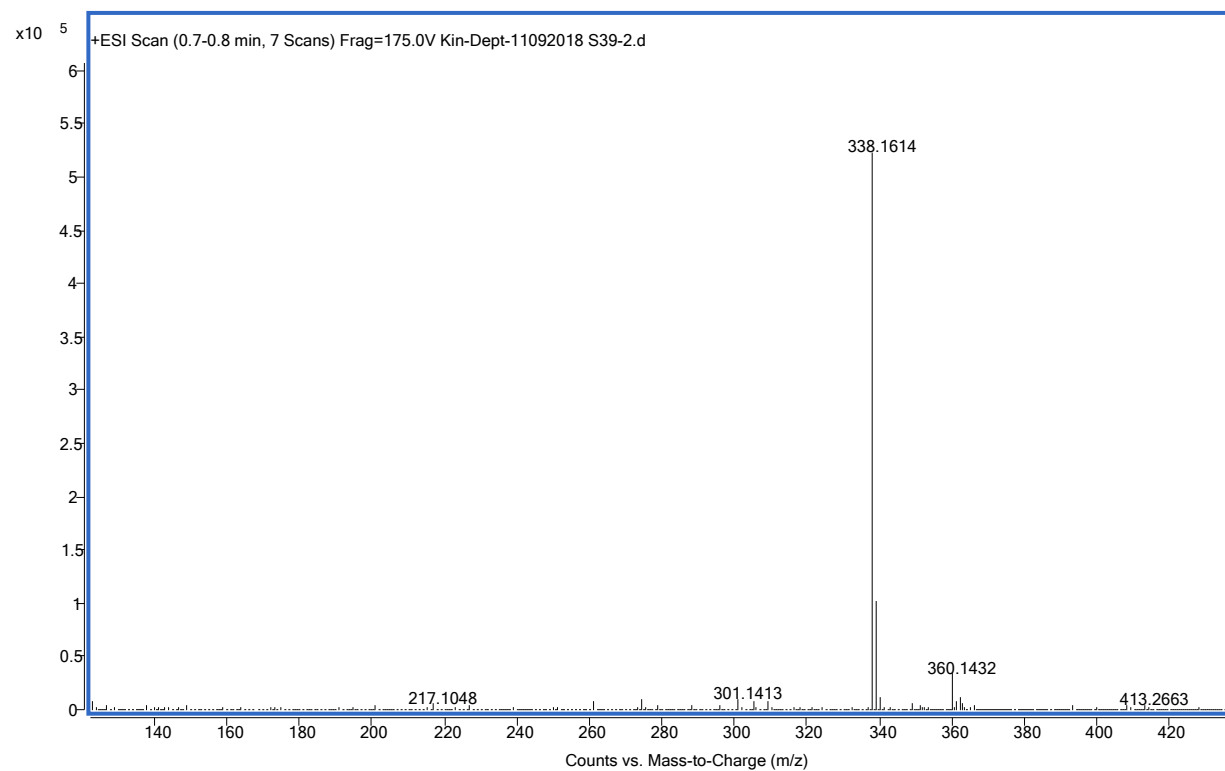
Field\_Strength = 11.62926421[T] (50  
 X\_Acq\_Duration = 1.74063616[s]  
 X\_Domain = 13c  
 X\_Freq = 124.5010059[MHz]  
 X\_Offset = 110[ppm]  
 X\_Points = 65536  
 X\_Prescans = 4  
 X\_Resolution = 0.5745026[Hz]  
 X\_Sweep = 37.65060241[kHz]  
 X\_Sweep\_Clipped = 30.12048193[kHz]  
 Irr\_Domain = Proton  
 Irr\_Freq = 495.13191398[MHz]  
 Irr\_Offset = 5[ppm]  
 Blanking = 2[us]  
 Clipped = FALSE  
 Scans = 2859  
 Total\_Scans = 2859

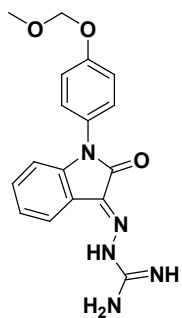
Relaxation\_Delay = 2[s]  
 Recvr\_Gain = 56  
 Temp\_Get = 22.9[dC]  
 X\_90\_Width = 11.36[us]  
 X\_Acq\_Time = 1.74063616[s]  
 X\_Angle = 45[deg]  
 X\_Atn = 9[dB]  
 X\_Pulse = 5.68[us]  
 Irr\_Atn\_Dec = 29.172[dB]  
 Irr\_Atn\_Dec\_Calc = 29.172[dB]  
 Irr\_Atn\_Dec\_Default\_Calc = 29.172[dB]  
 Irr\_Atn\_No = 29.172[dB]  
 Irr\_Dec\_Bandwidth\_Hz = 5.97826087[kHz]  
 Irr\_Dec\_Bandwidth\_Ppm = 12.07407703[ppm]



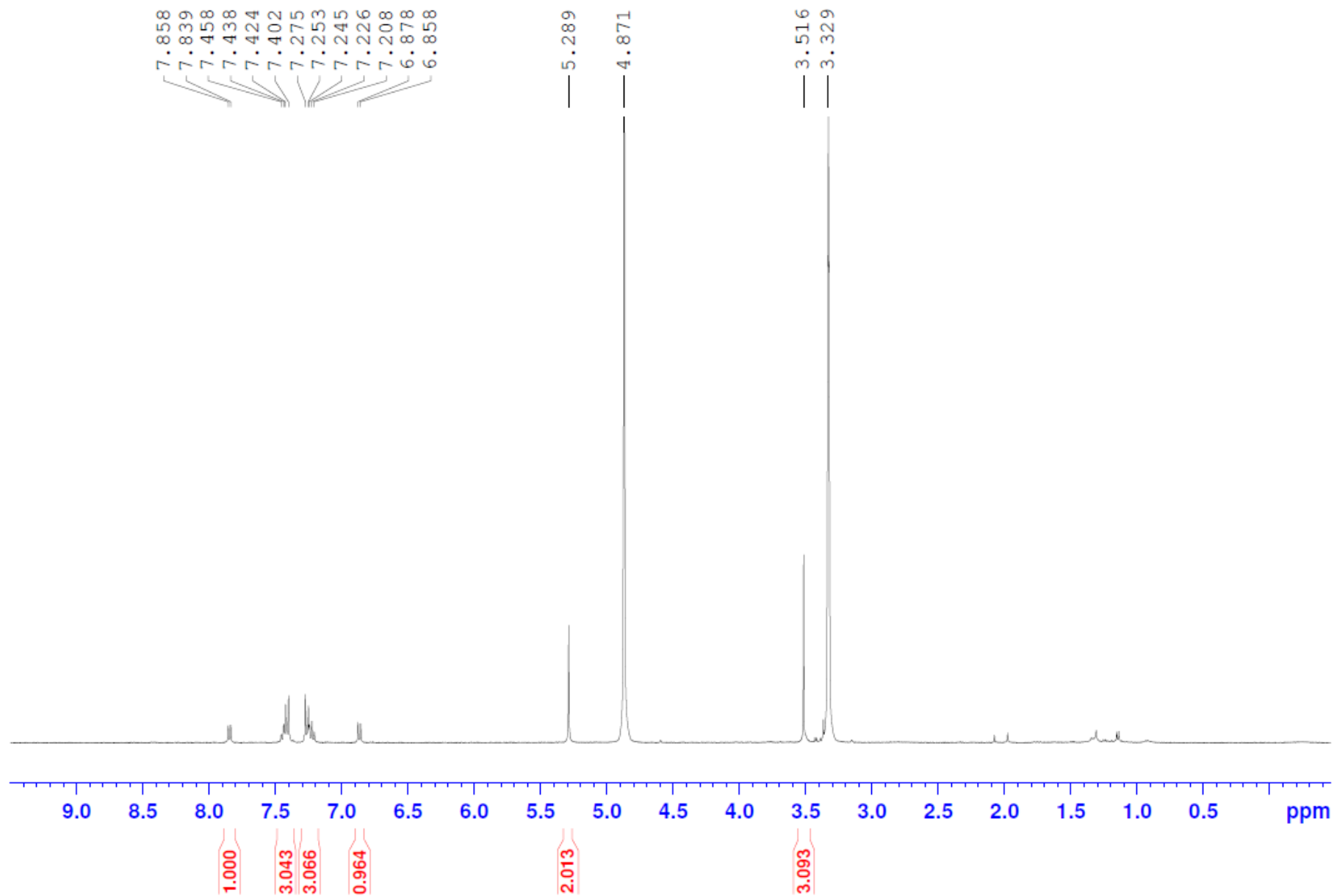


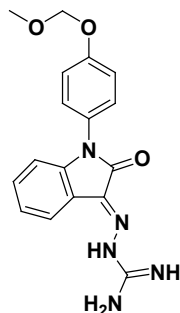
**5f**



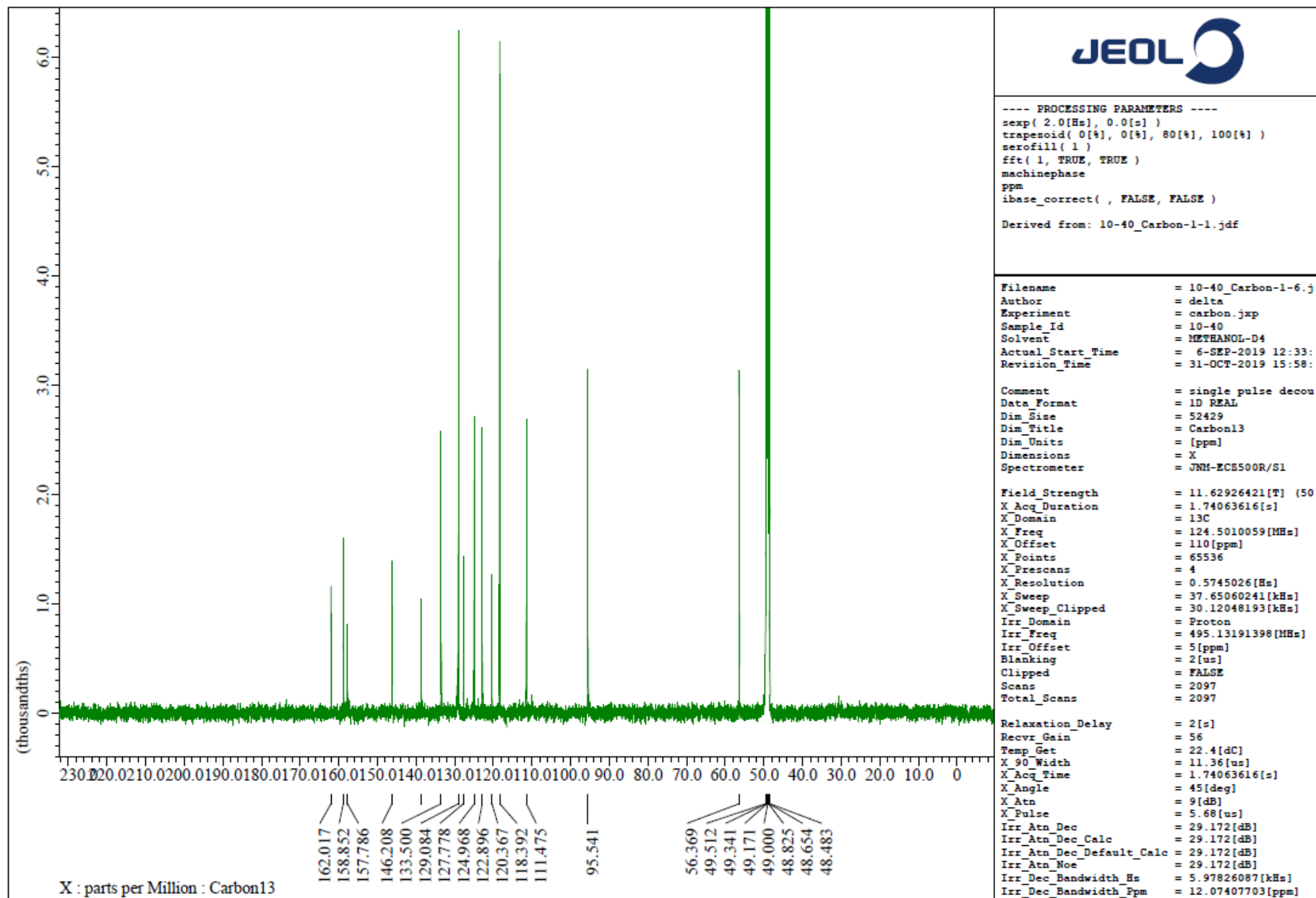


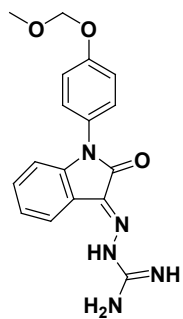
5g



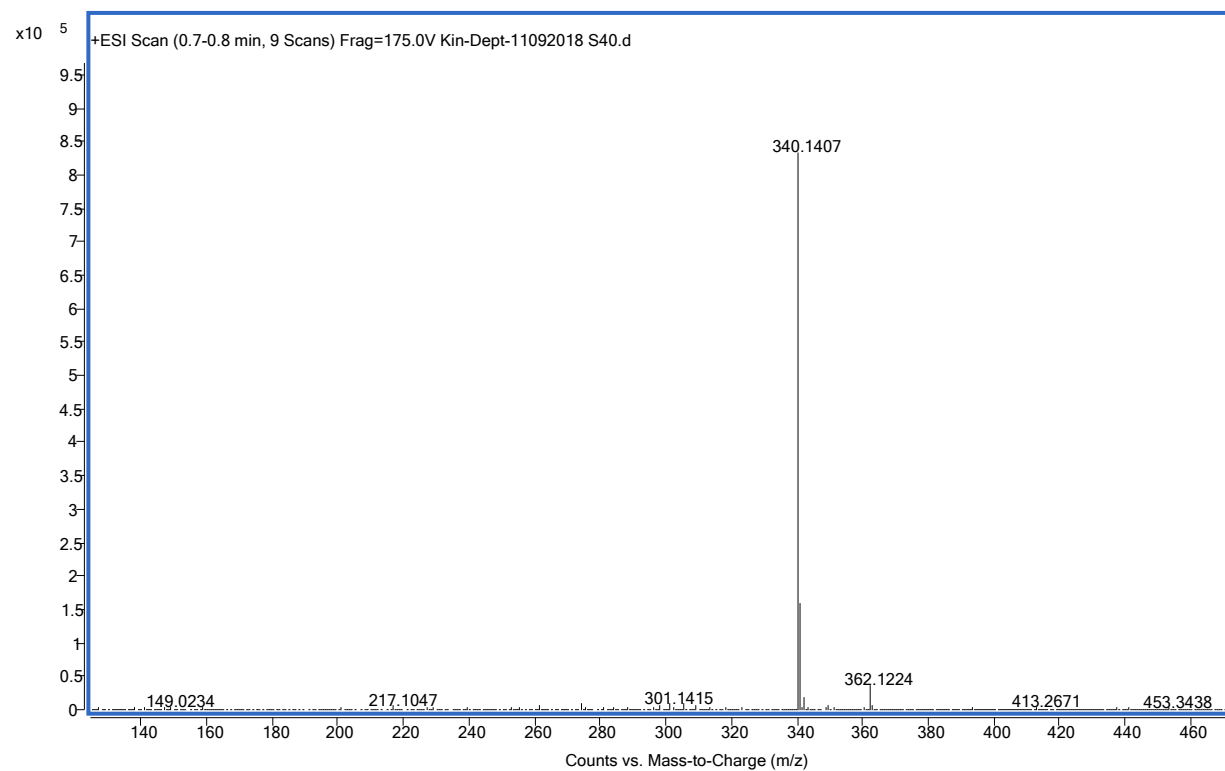


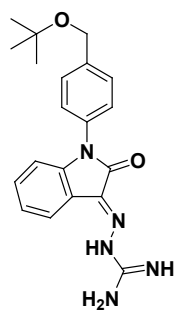
5g



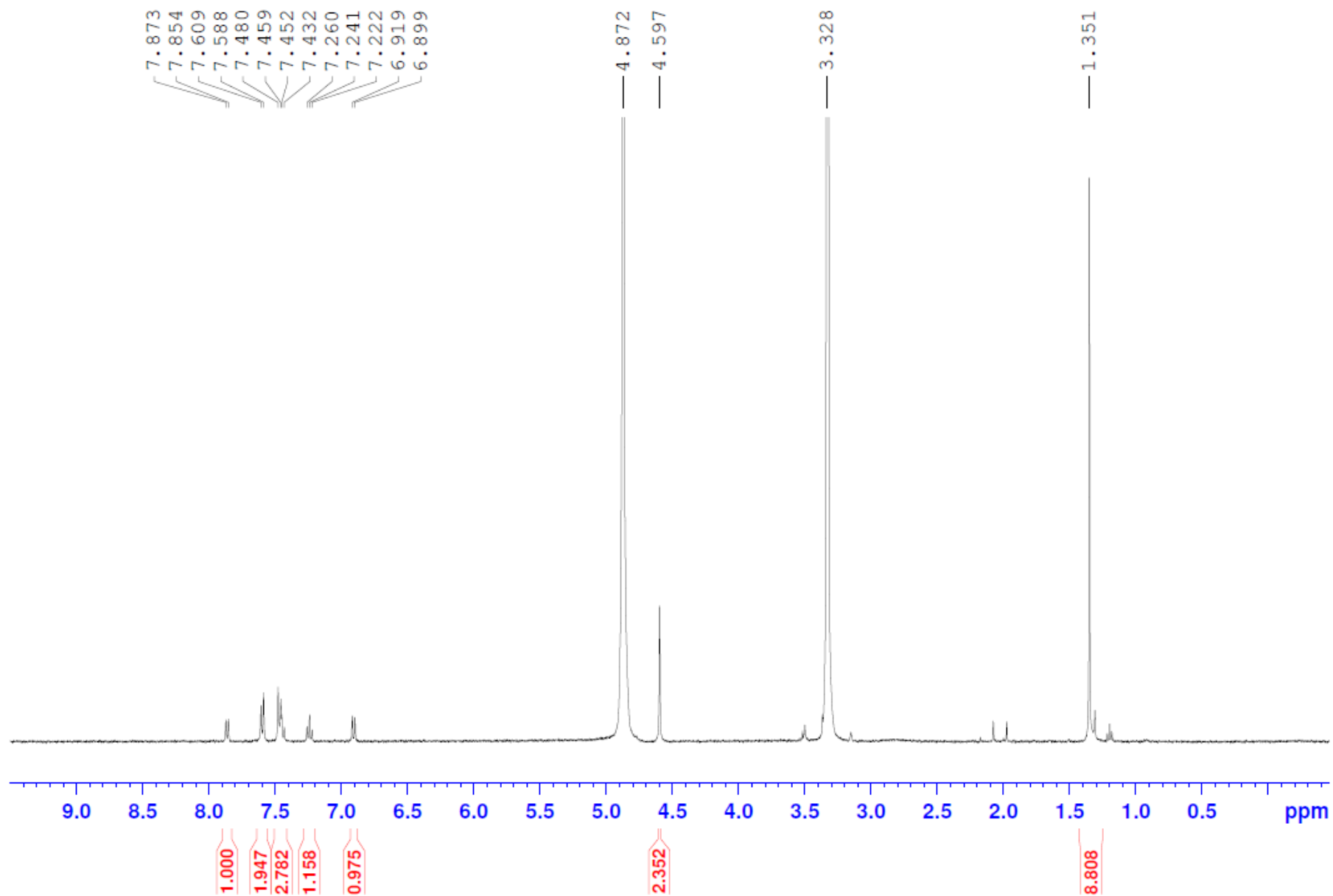


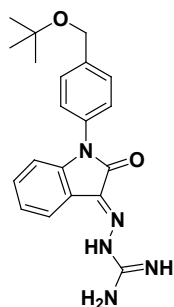
**5g**



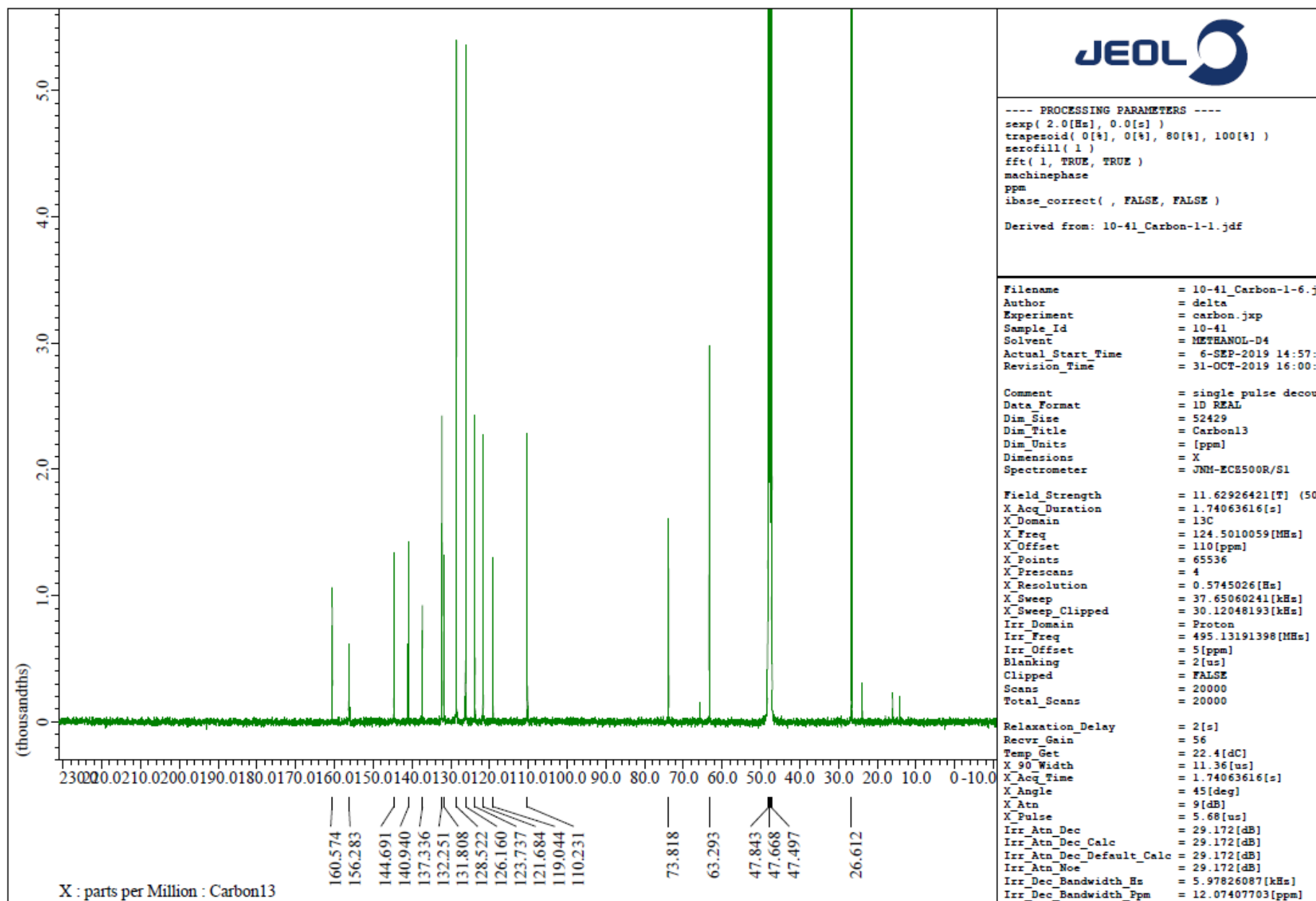


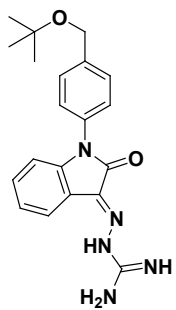
5h



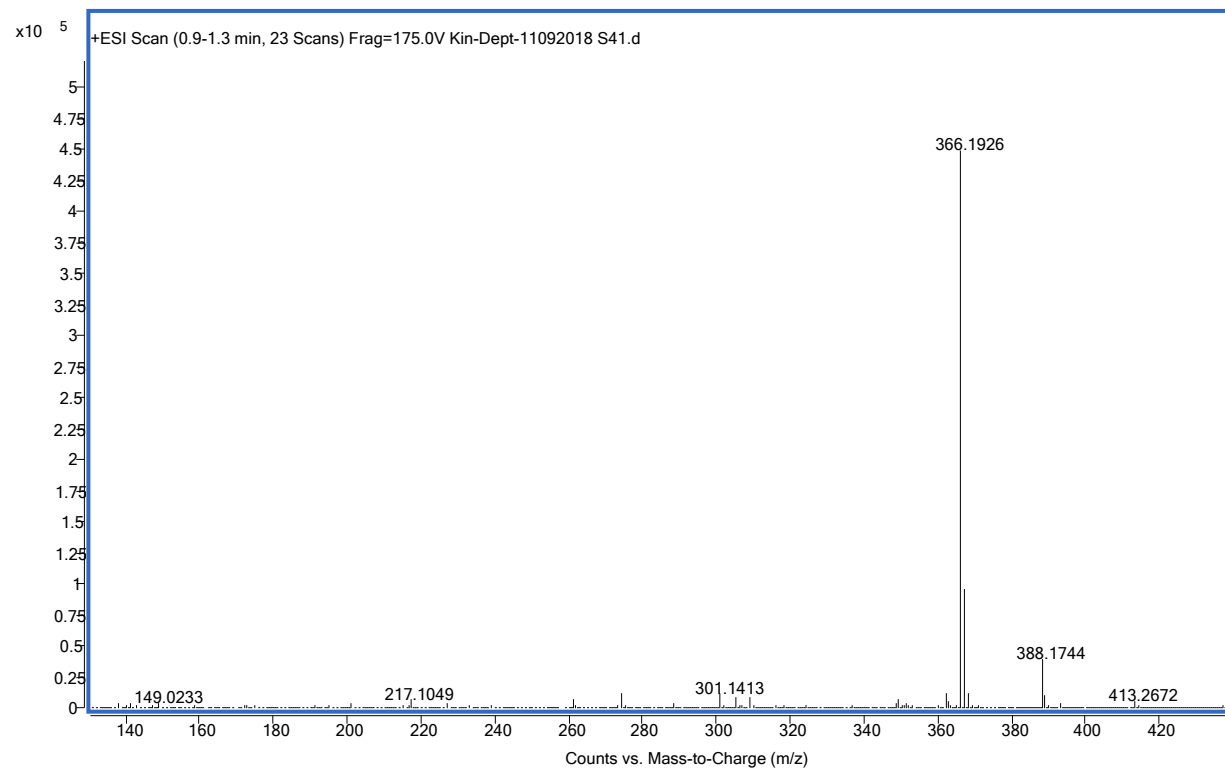


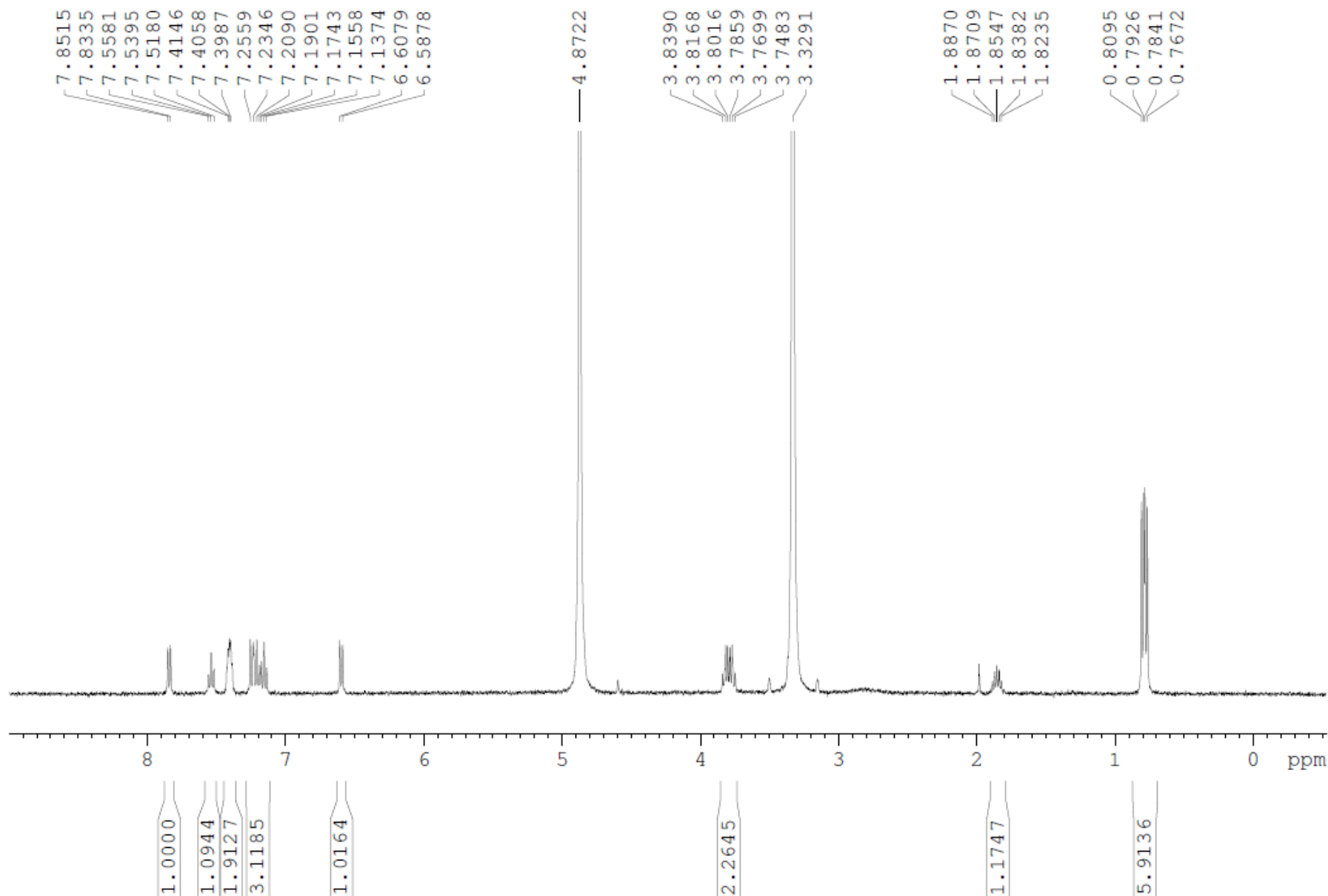
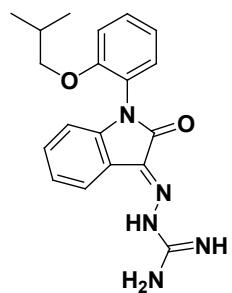
5h



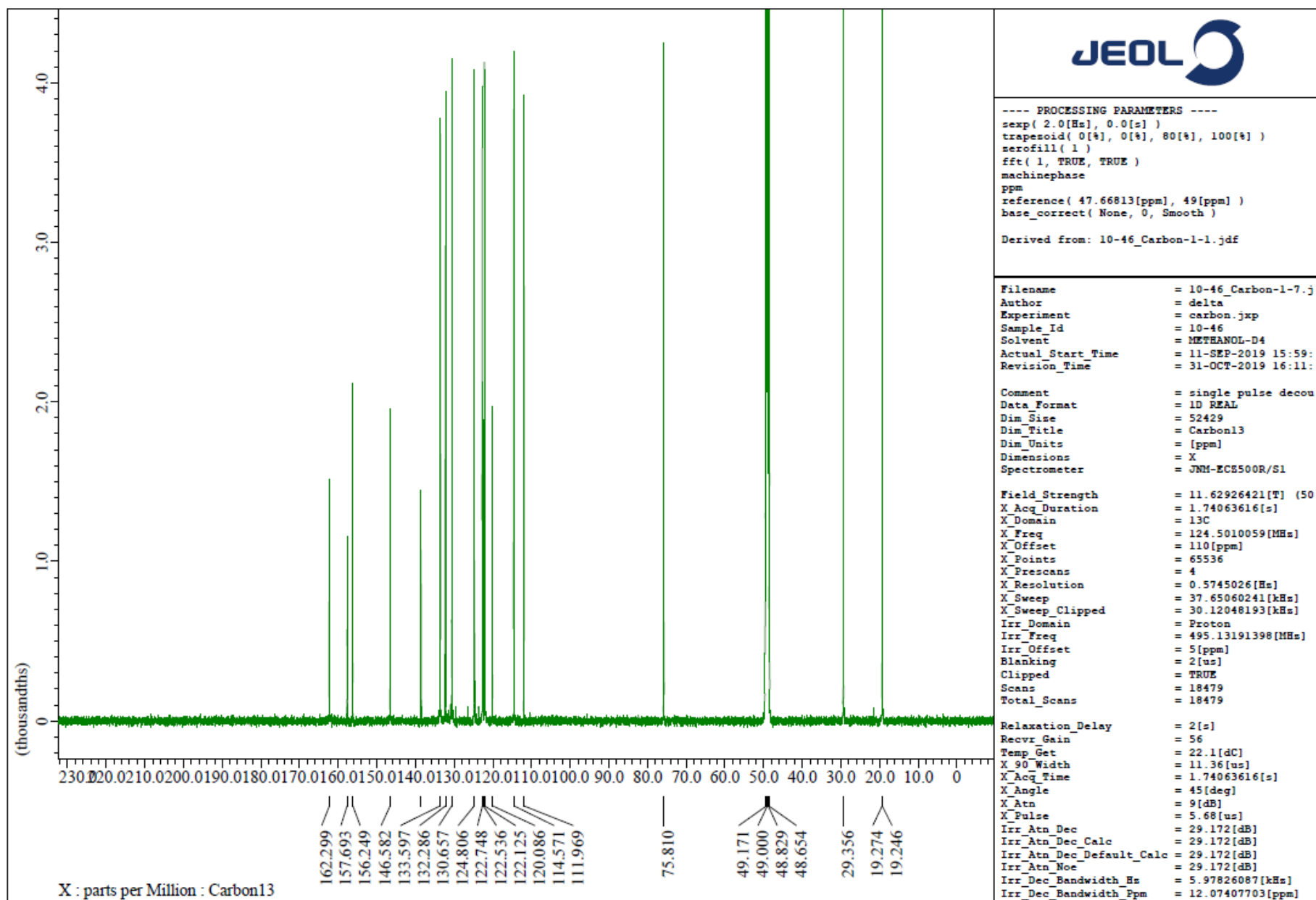
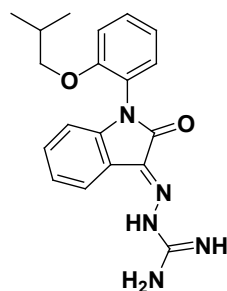


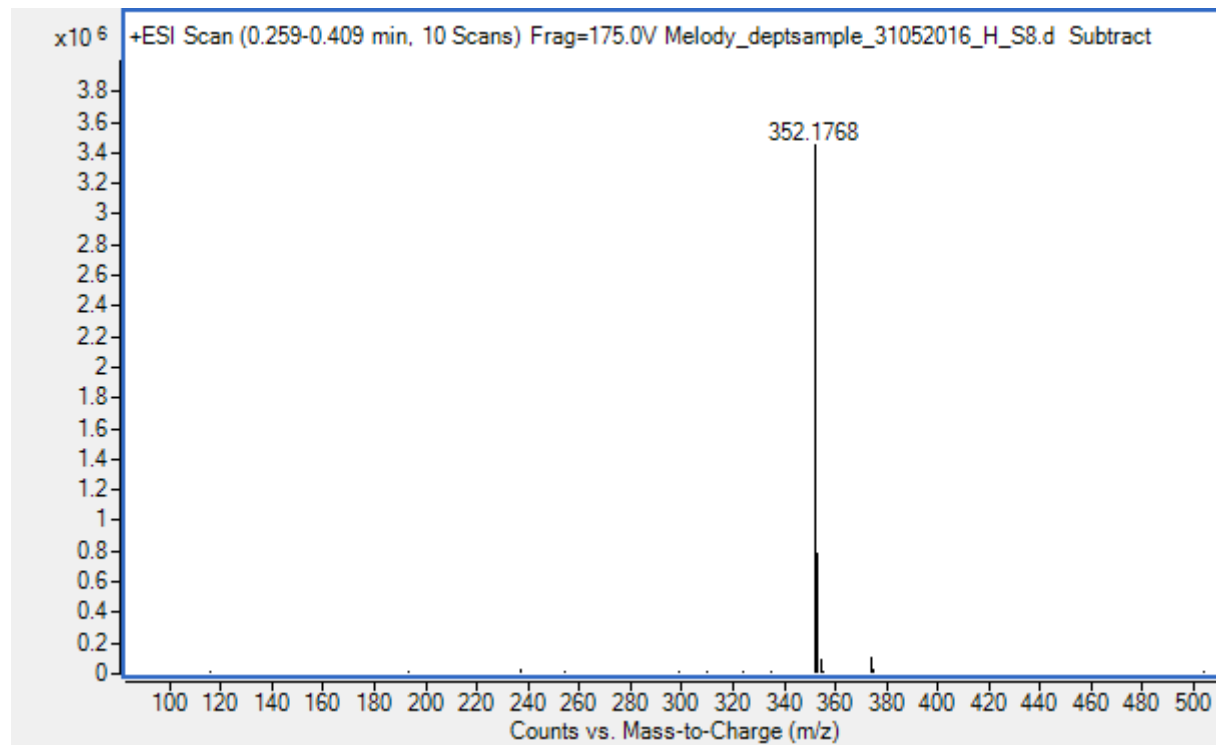
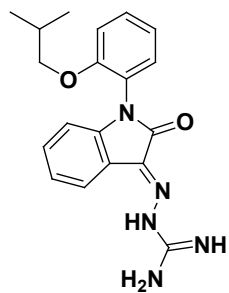
**5h**

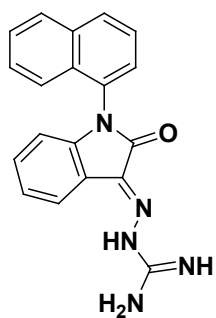




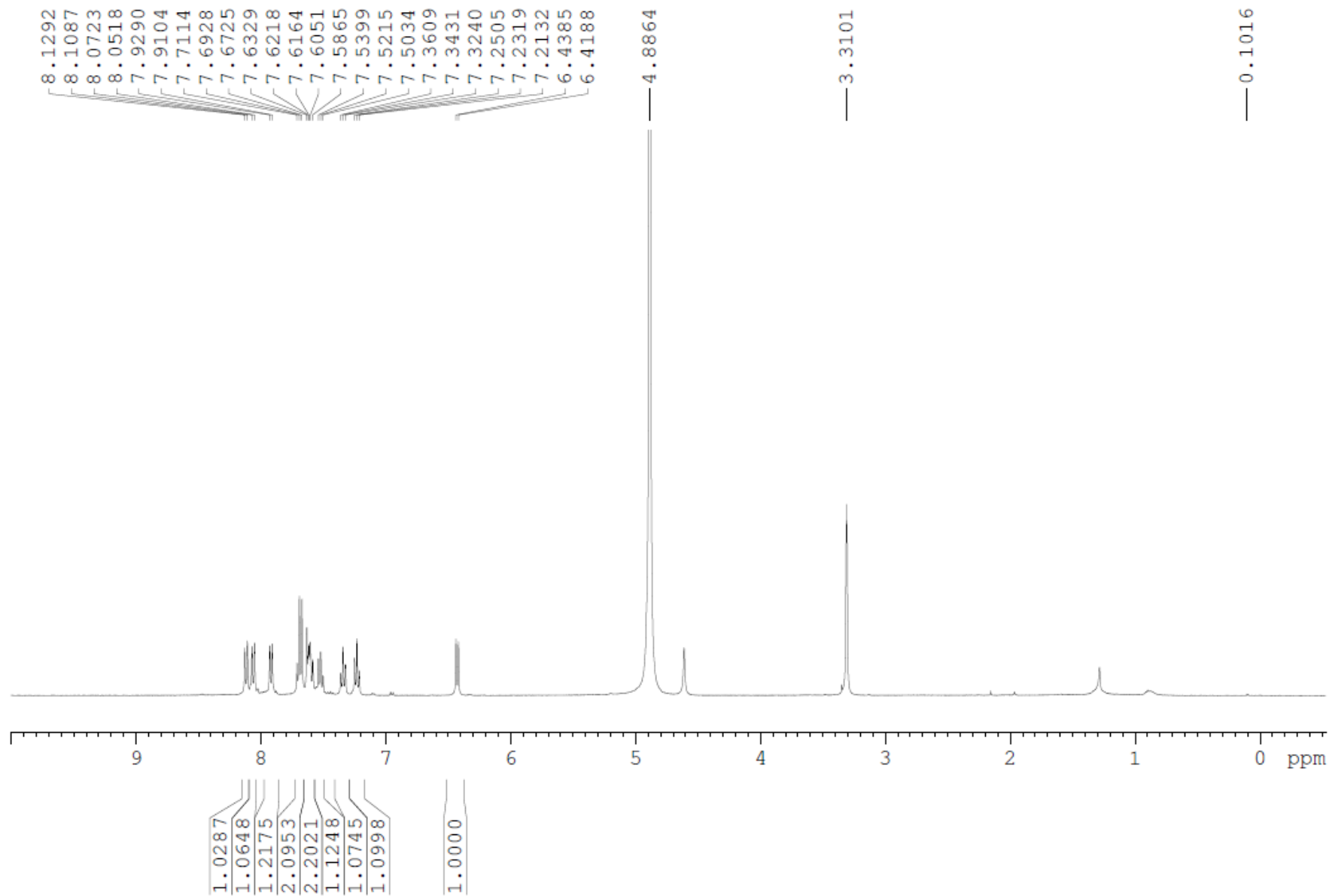


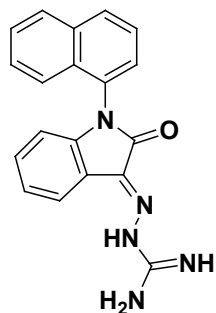




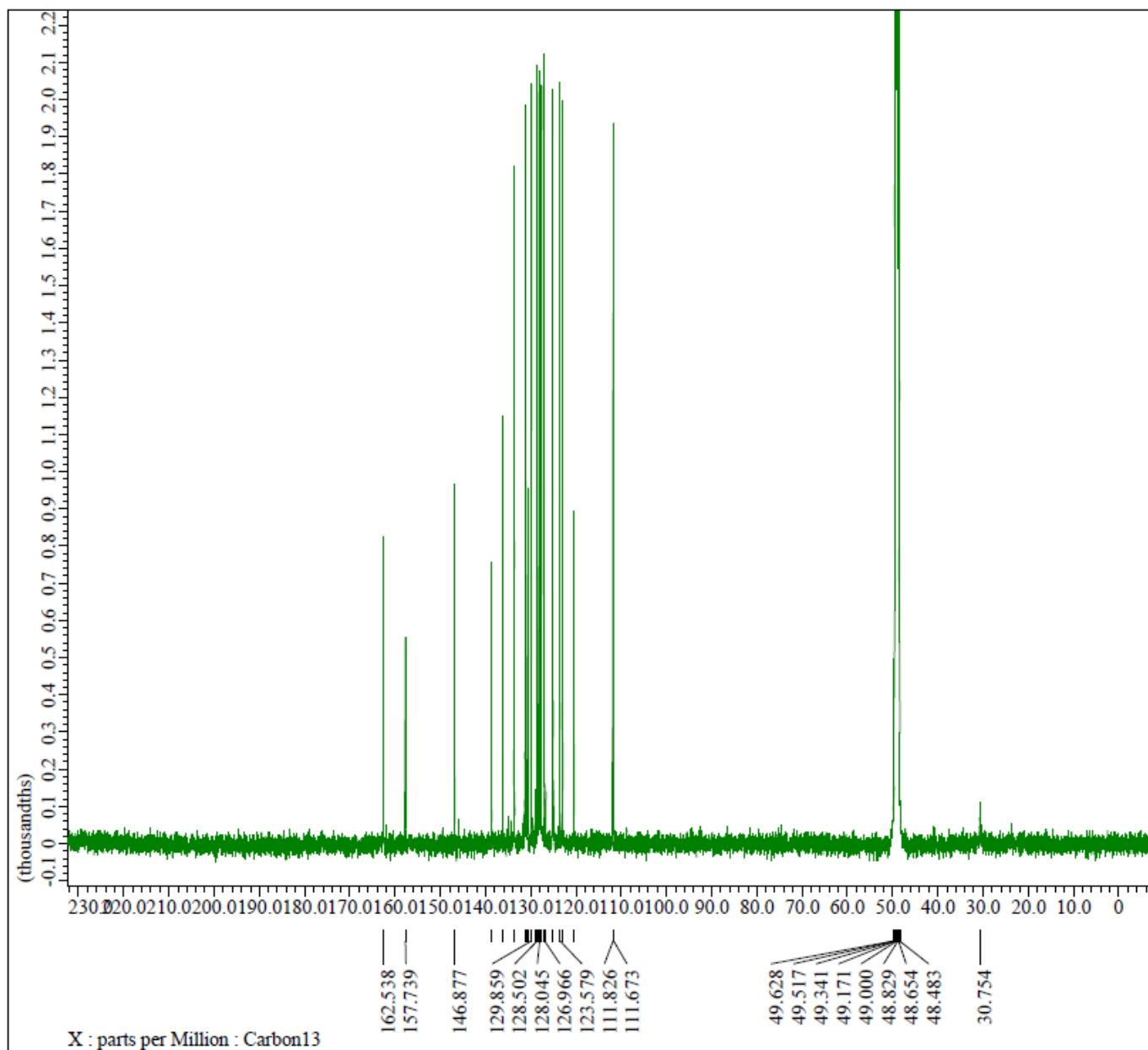


5j





5j



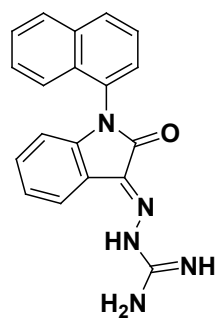
----- PROCESSING PARAMETERS -----  
 sexp( 2.0[Hs], 0.0[s] )  
 trapezoid( 0[%], 0[%], 80[%], 100[%] )  
 zerofill( 1 )  
 fft( 1, TRUE, TRUE )  
 machinephase  
 ppm  
 ibase\_correct( , FALSE, FALSE )  
 Derived from: 10-35\_Carbon-1-1.jdf

Filename = 10-35\_Carbon-1-6.j  
 Author = delta  
 Experiment = carbon.jxp  
 Sample\_Id = 10-35  
 Solvent = METHANOL-D4  
 Actual\_Start\_Time = 5-SEP-2019 13:45:  
 Revision\_Time = 31-OCT-2019 15:56:

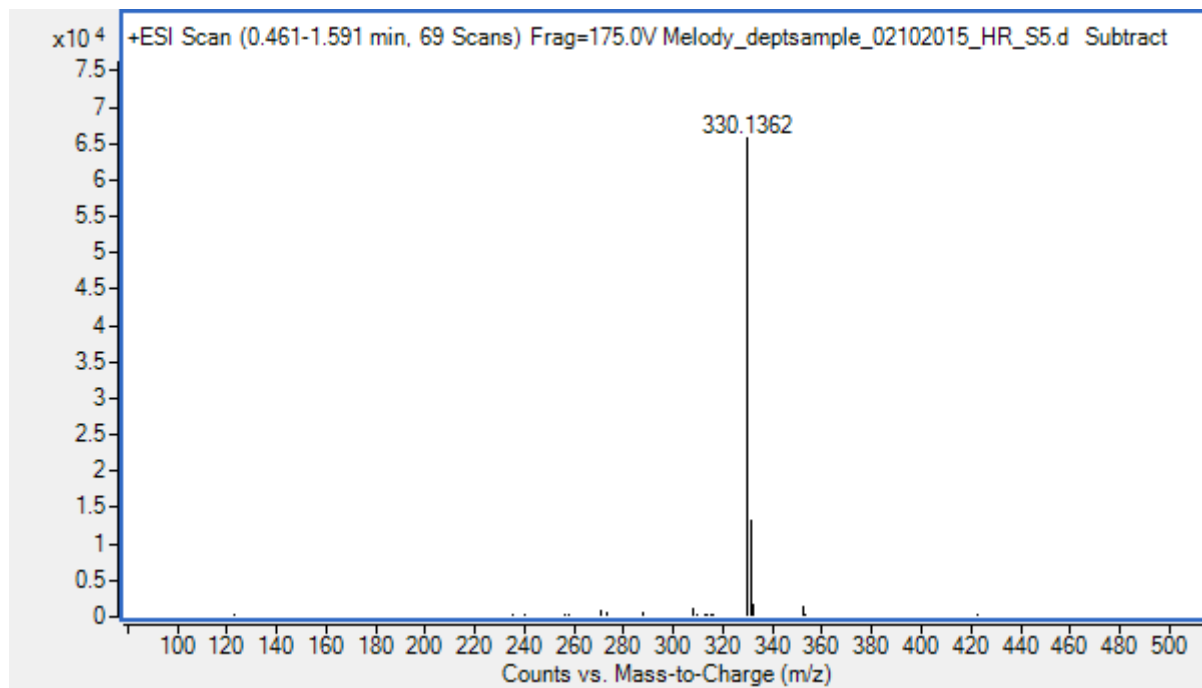
Comment = single pulse decou  
 Data\_Format = 1D REAL  
 Dim\_Size = 52429  
 Dim\_Title = Carbon13  
 Dim\_Units = [ppm]  
 Dimensions = X  
 Spectrometer = JNM-ECS500R/S1

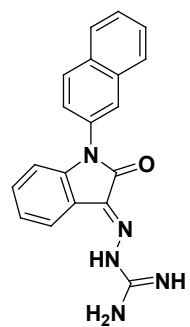
Field\_Strength = 11.62926421[T] (50  
 X\_Acq\_Duration = 1.74063616[s]  
 X\_Domain = 13C  
 X\_Freq = 124.5010059[MHz]  
 X\_Offset = 110[ppm]  
 X\_Points = 65536  
 X\_Prescans = 4  
 X\_Resolution = 0.5745026[Hs]  
 X\_Sweep = 37.65060241[kHz]  
 X\_Sweep\_Clippped = 30.12048193[kHz]  
 Irr\_Domain = Proton  
 Irr\_Freq = 495.13191398[MHz]  
 Irr\_Offset = 5[ppm]  
 Blanking = 2[us]  
 Clipped = FALSE  
 Scans = 20000  
 Total\_Scans = 20000

Relaxation\_Delay = 2[s]  
 Recvr\_Gain = 56  
 Temp\_Get = 22.4[dC]  
 X\_90\_Width = 11.36[us]  
 X\_Acq\_Time = 1.74063616[s]  
 X\_Angle = 45[deg]  
 X\_Atn = 9[dB]  
 X\_Pulse = 5.68[us]  
 Irr\_Atn\_Dec = 29.172[dB]  
 Irr\_Atn\_Dec\_Calc = 29.172[dB]  
 Irr\_Atn\_Dec\_Default\_Calc = 29.172[dB]  
 Irr\_Atn\_Noe = 29.172[dB]  
 Irr\_Dec\_Bandwidth\_Hz = 5.97826087[kHz]  
 Irr\_Dec\_Bandwidth\_Ppm = 12.07407703[ppm]

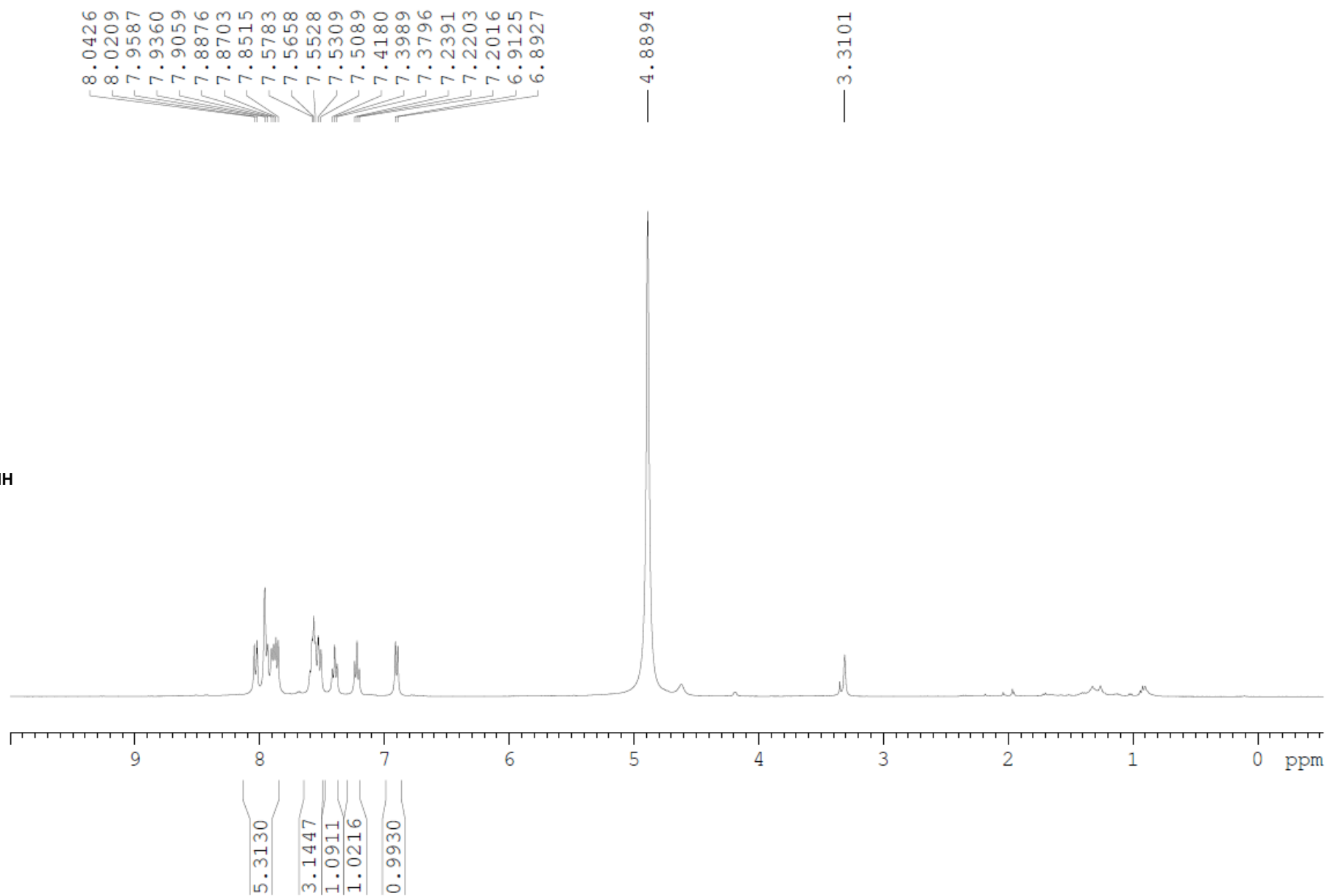


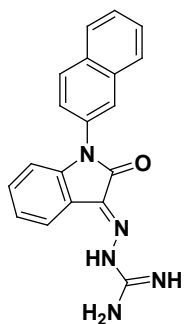
**5j**



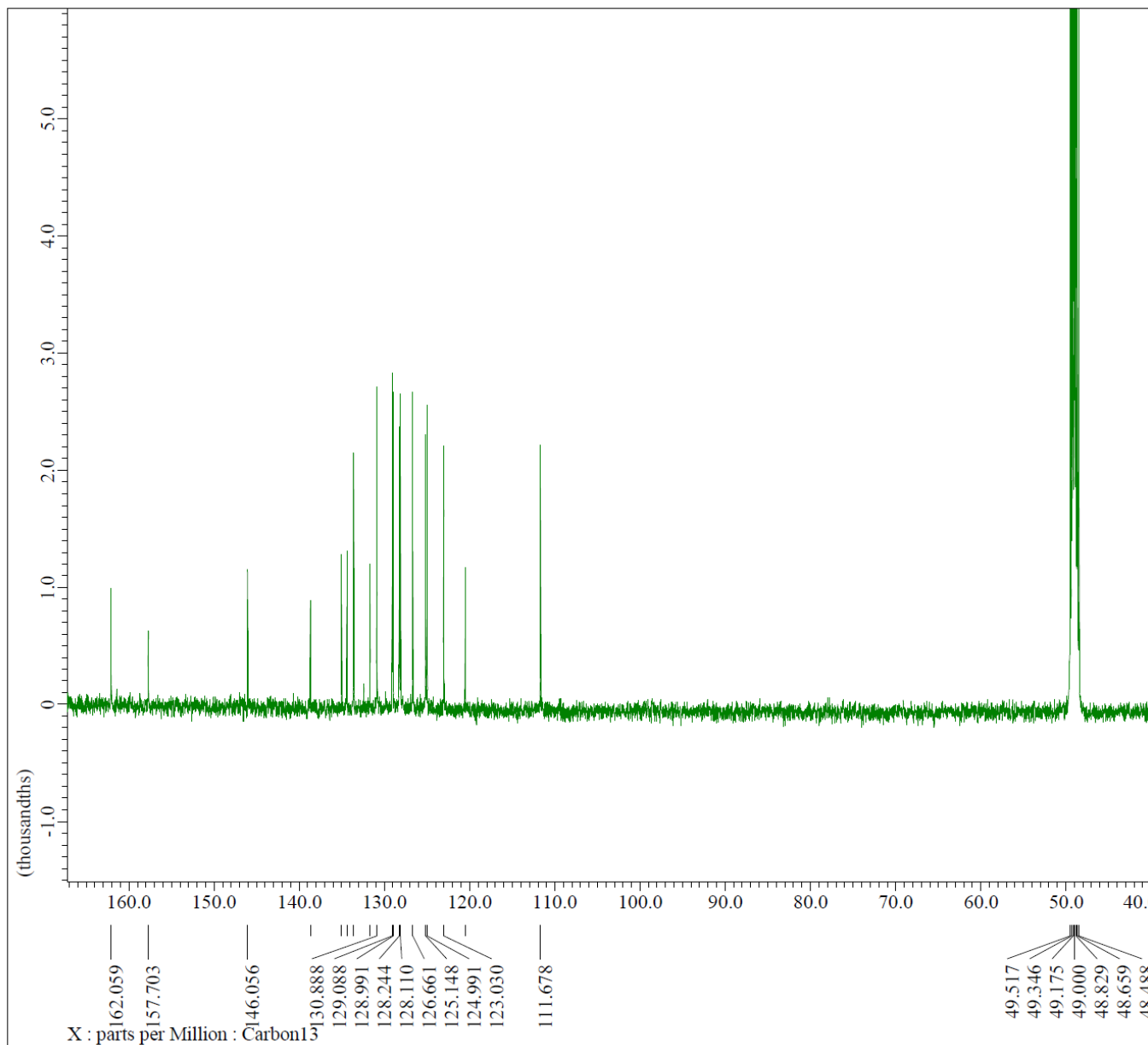


5k

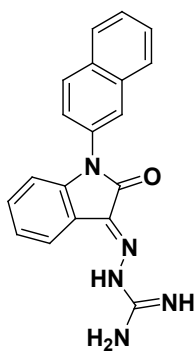




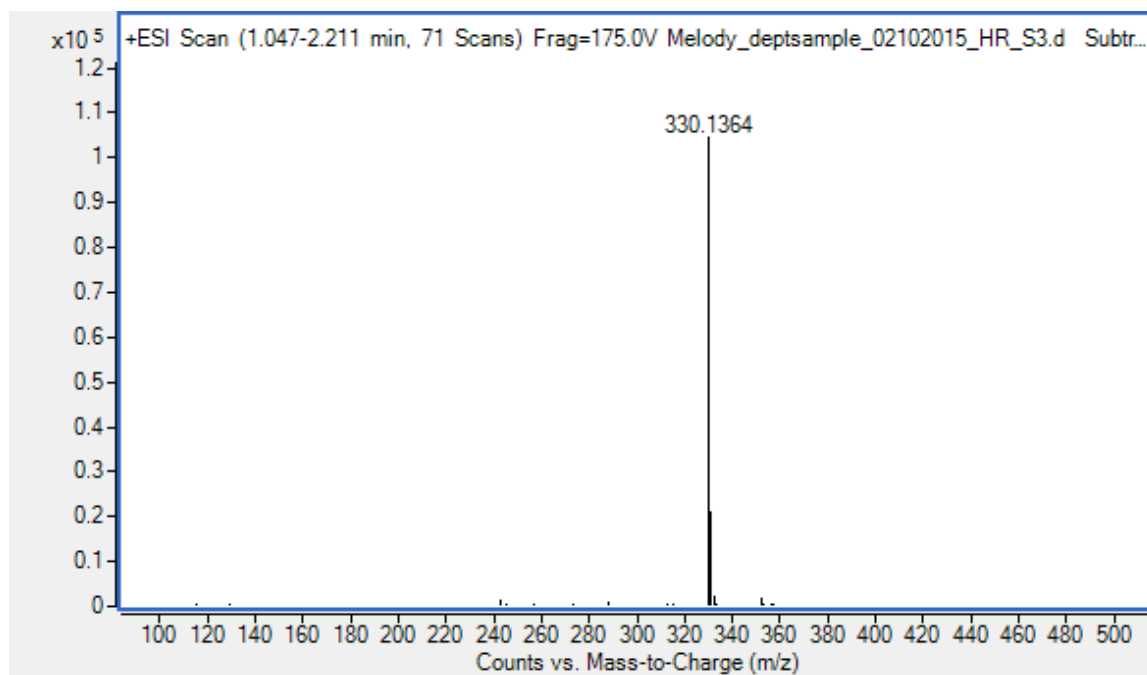
5k



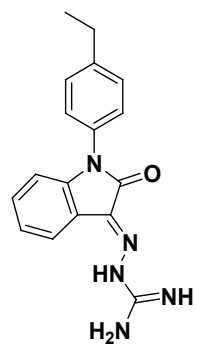
<pre> ----- PROCESSING PARAMETERS ----- sexp( 2.0[Hz], 0.0[s] ) trapezoid( 0[%], 0[%], 80[%], 100[%] ) zerofill( 1 ) fft( 1, TRUE, TRUE ) machinephase ppm Derived from: 10-36_Carbon-2-1.jdf </pre>	
Filename	= 10-36_Carbon-2-4.j
Author	= delta
Experiment	= carbon.jxp
Sample Id	= 10-36
Solvent	= METHANOL-D4
Actual Start Time	= 25-JUN-2019 13:54:
Revision Time	= 10-JUL-2019 12:11:
Comment	= single pulse decou
Data Format	= 1D COMPLEX
Dim Size	= 52429
Dim Title	= Carbon13
Dim Units	= [ppm]
Dimensions	= X
Spectrometer	= JNM-ECZ500R/S1
Field Strength	= 11.62926421[T] (50
X Acq_Duration	= 1.74063616[s]
X_Domain	= 13C
X_Freq	= 124.5010059[MHz]
X_Offset	= 110[ppm]
X Points	= 65536
X Prescans	= 4
X Resolution	= 0.5745026[Hz]
X Sweep	= 37.65060241[kHz]
X Sweep_Clippped	= 30.12048193[kHz]
Irr_Domain	= Proton
Irr_Freq	= 495.13191398[MHz]
Irr_Offset	= 5[ppm]
Blanking	= 2[us]
Clipped	= FALSE
Scans	= 2111
Total_Scans	= 2111
Relaxation_Delay	= 2[s]
Recvr Gain	= 56
Temp_Get	= 22.8[dC]
X 90_Width	= 11.36[us]
X_Acq Time	= 1.74063616[s]
X_Angle	= 45[deg]
X_Atn	= 9[dB]
X_Pulse	= 5.68[us]
Irr_Atn_Dec	= 29.172[dB]
Irr_Atn_Dec_Calc	= 29.172[dB]
Irr_Atn_Dec_Default_Calc	= 29.172[dB]
Irr_Atn_No	= 29.172[dB]
Irr_Dec_Bandwidth_Hz	= 5.97826087[kHz]
Irr_Dec_Bandwidth_Fpm	= 12.07407703[ppm]



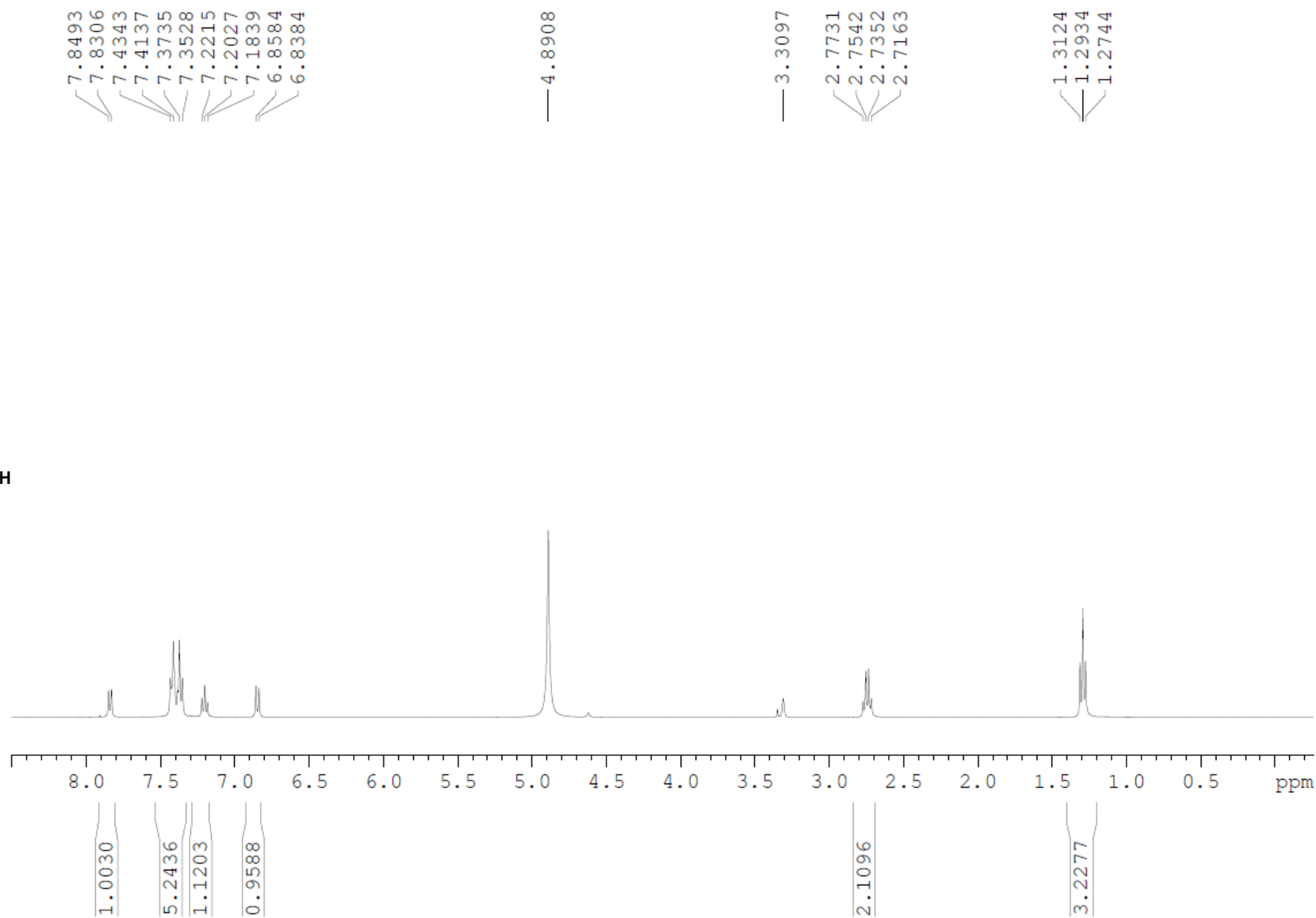
**5k**

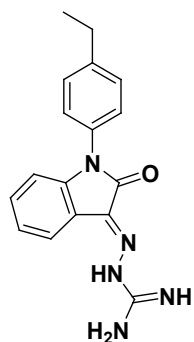




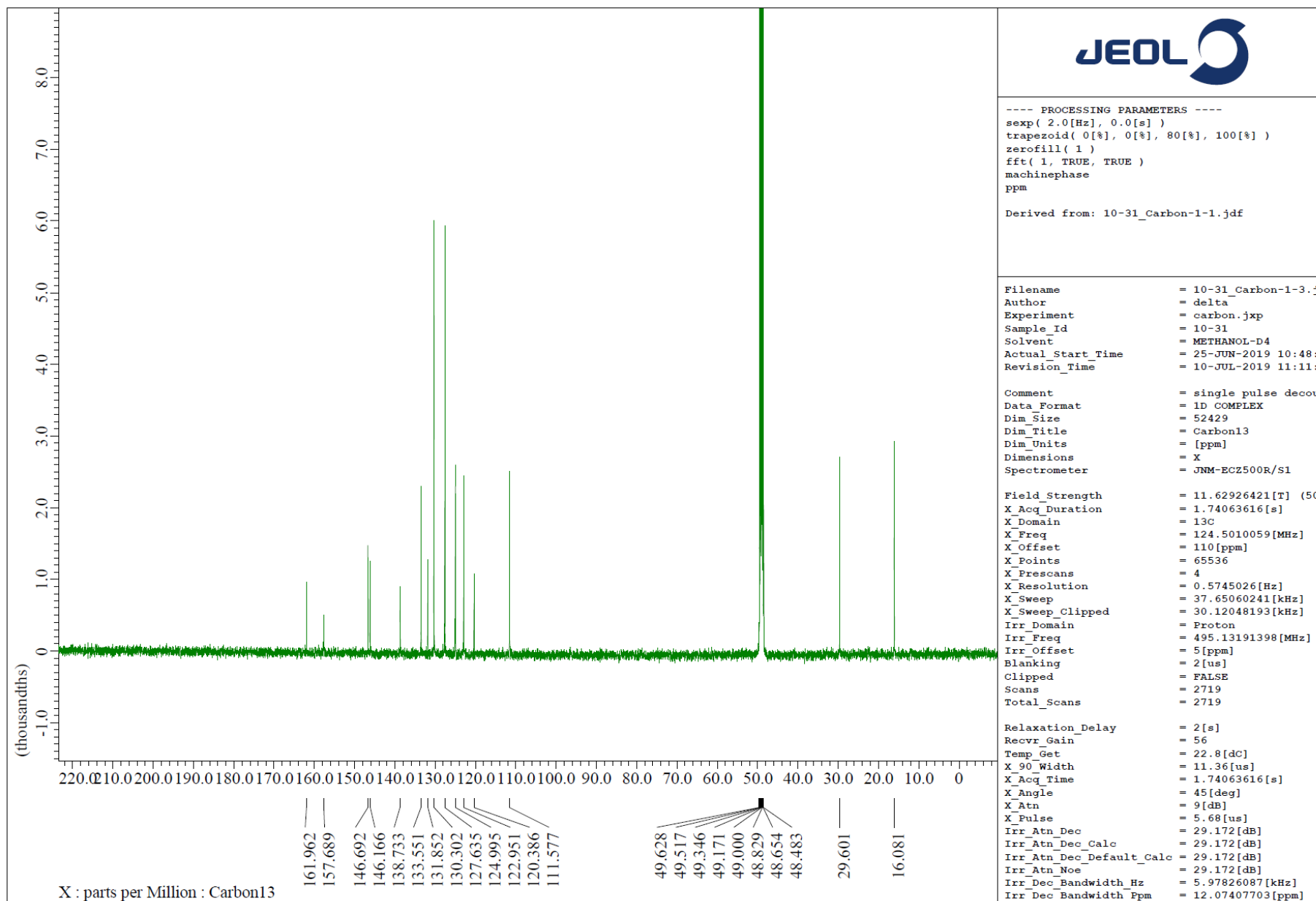


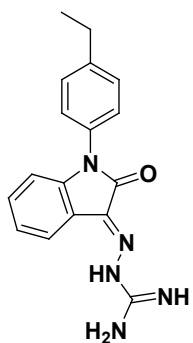
5l



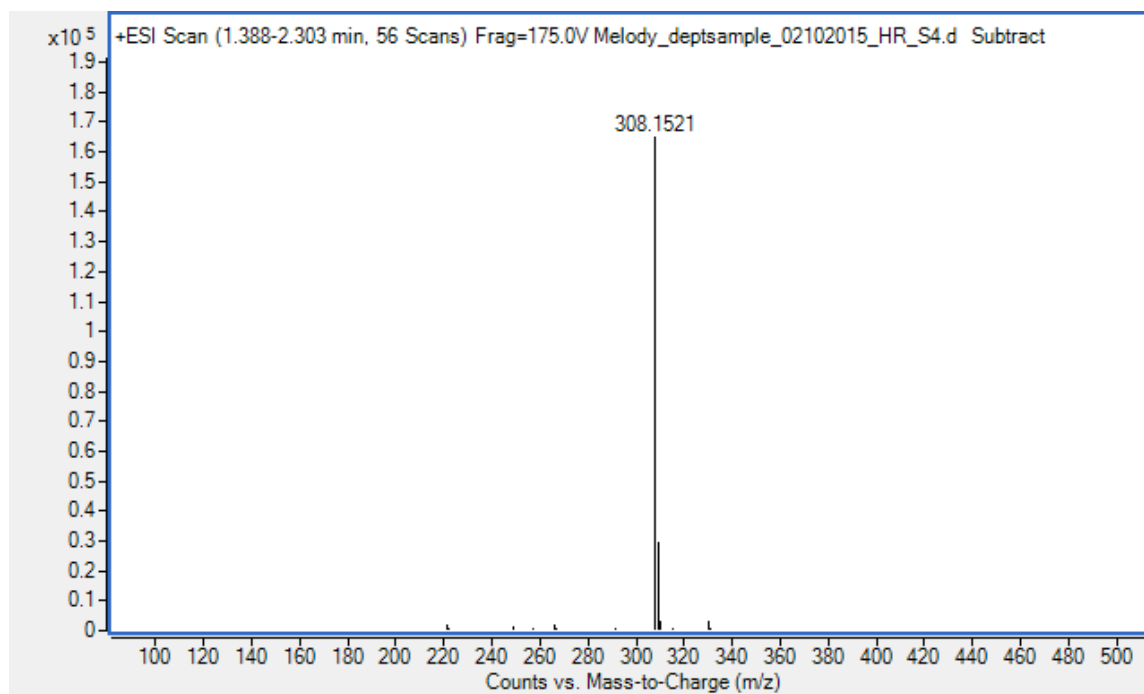


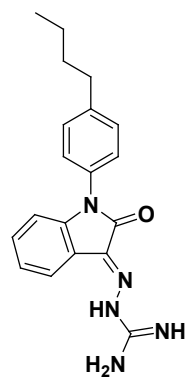
5l



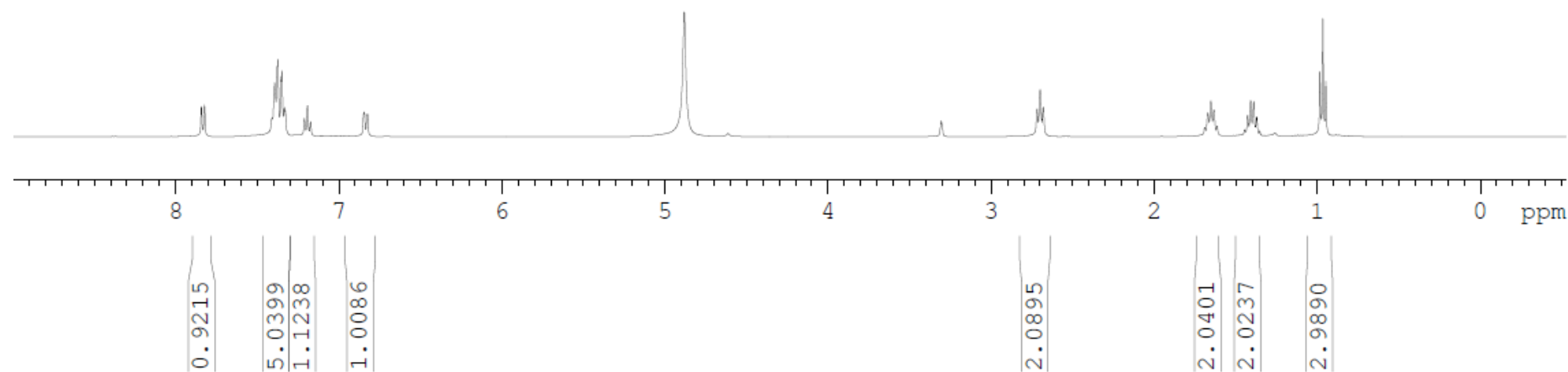


5l





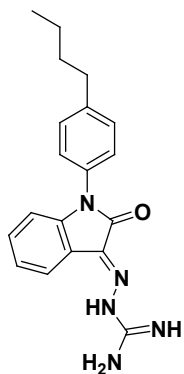
5m



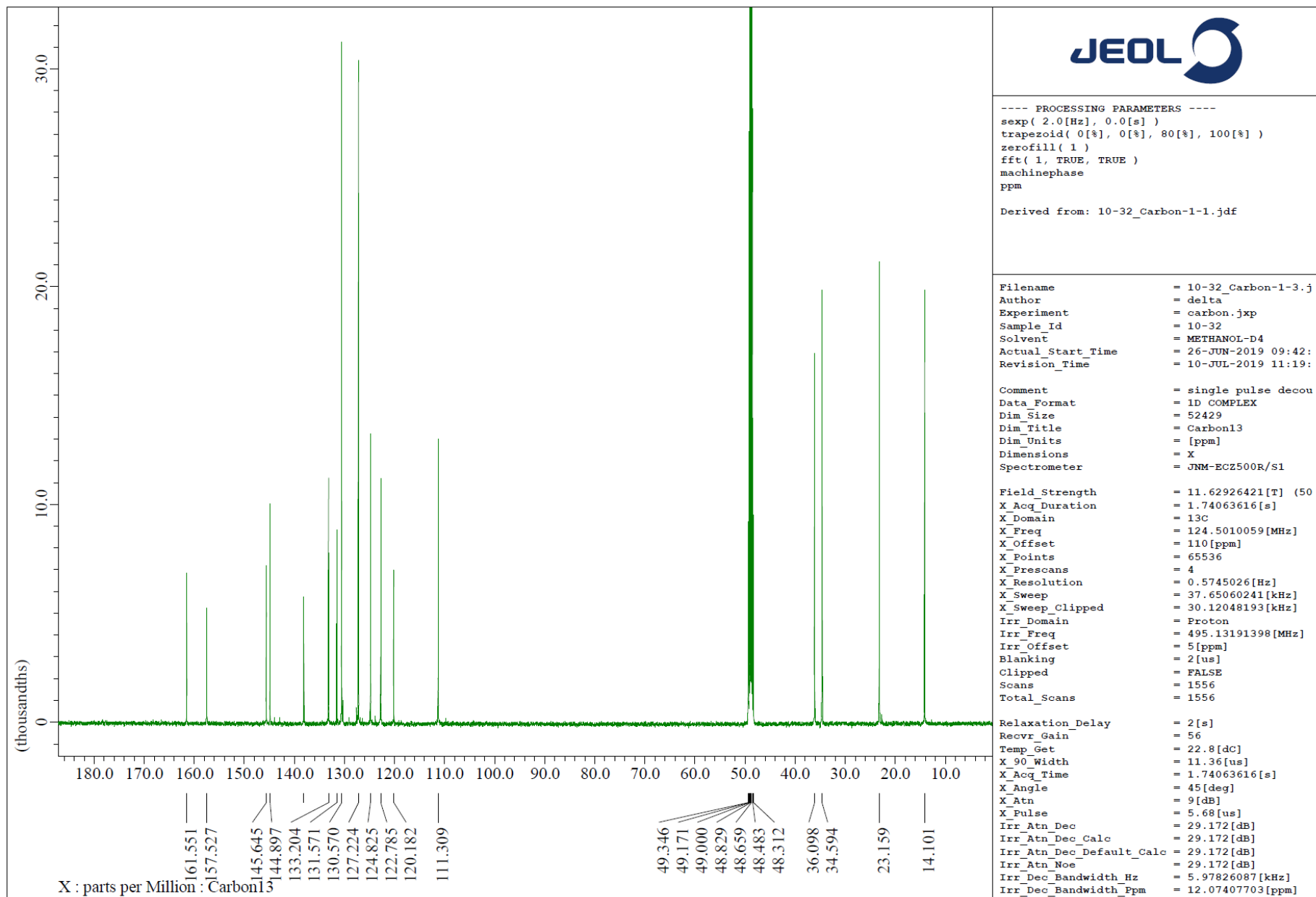
7.8425  
7.8238  
7.4108  
7.4077  
7.3937  
7.3783  
7.3737  
7.3543  
7.3484  
7.3332  
7.3278  
7.2113  
7.1923  
7.1735  
6.8438  
6.8239

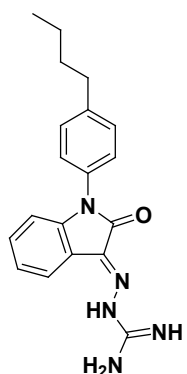
4.8820

3.3055  
2.7182  
2.6996  
2.6805  
1.6896  
1.6707  
1.6527  
1.6348  
1.6152  
1.4457  
1.4273  
1.4087  
1.3901  
1.3718  
1.3537  
0.9844  
0.9660  
0.9477

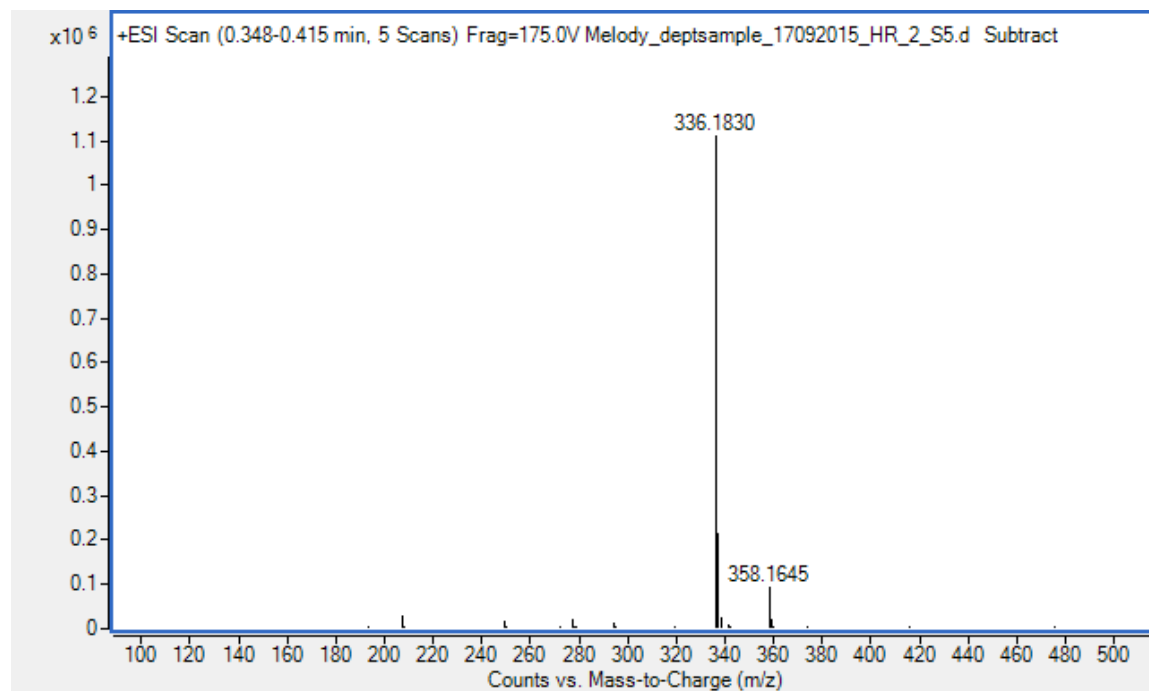


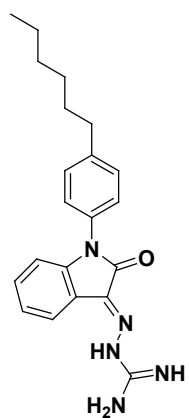
5m



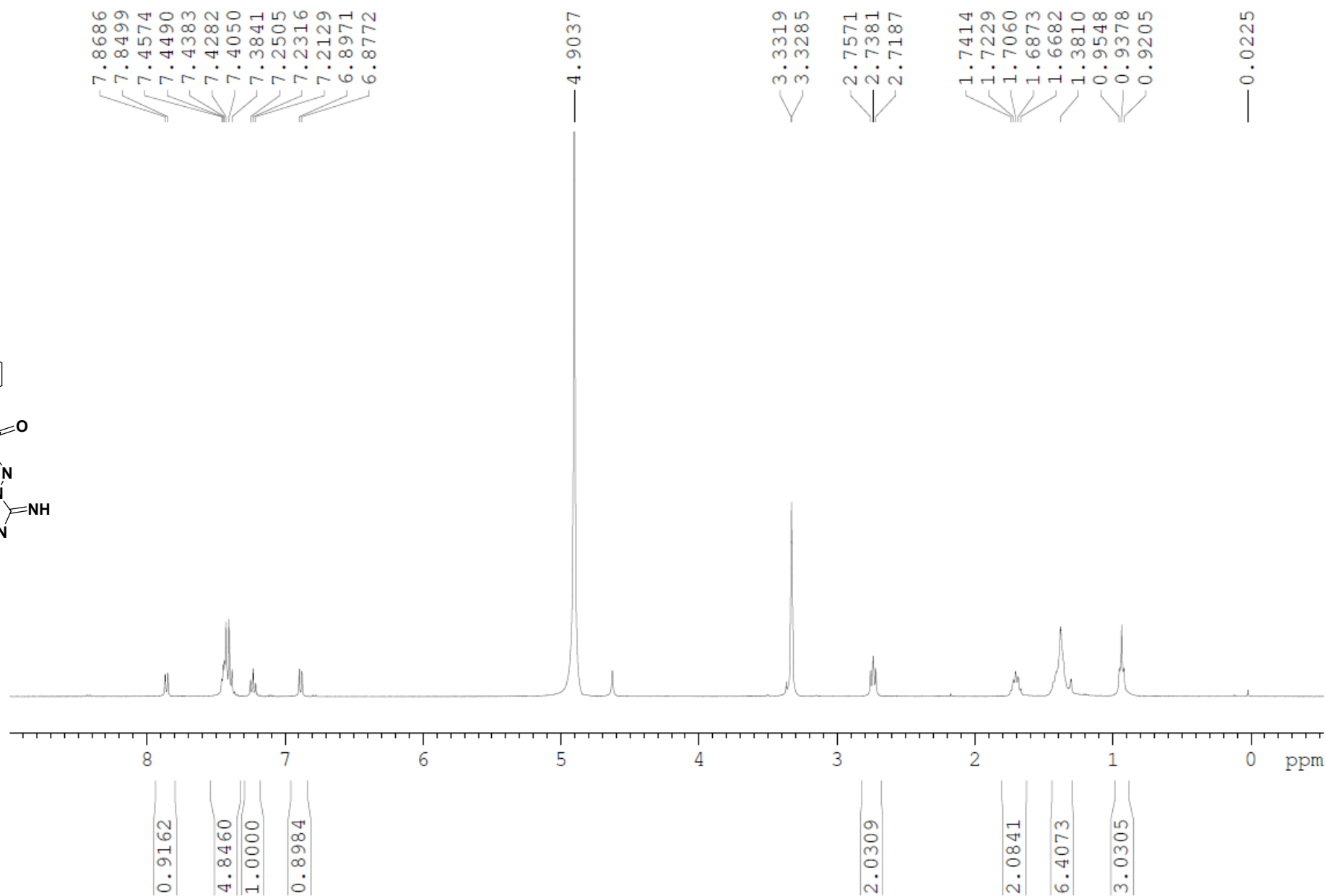


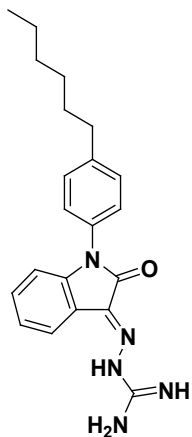
**5m**



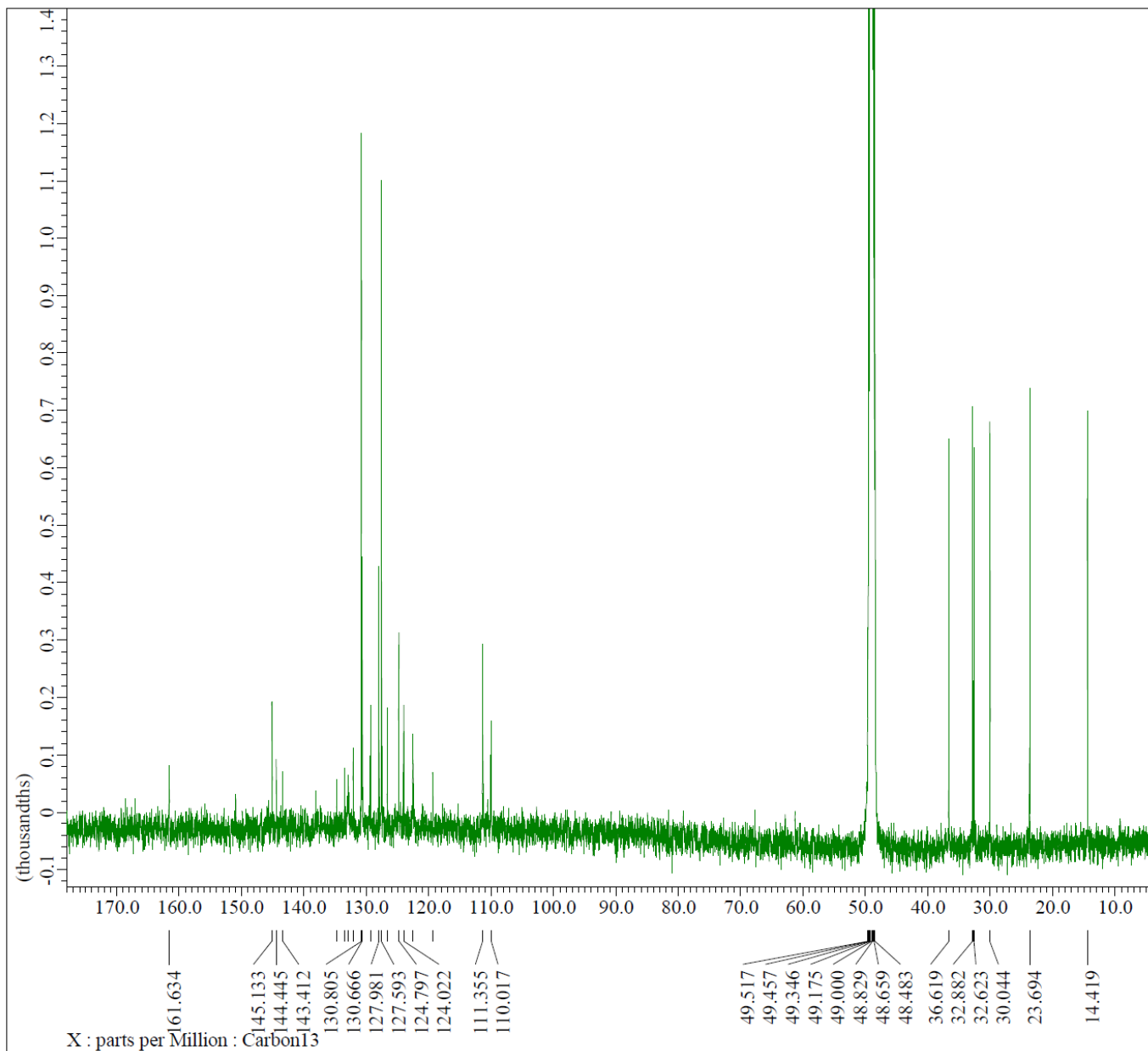


**5n**





5n



```

---- PROCESSING PARAMETERS ----
sexp( 2.0[Hz], 0.0[s] )
trapezoid( 0[%], 0[%], 80[%], 100[%] )
zerofill( 1 )
fft( 1, TRUE, TRUE )
machinephase
ppm

```

Derived from: 10-33\_Carbon-2-1.jdf

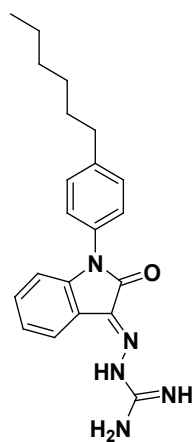
Filename	= 10-33_Carbon-2-3.j
Author	= delta
Experiment	= carbon.jxp
Sample Id	= 10-33
Solvent	= METHANOL-D4
Actual_Start_Time	= 26-JUN-2019 17:20:
Revision_Time	= 10-JUL-2019 12:00:

Comment	= single pulse decou
Data_Format	= 1D COMPLEX
Dim_Size	= 52429
Dim_Title	= Carbon13
Dim_Units	= [ppm]
Dimensions	= X
Spectrometer	= JNM-ECZ500R/S1

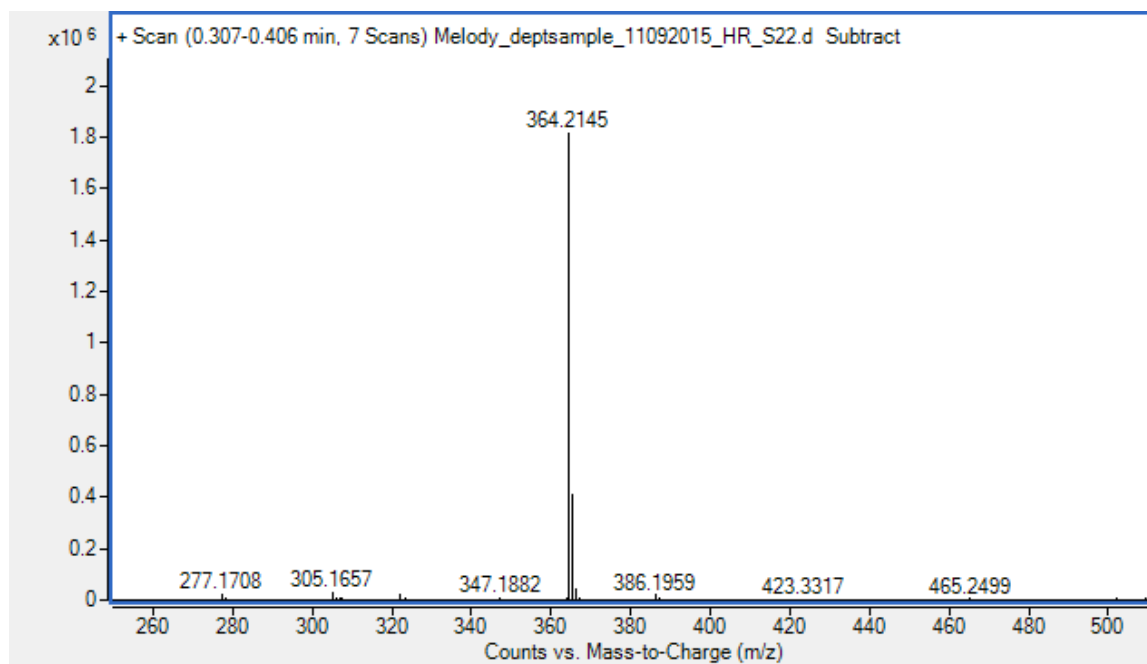
Field_Strength	= 11.62926421[T] (50
X_Acq_Duration	= 1.74063616[s]
X_Domain	= 13C
X_Freq	= 124.5010059[MHz]
X_Offset	= 110[ppm]
X_Points	= 65536
X_Prescans	= 4
X_Resolution	= 0.5745026[Hz]
X_Sweep	= 37.65060241[kHz]
X_Sweep_Clipped	= 30.12048193[kHz]
Irr_Domain	= Proton
Irr_Freq	= 495.13191398[MHz]
Irr_Offset	= 5[ppm]
Blanking	= 2[us]
Clipped	= FALSE
Scans	= 14910
Total_Scans	= 14910

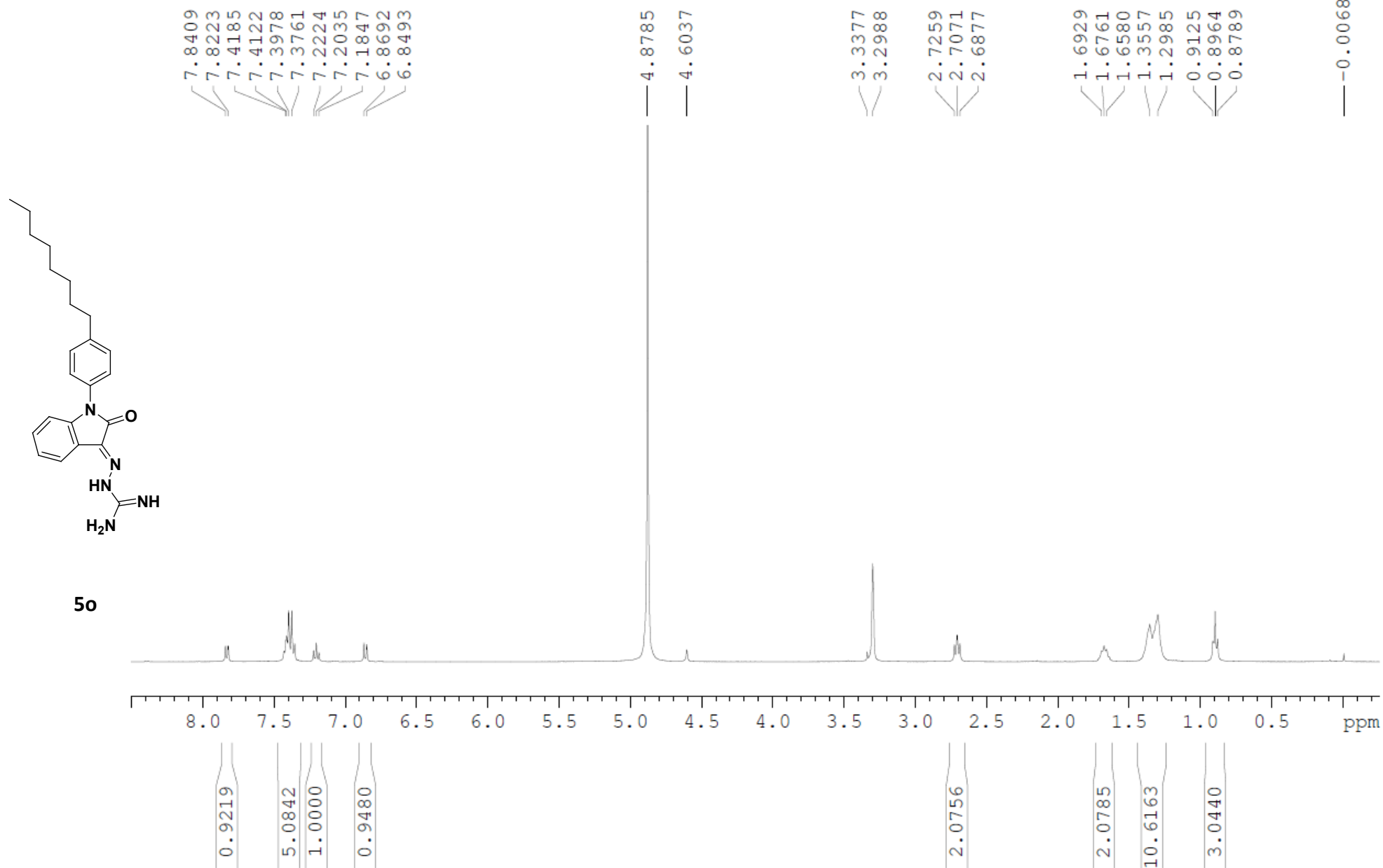
Relaxation_Delay	= 2[s]
Recvr_Gain	= 56
Temp_Get	= 22.8[dC]
X_90_Width	= 11.36[us]
X_Acq_Time	= 1.74063616[s]
X_Angle	= 45[deg]
X_Atn	= 9[dB]
X_Pulse	= 5.68[us]
Irr_Atn_Dec	= 29.172[dB]
Irr_Atn_Dec_Calc	= 29.172[dB]
Irr_Atn_Dec_Default_Calc	= 29.172[dB]
Irr_Atn_No	= 29.172[dB]
Irr_Dec_Bandwidth_Hz	= 5.97826087[kHz]
Irr_Dec_Bandwidth_Ppm	= 12.07407703[ppm]

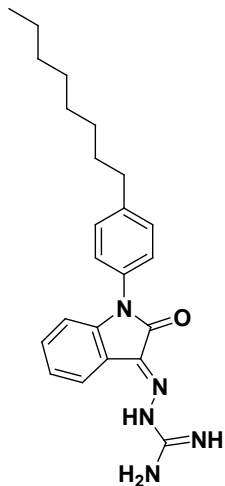




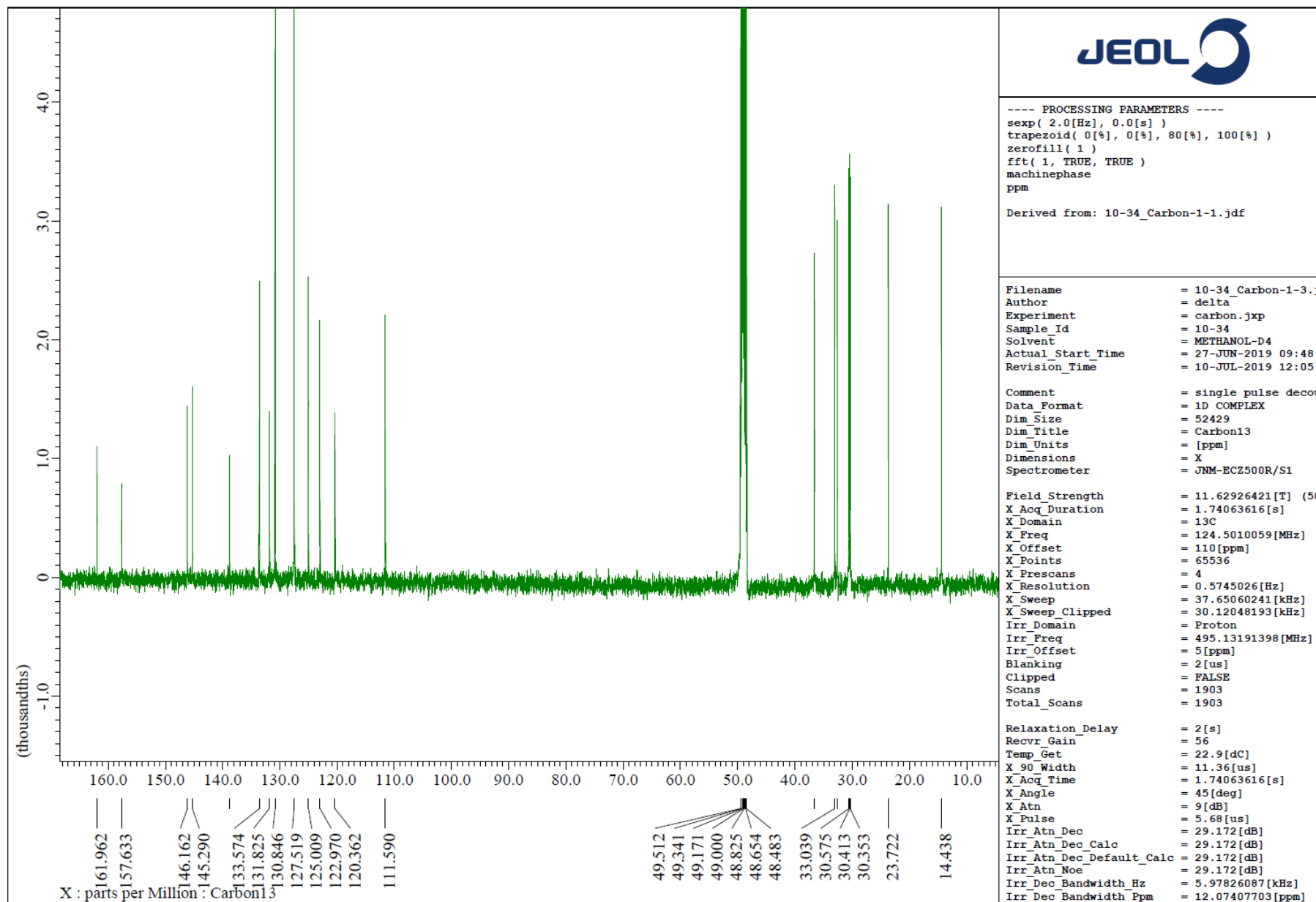
**5n**

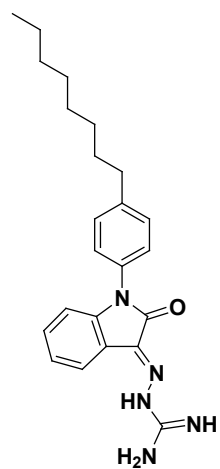




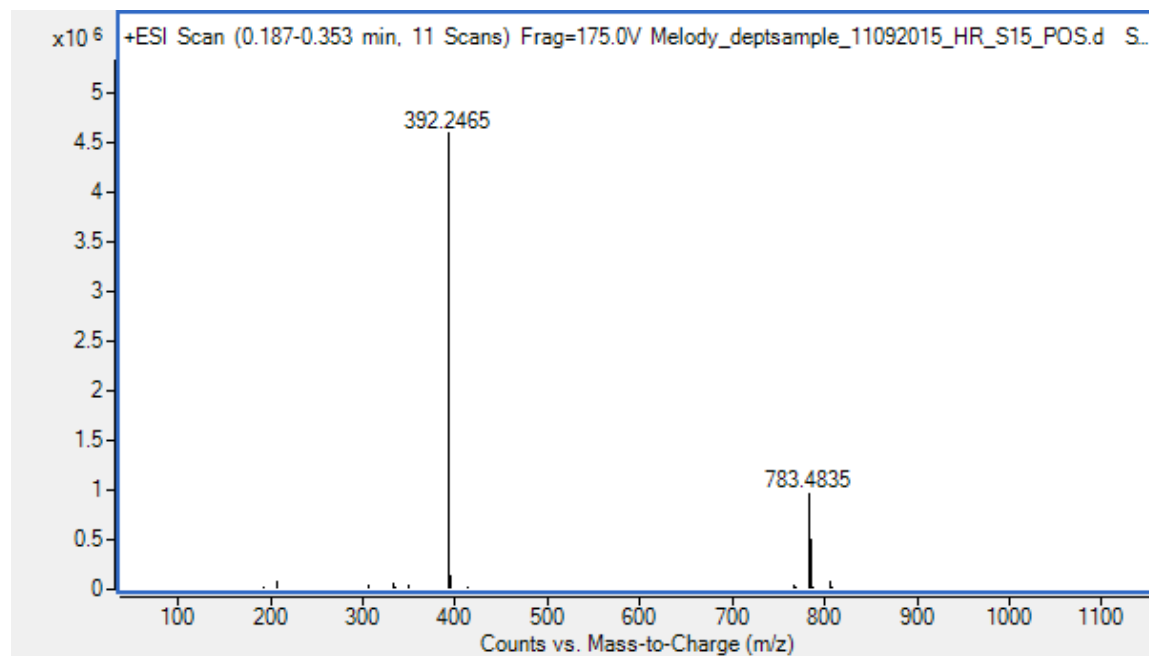


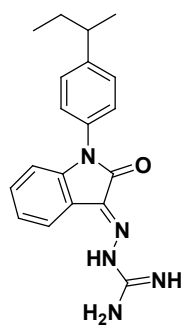
50



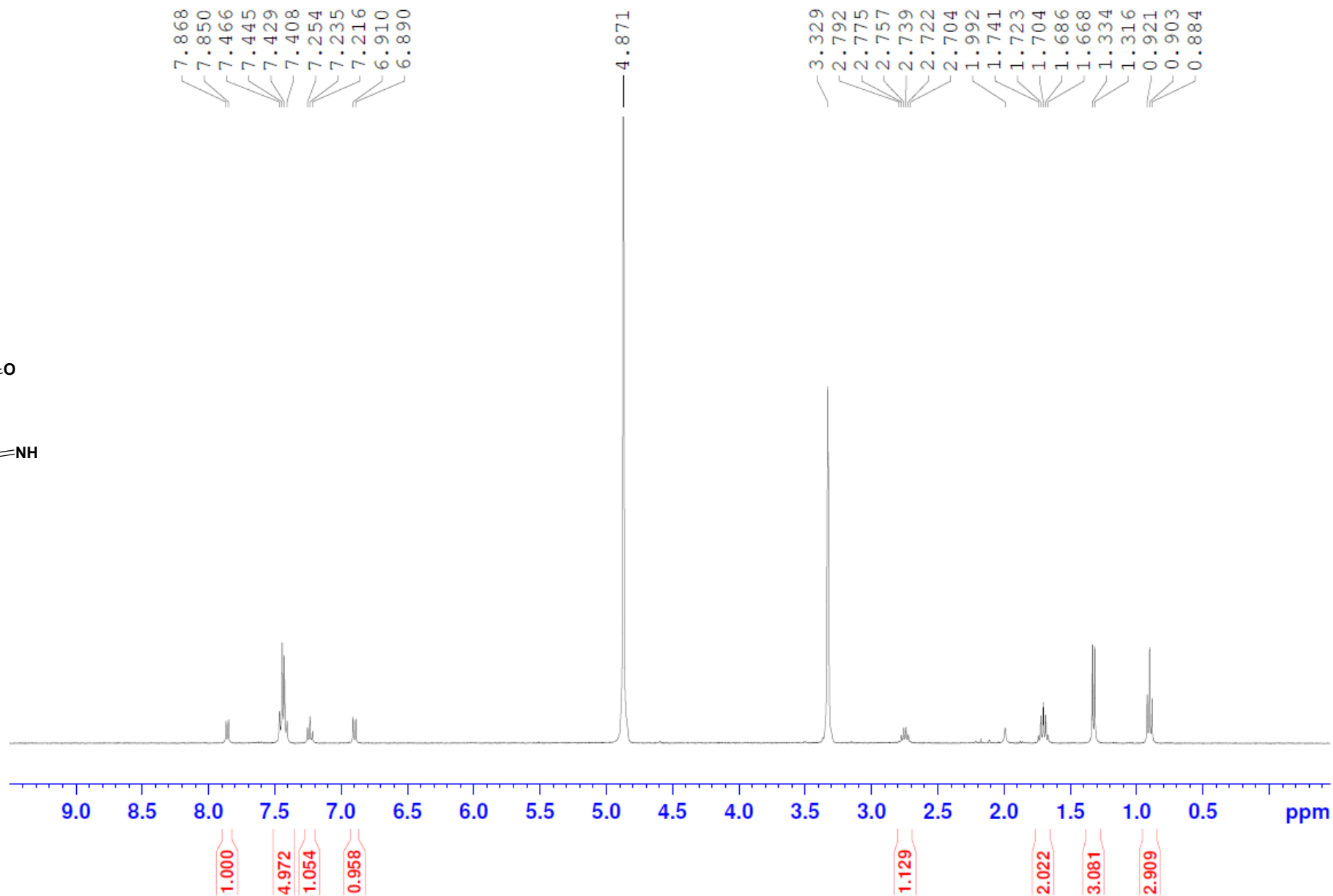


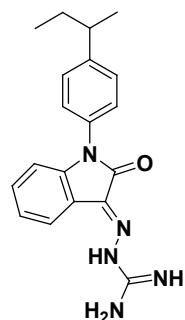
**5o**



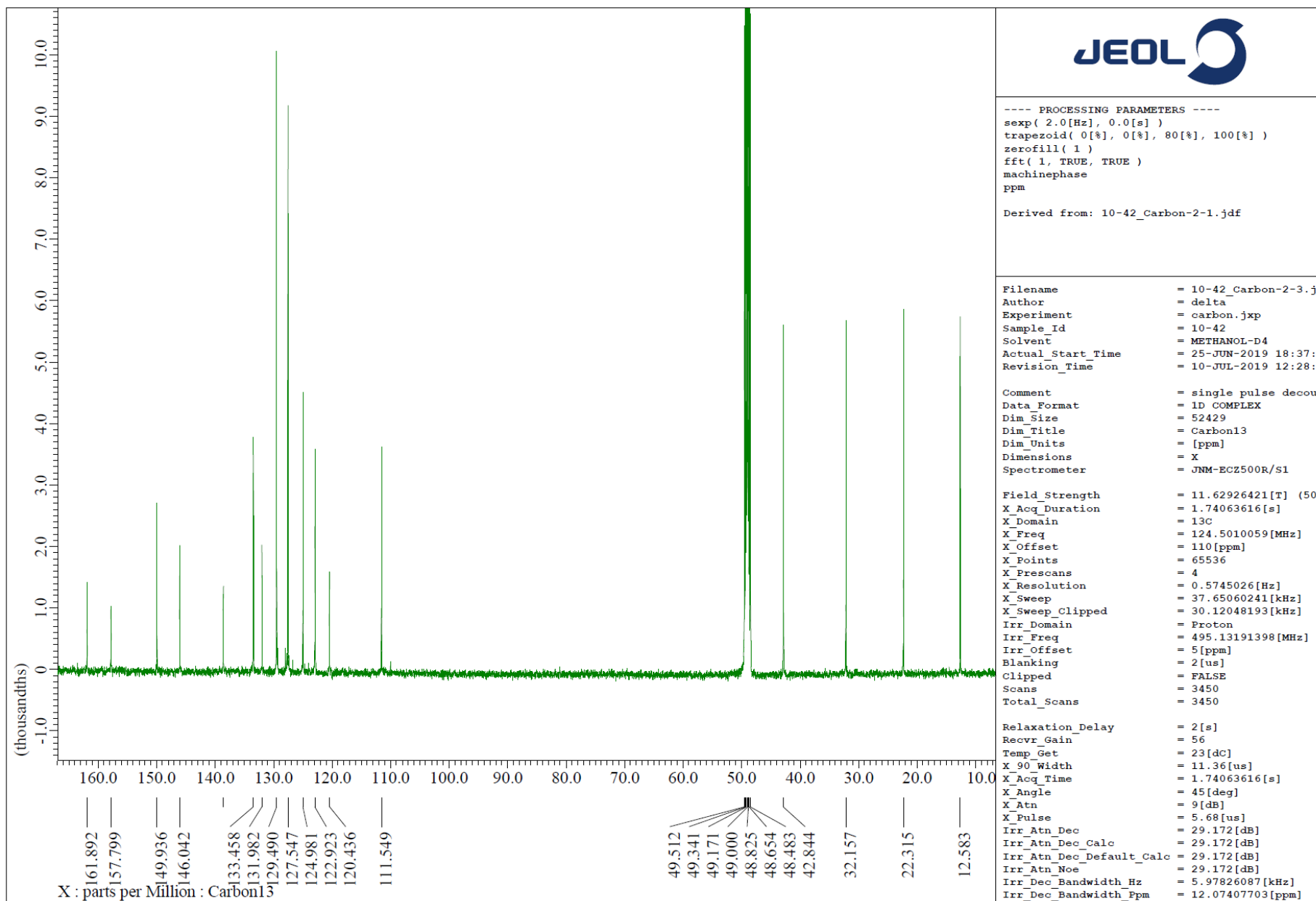


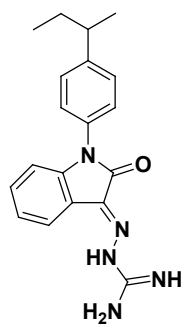
5p





5p





**5p**

